

CHAPTER 1

MATHEMATICAL MODELS OF EXCITATION AND PROPAGATION IN NERVE

Richard FitzHugh†

1. INTRODUCTION: MODELS OF AXONS

A model is something simple made by a scientist to help him understand something complicated. A model can consist of mathematical equations, an imaginary molecular structure obeying the laws of physics, or a machine which is physically different from the original phenomenon but which simulates its behavior. All three types of models are of use in neurophysiology.

Mathematical models have been used for a long time in theoretical physics, but it is only since the 1930s that serious attempts have been made to develop mathematical models of neurons (nerve cells). Since 1950, mathematical models have been developed which reproduce such neurophysiological facts as the threshold phenomenon, refractoriness, and the conduction of impulses along a nerve fiber.‡ This chapter describes some of the most useful of these models.

The physiological properties of a nerve fiber, or axon, originate in the thin nerve membrane which forms its surface. The real goal of studying the nerve membrane, not yet achieved, is to find out how it is made and how it works, i.e., to describe it by a detailed molecular model from which, by the use of physical laws, the chemical and electrical properties of the membrane can be derived. The development of purely mathematical models may seem to be irrelevant to this purpose. But until a satisfactory molecular model is forthcoming, mathematical models are valuable at their own level of abstraction, because they provide a translation of classical physiological concepts into a more definite and logical language than one composed of words alone. Future models will undoubtedly combine both physical and mathematical descriptions, but there is no reason for delaying

† This chapter was prepared at Bethesda, Md., with the sponsorship of the National Institutes of Health. *Reproduction for the purposes of the United States Government is permitted.*

‡ Appendix A contains a glossary of physiological terms. For an introduction to the physiology of nerve fibers, see Refs. 52 to 56.

the development of the mathematical side of the theory until it can be based on the laws of physics and chemistry. On the contrary, it is conceptually useful to construct different mathematical models, which emphasize one or another set of properties and omit others.

There are, unfortunately, difficulties of communication between the physiologists who have been concerned with the nerve cell for a long time and the relative newcomers with mathematical and engineering backgrounds, for whom this volume is mainly intended. Physiologists, on the one hand, are quick to recognize in the newcomers a lack of familiarity with the subtle complexities of the subject and to dismiss them as naive. On the other hand, many physiologists fail to understand not only the properties but even the necessity of mathematical models, because their own habits of thought, though highly effective in their own field, are unmathematical.[†]

In attempting to describe a nerve fiber mathematically, therefore, one has to face the problem of thinking in two different languages, that of the mathematician and that of the physiologist. A brief description in physiological language of the observable electrical properties of that much-studied nerve fiber, the isolated giant axon of the squid, might sound as follows.

In the absence of stimulation, the cylindrical axon maintains a constant potential difference, called the *resting potential*, across its surface membrane. This potential can be picked up between an internal and an external recording electrode, amplified, and recorded. If one applies a stimulus in the form of a brief outward current pulse (less than a millisecond duration) to the axon through a stimulating electrode touching the membrane, the resulting potential change depends on the amplitude of the stimulus. A very weak stimulus produces a temporary deviation of potential (negative outside) which dies away with a time constant of about a millisecond, is proportional to the stimulus amplitude, and decays with distance away from the electrode with a "space constant" (analogous to the time constant) of less than a centimeter. Such a response is called *passive* and *local*. As the stimulus strength is increased, the potential change starts increasing faster than the stimulus strength, but still remains below about 10 mV. This is called an *active response*; it is still local. Finally, above a critical stimulus level called the *threshold*, the recorded potential curve increases abruptly in amplitude to form a roughly triangular waveform about 100 mV high and lasting about a millisecond. Such a curve is called an *action potential*. Although it arises

[†] For two widely different opinions by biologists on the applicability of mathematics to biology, see T. H. Waterman, *Amer. Scientist*, **50**:548 (1962); and L. V. Heilbrunn, "An Outline of General Physiology," 3d ed., pp. 593-595, Saunders, Philadelphia, 1952. For other discussions of this problem, see N. Rashevsky, "Mathematical Biophysics," 3d ed., vol. 2, Dover, New York, 1960; J. A. Rafferty, *Amer. Scientist*, **38**:549 (1950); F. S. Grodins, "Control Theory and Biological Systems," Columbia University Press, New York, 1963.

locally, it immediately splits into two separate waves which travel away from the stimulating electrode in opposite directions along the fiber at a constant conduction velocity. (In a living animal, nerve impulses are normally produced only at the ends of fibers at synapses by chemical mechanisms, and propagated impulses occur singly, not in pairs.) The action potential of a nerve impulse, once it starts traveling, can be recorded at any point along the fiber as it passes, but there is no way to deduce from the record alone where it originated or the strength of the stimulus that produced it. The fact that one can record only the presence or absence of an impulse, without intermediates, is called the *all-or-none law*.

If one applies a second stimulus shortly after the first one, further phenomena appear. Following a first stimulus which is above threshold and which therefore produces an impulse, there is a time interval, called the *absolute refractory period*, during which a second stimulus (no matter how strong) is unable to produce a second impulse. The absolute refractory period outlasts the action potential by roughly a millisecond. Following this comes a *relative refractory period*, during which a second stimulus can produce an impulse, but the threshold value for this second stimulus is higher than the threshold of the resting fiber. During the relative refractory period, which is of indefinite duration, the threshold falls and gradually approaches its original resting value.

If the first stimulus is below threshold, it produces no impulse, but it does affect the response of the fiber to a second stimulus for a short time afterward. First comes an enhanced phase, lasting a millisecond or two, during which the threshold is lower than normal. The effects of two stimuli applied close enough together in time therefore combine, and the closer together they are the more effective they are in combination. After the enhanced phase, the fiber enters a depressed phase of indefinite duration, during which the threshold to the second stimulus is greater than at rest. The degree of enhancement and depression in these two phases increases with the strength of the first subthreshold stimulus.

A stimulus applied to the axon thus has a twofold effect, first excitatory, resulting in a propagated impulse if the stimulus is strong enough, followed by a sort of rebound phenomenon which makes the membrane less excitable than it was originally, and this secondary depression is greater, the greater the previous excitatory effect.

Finally, if, instead of a brief pulse of current as a stimulus, one applies a very long one ($\frac{1}{2}$ s or more), more than one impulse may result. Depending on the stimulus strength, there may be as many as four or five impulses in a burst that lasts no more than about 100 ms, the action-potential heights decaying somewhat during the burst.

We can start to unravel this whole complicated tangle of events by noting that we are dealing with phenomena of three different orders of magnitude

temporally. The fastest events, lasting about 0.1 to 1 ms, are concerned with the threshold phenomenon, with the rising phase of the action potential, and with the temporal summation of two stimuli. Then come the events which take longer to develop (1 to 10 ms), the falling phase of the action potential and the subsequent refractory phases, and the depressed phase which follows the enhanced phase after a subthreshold stimulus. Finally, there is the still slower development of adaptation, with very long stimulus pulses, which outlasts several impulses and causes the decay of action-potential height and finally the cessation of firing.

This division of events occurring in a nerve fiber according to general duration or time constant helps in classifying the mathematical variables to be used in modeling. All the models to be described here are based on the concept of variables of state, which specify the state of the system, and which mathematically are the dependent variables of a set of differential equations. The variables of state used in neuron models fall into several distinct classes. The most easily measurable ones are membrane current and potential. In the current clamp experiment, current is an input variable and potential an output variable. Other output variables appear in mathematical models; they are not directly measurable experimentally, but influence the time course of the potential. These output variables can be classified into four types, according to their function and the general order of magnitude of their relaxation times,† as follows:

1. *Membrane potential.*
2. *Excitation variables.* The current-potential relation of most models is linear. Excitation variables vary this relation so as to provide either a negative resistance or a switching operation in the equivalent circuit of the model, to provide the regenerative action necessary for excitation. Variables of types 1 and 2 have the shortest relaxation times.
3. *Recovery variables.* These variables react on the type-1 and 2 variables so as to eliminate the excitability of the model after excitation has occurred and bring about recovery and the end of the impulse. Their relaxation times are usually an order of magnitude greater than those of types 1 and 2. If still greater, a prolonged plateau action potential results.
4. *Adaptation variables.* These also act to decrease excitability, but have longer relaxation times than those of type 3. Their effect builds up slowly and can result in the decrease in frequency of a train of impulses. If their effect is strong enough, they cut off the train completely. In the Hodgkin-Huxley (HH) model described in Sec. 4, potential V is of

† Relaxation times are defined in Appendix B. They are "time constants" which are not necessarily constant and provide an approximate measure of the relative rapidity of variation of a variable.

type 1, sodium activation m is of type 2, sodium inactivation h and potassium activation n are of type 3, and there is no type-4 variable.

The roles of these different types of variable can be briefly explained in engineering terms. The type-1 and 2 variables together form a subsystem of the model that acts like a bistable multivibrator. With zero current input, this subsystem remains in a resting state, but a sufficiently strong current shock puts it into an excited state.[†] The change of potential resulting from passing to the excited state causes a delayed change in the type-3 variables, which reacts on the bistable system so as to make it monostable, eliminating the excited state. This is the recovery process that forces the excited subsystem to return to its original resting state. The momentary occurrence of an excited state constitutes the nerve impulse. If the current shock is too weak to evoke an impulse, lesser changes of the type-3 variables still occur which make it harder for a second shock to evoke an impulse.

If, instead of a brief shock, a sufficiently strong step current is applied to a model containing only type-1, 2, and 3 variables, it converts it into a free-running multivibrator which produces a train of impulses. Type-4 variables, which are the slowest of all, react on such a train of impulses either by reducing their frequency or by quenching the oscillation completely. In the latter case, the complete model responds to a step-current input by giving only a finite burst of impulses.

The fact that some of these variable types have relaxation times that vary considerably from one another makes it possible to simplify the analysis of the equations by using the method of reduced systems. If one makes the relaxation times of the faster variables zero, or those of the slower ones infinite, the approximate behavior of the remaining variables can be studied in isolation. How this is done is shown in later sections.

The most useful class of models is based on an equivalent circuit consisting of a capacitor in parallel with a conductor, the current through which is a function of one or more variables of state (denoted here by W_1, W_2, \dots, W_μ) of types 2, 3, and 4 (Figs. 3-1 and 4-1). If V is the membrane potential, I the total membrane current density (per unit area of membrane), I_i the current density (per unit area) through the conductor, and C the membrane capacitance (per unit area), a membrane element is described by a set of differential equations of the form

$$\begin{aligned} \frac{dV}{dt} &= \frac{1}{C} [I - I_i(V, W_1, \dots, W_\mu)] \\ \frac{dW_j}{dt} &= F_j(V, W_1, \dots, W_\mu) \quad j = 1, \dots, \mu \end{aligned} \tag{1-1}$$

[†] As far as this property is concerned, there is no distinction between type-1 and type-2 variables. The distinction appears under potential control when the presence of a type-2 variable delays the development of the current in response to a sudden change of potential.

The BVP (Bonhoeffer-van der Pol) and HH models described in Secs. 3 and 4 belong to this class, and newer models of various nerve and muscle membranes have appeared that are built on the same plan.

Excitation and propagation in neurons are essentially nonlinear phenomena, for which mathematical methods are much less well developed than for the linear phenomena comprising much of theoretical physics. The nonlinear differential equations used cannot usually be solved explicitly, but require the use of two approximate methods for their solution: nonlinear mechanics and computation. Analytic results from the theory of nonlinear differential equations (nonlinear mechanics) are given in Appendix B. A fuller introduction to these concepts can be found in the books on this subject which are listed in the bibliography.

The use of computers in studying nerve models is discussed in Appendix C. Appendix D is a list of mathematical symbols.

Because interest in this chapter is focused on the nonlinear properties of excitation and propagation, little is said about the use of linear methods to study the electrical properties of axons (nerve fibers) as an approximation when the signals involved are small. These applications of cable theory to neurons are covered by R. E. Taylor [40].

In addition to models of single nerve fibers, mathematical models of more complicated nervous structures are now being developed: the nerve cell body with its attached shrubbery of dendrites, synapses, which are connections between different neurons, and networks of interconnected neurons and sensory cells.†

Much remains to be done in comparing theoretical and experimental results. The principal emphasis in this chapter is on providing an understanding of the models themselves, rather than on comparing them with experiments, and such comparisons as are in the literature are mostly quoted without criticism.

2. EARLY MODELS OF EXCITATION

During the 1930s research workers began to construct mathematical models to explain excitation and impulse conduction in axons. In the absence of any detailed information on the molecular structure and function of the membrane (which is still largely missing), two general approaches were used. The first was to set up an equivalent circuit of conventional

† An interesting modern development of this work is that the mathematical complexities inherent in such structures have inspired the construction of electronic circuits which are analogs of single neurons and which can be interconnected electrically to simulate neuronal networks. It is too early to tell how well the behavior of the nervous system can be duplicated in this way (the principal difficulty being a lack of information on how the nervous system itself works), but the possibilities of creating new brainlike automata and computers is an exciting one which has aroused much interest among engineers.

circuit elements, including a switch or relay which closed when the membrane potential reached a certain triggering value. The models of Rushton and of Offner, Weinberg, and Young are of this kind. These models were used to predict the propagated action potential. However, the excitation mechanism assumed was inadequate to explain such things as strength-duration curves or the time course of excitability changes. A discussion of these models will be postponed until the explanation of models of propagation, below, in Sec. 6.

The second type of early model was based on a realization that it would be useful to have a purely mathematical model in which the variables of state correspond to physiological concepts such as degree of excitation or accommodation, as well as purely electrical quantities.

These models are the so-called "one- and two-factor theories" of Blair, Rashevsky, Hill, Monnier, and Young. (The word *factor* means a variable of state and will be replaced by *variable* in what follows.) Although these early models have been replaced by later ones, they are described here to show that the later models did not appear suddenly in a fairly highly developed form, but were partly the result of earlier searching, and also because some of these early models introduced ideas regarding the different types of variables of state which are still useful. Only one of these models, that of G. Young [42], is considered in detail here, since all the others are special examples of it.[†]

Instead of the purely analytical mathematical analysis generally used in describing such models, a phase-plane representation is employed here, for three reasons: (1) to introduce the use of the phase plane in a simple example to readers who may be unfamiliar with it, (2) to make the properties of the model somewhat clearer, and (3) to show, by comparison with the BVP phase plane (described below in Sec. 3), the relation between Young's model and the more complete nonlinear models developed later.

The two variables of state of Young's and related models have been given various interpretations by different authors. In the light of subsequent developments it seems best to identify them as V , the membrane potential (a type-1 variable) and U , the accommodation variable (type 3). The input variable is I , the stimulating current applied to the neuron through an electrode. Young's equations are:[‡]

$$\begin{aligned}\dot{V} &= k_{11}(V - V_R) + k_{12}(U - U_R) + aI \\ \dot{U} &= k_{21}(V - V_R) + k_{22}(U - U_R)\end{aligned}\tag{2-1}$$

[†] For description of the other models see particularly A. V. Hill [30], B. Katz [34], and N. Rashevsky [38].

[‡] Young's original equations contain a term $+bI$ on the right side of the second equation (2-1). Since interest here is in models of the type (1-1), in which only V is directly affected by I , b is made zero here.

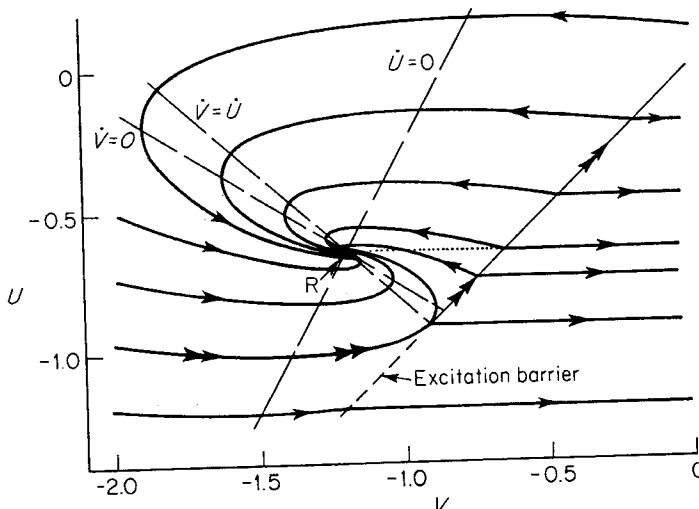


FIG. 2-1. Phase plane of Young's model for zero stimulating current. Equations (2-1) apply above the excitation barrier ($V = U$). Isoclines (broken lines labeled $\dot{V} = 0$, $\dot{U} = 0$, $\dot{V} = \dot{U}$) intersect at +stable resting singular point R . Arrowheads indicate trajectories. When the state point traveling along a trajectory reaches the excitation barrier, excitation occurs. Trajectories below barrier, though not actually specified by the model, are shown as horizontal lines for comparison with Fig. 3-2. Double arrowheads denote the threshold separatrix, composed of a straight segment of the excitation barrier and a curved segment of the trajectory tangent to the barrier. For values of constants in Eq. (2-1), see text.

where $\dot{V} = dV/dt$, $\dot{U} = dU/dt$, and V_R , U_R , and the k 's are constants, with $V_R < U_R$. In the UV phase plane (Fig. 2-1),† the solutions of Eqs. (2-1) are drawn as curves with arrowheads, called *trajectories*, along which the *state point*, representing the state of the system, moves.

Equation (2-1) holds only in the region of the phase plane where $V < U$. When the state point reaches the *excitation barrier* ($V = U$) for the first time along any trajectory, excitation is assumed to occur, but the events thereafter are not specified. Young's model does not describe the latency and shape of the impulse nor the subsequent recovery of excitability.

In addition to the excitation barrier, there are three other important lines on the phase plane, the *vertical*, *horizontal*, and *unity isoclines*, where

† The parameter values used in Fig. 2-1 were chosen so as to make the model approximate to the BVP model illustrated in Fig. 3-2. The values are $V_R = -1.199$, $U_R = -0.656$, $k_{11} = -0.439$, $k_{12} = -0.667$, $k_{21} = 0.12$, $k_{22} = -0.064$. These values were obtained by (1) linearizing the BVP model at its resting point, (2) locating the straight-line excitation barrier so as to pass through the point on the horizontal dotted line in Fig. 2-1 where it intersects the threshold separatrix, with a slope equal to that of the phase-velocity vector there, and (3) transforming W by the formula $W = 0.667 (U - 0.28)$ so as to make the excitation barrier coincide with the line $V = U$.

$\dot{V} = 0$, $\dot{U} = 0$, and $\dot{W} = \dot{U}$, respectively.[†] The equations of the three isoclines are, from Eq. (2-1),

$$\begin{aligned}\dot{V} = 0 \quad & k_{11}(V - V_R) + k_{12}(U - U_R) + aI = 0 \\ \dot{W} = 0 \quad & k_{21}(V - V_R) + k_{22}(U - U_R) = 0 \\ \dot{V} = \dot{W} \quad & (k_{11} - k_{21})(V - V_R) + (k_{12} - k_{22})(U - U_R) + aI = 0\end{aligned}\tag{2-2}$$

For a given value of I , a singular point exists at the common intersection of the isoclines, at the point (V_S, U_S) , the values of which are found by solving the first two equations (2-2) simultaneously for V and W . The stability of the singular point is found by calculating its eigenvalues.[‡] These are the roots p_1 and p_2 of the characteristic equation [Eq. (B-29) of Appendix B].

$$p^2 + (-k_{11} - k_{22})p + (k_{11}k_{22} - k_{12}k_{21}) = 0\tag{2-3}$$

The roots of Eq. (2-3) are given by the usual formula for the solution of a quadratic equation. They are either both real or a complex conjugate pair. One advantage of using Young's model rather than the special cases studied by Hill and Rashevsky is that the latter have only real eigenvalues, whereas experimental transients in the form of damped oscillations require the eigenvalues to be complex [16]. The example shown in Fig. 2-1 has complex eigenvalues.

In order to guarantee that the singular point is +stable (i.e., that it is approached by all neighboring trajectories), it is necessary that the two quantities in parentheses in Eq. (2-3) be positive [1, 4, 5].[§] The singular point represents a steady state corresponding to the given value of I . There is one trajectory that is tangent to the excitation barrier, at the point where the unity isocline intersects the latter. An arc of this trajectory, plus its extension forward along the excitation barrier, is called the *threshold separatrix* and is marked with double arrowheads in Fig. 2-1. Any state point below the separatrix is either already within the region of excitation (below the barrier) or soon reaches the barrier by traveling along its trajectory. In either case excitation occurs. Any state point above the separatrix never reaches the barrier, but instead approaches the singular point. The separatrix thus divides the phase space locally into two zones, depending on whether or not state points in them reach the excitation barrier.

Consider first a step-current input, in which the current jumps from zero to a positive value I at $t = 0$ (Fig. 2-2).^{||} When the current is zero, the

[†] The isoclines are so named because they are crossed everywhere by trajectories that have a certain direction at the point of intersection, either vertical, horizontal, or of unit slope in the phase plane.

[‡] Definitions of mathematical terms used and derivations of Eqs. (2-3) and (2-4) are given in Appendix B.

[§] Note that the stability of the singular point is the same for all values of I .

^{||} Physiologically, this represents a cathodal stimulus. For definitions of cathodal and anodal stimuli see Appendix A.

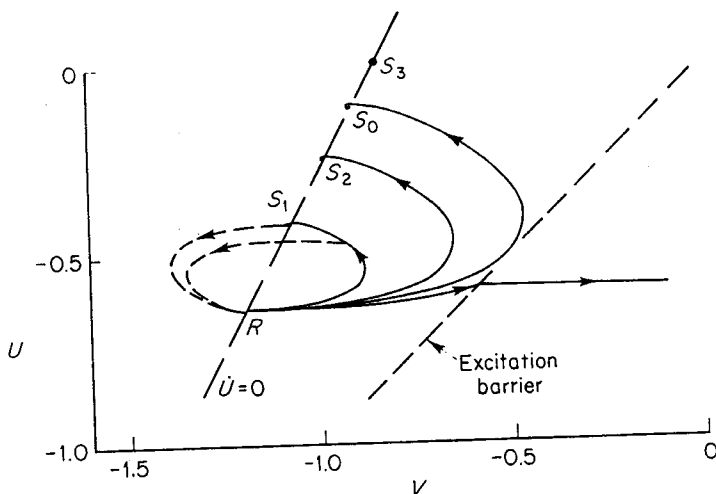


FIG. 2-2. Phase plane of Young's model showing trajectories for various step currents I . Model initially at resting point R . S_0 is the singular point for rheobasic current ($I = I_0$). S_1 and S_2 are for subrheobasic currents, and S_3 for a suprarheobasic one. Lowest trajectory corresponds to S_3 and crosses barrier. Broken trajectories show return of state point to R after the end of two rectangular pulses, one of finite duration and the other infinitely long.

singular point is at $V = V_R$, $U = U_R$. This is the *resting state* R . Changing the current to a positive I does not change the horizontal isocline, but displaces the vertical isocline to the right (Eq. 2-2). This moves the singular point to a new location S on the horizontal isocline, and the whole pattern of trajectories is displaced with a new separatrix. For $I > 0$, R is not a singular point, but is the initial point at $t = 0$ for the resulting trajectory. Whether excitation occurs or not depends on whether the initial point R is above or below the new separatrix. The value I_0 of I for which the new separatrix passes through R is called the *rheobase*, given by Eq. (2-4) below.

Now let I be the amplitude of a rectangular current pulse starting at $t = 0$ and ending at $t = T$. The trajectories during the interval $0 \leq t \leq T$ are the same as they were for the step current. For $t > T$, the phase plane is again that for $I = 0$, with the singular point at R . The initial point at $t = T$ for each trajectory during the interval $t > T$ is the point reached by the state point at time T , at the end of the pulse. Figure 2-2 shows that if the state point has not reached the barrier by time T , it will not do so at all, since after the pulse is finished, the state point moves away from the barrier and returns toward R (broken trajectories). If $I > I_0$, and if the state point just touches the barrier at $t = T$ (e.g., the lowermost trajectory in Fig. 2-2), I is called the *threshold stimulus amplitude* for a pulse of duration T . If I is plotted against T , the resulting curve is a *strength-duration curve*.

Since Young's differential equations (2-1) are explicitly solvable, a formula for the strength-duration relation can be derived [Eq. (B-38) of Appendix B]:

$$0 < T \leq T_0 \quad I(T) = \frac{1}{K_1(e^{p_1 T} - 1) - K_2(e^{p_2 T} - 1)} \quad (2-4)$$

$$T_0 < T \quad I(T) = I_0 = I(T_0)$$

T_0 is the *utilization time*, defined by Eq. (B-37), and K_1 and K_2 are constants. In the limit as T approaches zero,

$$IT \rightarrow \frac{1}{K_1 p_1 - K_2 p_2} = Q \quad (2-5)$$

Equation (2-5) expresses the *constant quantity law* of excitation for rectangular stimulating pulses. This law says, in general, that for very short pulses it is not the shape of the pulse but rather the total charge (area under the current pulse) that determines whether excitation takes place. If an instantaneous pulse, $I = Q \delta(t)$, where $\delta(t)$ is the unit impulse or Dirac delta function, is applied to the model as a stimulus, the threshold value of Q is given by Eq. (2-5). This is the limiting case in which the pulse duration is infinitesimal.

By solving Eq. (2-1) it can be shown that an instantaneous current pulse displaces the state point horizontally in the phase plane for a distance equal to Q . The threshold to an instantaneous pulse is thus equal to the horizontal distance from any point in the phase plane to the excitation barrier. Since points R and S in Fig. 2-2 are not equidistant from the barrier, the threshold to an instantaneous shock is changed by the application of a long-lasting subrheobasic step current. The degree of accommodation in a real axon varies considerably with the condition of the axon, and H. O. Parrack† found that in nerves, left in frogs with intact circulation instead of being excised, accommodation in this steady-state sense is absent. However, transient changes in accommodation following a stimulus still occur, and are provided for by type-3 variables, such as U in Young's model.

In addition to providing a formula for the strength-duration curve, Young's model shows in very simple mathematical form the basic idea that variables of at least two types are necessary to describe excitation, one representing membrane potential (type 1), and a second, not yet physically identified, representing changes of excitability as expressed in the phenomenon of accommodation (type 3). Variables of types 2 and 4 will be introduced in later sections and their significance explained. In Hill's model [30], which is a special example of Young's model, there is no steady-state accommodation.

† Amer. J. Physiol., 130:481 (1940).

In Hill's model the relaxation times[†] of V and U (which Hill calls the "threshold"[‡]) are k and λ , respectively. The ratio λ/k of these two relaxation times was usually taken by Hill to lie between 10 and 200. In later models, such as that of Hodgkin and Huxley, this ratio is of the order of magnitude of 10. An extension of Hill's formulation has been made by B. Katz[§] to explain finite trains of impulses in response to step-current stimulation. Hill's equations can be written as^{||}

$$\begin{aligned}\dot{V} &= \frac{-(V - V_R) + cI}{k} \\ \dot{U} &= \frac{(V - V_R) - (U - U_R)}{\lambda}\end{aligned}\tag{2-6}$$

Katz changes Hill's original assumption that the model ceases to describe events following the arrival of the state point at the excitation barrier in the phase plane. To quote Katz [34, p. 45]:

If λ is large, the "local potential" V remains above threshold U for a long time during which repetitive responses may be expected to occur. The rhythmical intervention of the refractory period which, strictly speaking, prevents V from remaining above U each time an impulse is started off has been left out of this scheme; the local changes, due to a persisting stimulus, are considered, for simplicity, as separate, and as proceeding independently of the success or failure of the stimulus in setting up a propagated disturbance.

In fact, this is a new model, which is of the same mathematical form as that of Hill, but in which the variables have different physiological significance. This is shown by the fact that the values of λ/k calculated from experimental results by Katz go as high as 500, instead of from 10 to 200. In this "Hill-Katz model," U is not a type-3 variable, but a type-4 variable that represents adaptation, a phenomenon that is expressed in the slow decay of the frequency of a train of nerve impulses resulting from a constant stimulation. Adaptation may be either complete (the impulse frequency drops to zero, and the train of impulses is finite) or incomplete (the impulse frequency does

[†] See Appendix B.

[‡] This meaning of the term *threshold* is different from that used elsewhere in this chapter, where it indicates the smallest value of the stimulus (the input variable of the neuron) at which an impulse appears in the membrane potential (the output variable). The latter definition is a purely operational one, whereas Hill's usage represents a concept of threshold characteristic of the neurophysiological thinking of the time.

[§] *J. Physiol.*, 88:239 (1936).

^{||} Making λ infinite gives as a special case a reduced system with only one differential equation (for V). This is equivalent to the model of H. A. Blair (*J. Gen. Physiol.*, 15:709, 731; 16:165, 177 (1932); 18:755 (1935); *Amer. J. Physiol.*, 111:515; 112:277 (1935); *J. Cellular Comp. Physiol.*, 6:291 (1935); *Cold Spring Harbor Symp. Quant. Biol.*, 4: 63 (1936).

not decrease to zero, and the train of impulses lasts as long as the stimulus is applied).†

If k is taken to be very small compared with λ , \dot{V} can be made zero in Eq. (2-6), which thus has the approximate solution

$$V = V_R + cI \quad (2-7)$$

Let $I(t)$ be a step function starting at $t = 0$, and I_1 its amplitude. Define a new variable of state $Z = V - U$ which obeys the differential equation

$$\dot{Z} = cI - \frac{Z - Z_R}{\lambda} = cI_1 \delta(t) - \frac{Z - Z_R}{\lambda} \quad (2-8)$$

where $Z_R = V_R - U_R$. The solution of Eq. (2-8) is

$$Z = \begin{cases} Z_R & t \leq 0 \\ Z_R + cI_1 e^{-t/\lambda} & t > 0 \end{cases} \quad (2-9)$$

According to Katz' assumption, the neuron discharges repetitively when Z is positive. Since Z_R is negative, Z is positive only if $cI_1 > -Z_R$, and then only in the interval $0 < t < t_1$, where

$$t_1 = \lambda \ln \frac{-cI_1}{Z_R} \quad (2-10)$$

t_1 is thus the duration of the train of impulses.

The Hill-Katz model can be used to provide adaptation for any model that does not include an adaptation variable by simply considering $Z - Z_R$ rather than I to be the effective stimulating current, and $-Z_R$ to be the threshold for a repetitive response. RC filters to accomplish this purpose have been used by Harmon [29] to provide adaptation in his electronic neuron models. That this simple method is not adequate to reproduce accurately all features of finite trains of impulses, including the rise of the undershoot, has, however, been shown by computations (unpublished) with the HH model, made in an attempt to reproduce the experimental curves of Hagiwara and Oomura [44]. These are discussed in more detail in Sec. 4.

† The term *adaptation* was introduced by E. D. Adrian, "The Basis of Sensation," Norton, New York, 1928, to apply to either axons or sense organs. Adaptation is usually complete in axons and incomplete in sense organs. Other authors, e.g., Katz, used the word *accommodation* to denote this phenomenon in axons, distinguishing this *slow accommodation* from the *rapid accommodation* evidenced by the changes of excitability during a subthreshold stimulus. In this chapter Adrian's original terminology is retained, and these two phenomena will be called simply accommodation and adaptation. They correspond to state variables of types 3 and 4, respectively.

3. A DESCRIPTION OF NERVE-MEMBRANE PROPERTIES USING A NONLINEAR TWO-VARIABLE MODEL

For some purposes it is useful to have a model of an excitable membrane that is mathematically as simple as possible, even if experimental results are reproduced less accurately. Such a model is useful in explaining the general properties of membranes, and as a pilot model for performing preliminary calculations. The use of a qualitative rather than a quantitative model to represent a nonlinear system goes back to B. van der Pol.[†] His equation for a relaxation oscillator has been valuable for understanding real systems, in spite of the fact that it does not very accurately predict the waveform of the output of most real oscillators.

A useful two-variable model of an excitable membrane can be developed from van der Pol's cubic (third-degree polynomial) equation by the addition of terms which make it monostable rather than astable (free running). Although it normally shows a threshold phenomenon rather than an oscillation, it can also be made to show the latter under appropriate input conditions. Since the resulting model resembles qualitatively the phase-plane model of K. F. Bonhoeffer[‡] describing the passivated iron-wire model of an axon, the new equations are called the *cubic BVP* (Bonhoeffer-van der Pol) *equations*. Many qualitatively similar two-variable systems, based on nonlinear current-potential characteristics with negative-resistance regions, behave similarly, even though their nonlinearities are not cubic. They will be referred to collectively as *BVP models*.

Before the properties of the BVP equations are analyzed, one of their equivalent circuits will be described. Figure 3-1 shows the tunnel-diode model of Nagumo, Arimoto, and Yoshizawa [35], used by them to simulate many of the properties of axons. The circuit equations are

$$\begin{aligned} C\dot{V} &= I - F(V) - W \\ L\dot{W} &= E - RW + V \end{aligned} \quad (3-1)$$

where $F(V)$ is the current through the tunnel diode expressed as a function of the potential V across it. These equations are similar in form to the cubic BVP equations (3-6); the latter have a cubic nonlinearity in place of the tunnel-diode current-potential relation.

To derive the cubic BVP equations, start with the equation for a linear oscillator:

$$\ddot{V} + k\dot{V} + \phi V = 0 \quad (3-2)$$

[†] *Phil. Mag.*, 2:978 (1926). For an early electronic model of the heart, see B. van der Pol and J. van der Mark, *ibid.*, 6 (suppl.):763 (1928), and *Arch. Neerl. Physiol.*, 14:418 (1929)..

[‡] *J. Gen. Physiol.*, 32:69 (1948); *Naturwissenschaften* 40:301 (1953).

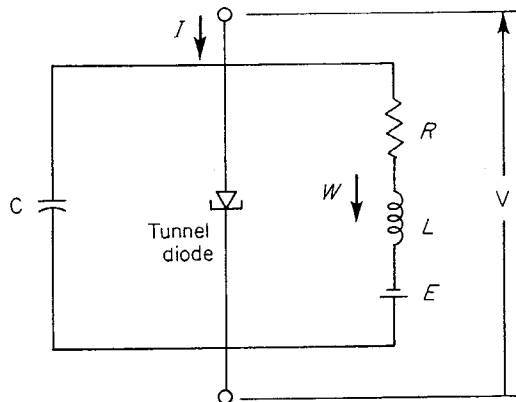


FIG. 3-1. Circuit diagram of the tunnel-diode nerve model of Nagumo, Yoshizawa, and Arimoto [35, fig. 2, redrawn].

Replace the constant k by a quadratic function of V :

$$\ddot{V} + (V^2 - 1)\dot{V} + \phi V = 0 \quad (3-3)$$

This is the van der Pol equation for a relaxation oscillator. Roughly described, it has negative damping (increasing amplitude) for small oscillations and positive damping (decreasing amplitude) for large ones. The amplitude of the oscillations therefore tends toward a fixed intermediate value.

To get this equation into a more useful form, apply the Liénard transformation [5]

$$W = -\dot{V} + V - \frac{V^3}{3} \quad (3-4)$$

to get the following differential equations:

$$\dot{V} = V - \frac{V^3}{3} - W \quad (3-5)$$

$$\dot{W} = \phi V$$

It can be shown by the methods of Appendix B that the vw phase plane of these equations has a $-$ stable singular point at the origin, surrounded by a $+$ stable limit cycle. The singular point is moved and made $+$ stable by adding terms to Eqs. (3-5) as follows, to form the cubic BVP equations:

$$\dot{V} = V - \frac{V^3}{3} - W + I \quad (3-6)$$

$$\dot{W} = \phi(V + a - bW)$$

where a , b , and ϕ are positive constants. V is the membrane potential. I is the membrane current, an input variable which is defined as any arbitrary

function of time; for the moment let $I = 0$. t is time. W is the recovery variable. In terms of the classification of variables introduced in Sec. 1, V is of type 1 and W of type 3; there is no variable of type 2, as there is in the HH equations (Sec. 4).† V , I , W , and t are dimensionless, since this model is not meant to represent any actual nerve membrane.

Equations (3-6) are a special case of Eqs. (1-1), obtained by setting $C = 1$, $I_i = -V + V^3/3 + W$, $\mu = 1$, $W_1 = W$, $F_1 = \phi(V + a - bW)$.

The equations for the vertical ($\dot{V} = 0$) and horizontal ($\dot{W} = 0$) isoclines are as follows:‡

$$\begin{aligned}\dot{V} = 0 \quad W &= V - \frac{V^3}{3} + I \\ \dot{W} = 0 \quad W &= \frac{V + a}{b}\end{aligned}\tag{3-7}$$

Figure 3-2 shows the phase plane of the BVP model for $a = 0.7$, $b = 0.8$, $\phi = 0.08$.

The encircled letters in Fig. 3-2 indicate various physiological states, identified in the legend. These labels serve to convert the phase plane into a useful map of the physiological states of the model. Since a single state of the model corresponds to a single point on the phase plane, each labeled region corresponds to a two-dimensional continuum of states. There are no definite boundaries between the labels, but a continuous gradation of intermediate states. The trajectories show the routes of travel through the physiological states from initial points which are reached as the result of applying current shocks I of various forms.

After the model has been left for a long time with $I = 0$ (zero applied current) it will be at the resting state R , which is a $+/-$ stable singular point. Its coordinates, obtained by solving Eqs. (3-7) simultaneously with $a = 0.7$ and $b = 0.8$, are $V = V_R = -1.1994$, $W = W_R = -0.6243$. Consider stimulation by a current shock. The simplest example is that of an instantaneous pulse of current, with I proportional to a delta function. The area Q under the pulse is the total charge transferred. This charge appears on C , changing V discontinuously by an amount Q/C but not changing W . In Fig. 3-2 this appears as a displacement of the state point along the horizontal dotted line through R , for a distance equal to Q/C . If Q is positive

† One can, for comparison with the HH model, consider that in constructing the BVP model, a type-2 variable, corresponding to the HH variable m , has been eliminated by making its relaxation time zero, thus providing a nonlinear current-potential relation with a region of negative slope.

‡ Equations (3-5), describing the van der Pol model, are a special case of Eqs. (3-6), with $a = b = I = 0$. The phase plane of the van der Pol equations differs from that of Fig. 3-2 in that the horizontal isocline is vertical, rather than sloping, and the singular point is at the origin and $-/-$ stable. There is also a limit cycle resembling that in Fig. 3-4.

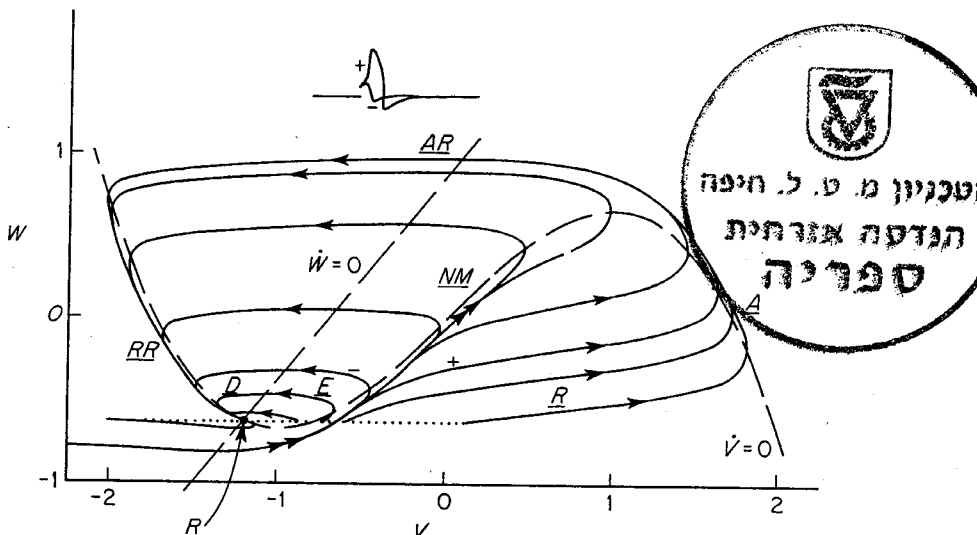


FIG. 3-2. Phase plane of cubic BVP equations (3-6), for instantaneous current I shocks of various amplitudes. Broken curves are isoclines. Shock displaces state point from resting point R to a point on dotted line. Double arrowheads denote the threshold separatrix. In this and subsequent figures, + and - indicate a pair of trajectories, one for a stimulus slightly above (+) and one slightly below (-) threshold. $a = 0.7$, $b = 0.8$, $\phi = 0.08$. Encircled letters denote physiological states as follows: A = active, AR = absolutely refractory, D = depressed, E = enhanced, NM = no man's land, R = regenerative, RR = relatively refractory. Inset: curves of V versus t , showing an action potential (+) and an active subthreshold response (-).

(cathodal stimulus), the displacement is to the right. Compare the two trajectories labeled plus and minus, which result from slightly different values of Q . Minus returns to R after passing through the enhanced and depressed regions, but plus returns to R by a more circuitous route through the regenerative, active, absolutely refractory, and relatively refractory regions. Plus corresponds to a nerve impulse; minus to no impulse.

The trajectories that represent impulses are separated from those that do not by a barrier in the form of a trajectory, the threshold separatrix, which travels upward just to the right of the middle branch of the vertical isocline. This trajectory is hard to obtain with an analog computer, because it is highly unstable, in the sense that small deviations from it grow rapidly and make the phase point veer off to one side or the other, instead of following the separatrix.[†] The separatrix extends into the region called *no man's land*. This unphysiological term was chosen to express the fact that this region is

[†] The separatrix curve in Fig. 3-2 was actually computed by reversing the sign of time in the differential equations and computing the trajectory backward. This changes the trajectory from unstable to stable and makes it easy to compute. Incidentally, as pointed out in Sec. 5, the separatrix trajectory is not uniquely defined mathematically.

very hard to reach from elsewhere in the phase plane, because of the instability of the separatrix. The entire separatrix trajectory is, however, not unstable—only that part of it that lies in no man's land.

In order for a stimulus to produce an impulse, the displaced state point must cross the separatrix. A shock that displaces the state point exactly onto the separatrix is called *threshold*; a smaller one is *subthreshold*, a larger one *suprathreshold*. If the state point is anywhere on the phase plane to the left of the unstable part of the separatrix, the model has an instantaneous value of threshold for excitation equal to the horizontal distance from the state point to the separatrix. In the relatively refractory region, for instance, the threshold is higher than in the resting state. The depressed region is similar, but with somewhat smaller thresholds. In the enhanced region, the threshold is lower than at rest.†

When the state point is in the absolutely refractory region, it is above the separatrix and cannot reach the separatrix by shock stimulation. The model is therefore inexcitable.

The BVP model can be used to explain a number of other physiological properties of the nerve membrane: stimulation by constant currents to produce a single impulse or an infinite train of impulses, stimulation by rectangular positive current pulses of different durations, anodal break excitation after the end of a negative pulse, the abolition of an impulse by a negative pulse (this process also shows a threshold phenomenon), and the phenomenon of break reexcitation found by Cranefield and Hoffman in heart muscle.‡ Space will permit consideration here only of constant-current stimulation and impulse trains. For the other phenomena, see Ref. 24.

Next, instead of a brief shock, let I be a constant current of amplitude I_1 switched on at $t = 0$. I is now a step function of t instead of a delta function. Equations (3-6) describe the phase plane. In Fig. 3-2, $I_1 = 0$, but making I_1 positive raises the vertical isocline in the WV plane, as shown in Fig. 3-3. When the isocline is moved, the singular point and the whole pattern of trajectories shifts, including the separatrix. Let R denote the position of the singular point for $I_1 = 0$, and S its new position for a different value of I_1 . S also lies on the horizontal isocline, but above and to the right of R . If I is changed discontinuously at $t = 0$ from zero to a positive value I_1 , the initial point for the trajectory is R , which is no longer a singular point. Whether excitation occurs or not depends on whether the separatrix has moved far enough to pass point R . Figure 3-3 shows two cases, one subthreshold and one suprathreshold. In the latter, I_1 is just large enough to

† These states were studied experimentally in nerve after the application of subthreshold shocks by Erlanger and Blair, *Amer. J. Physiol.*, 99:108 (1931).

‡ P. F. Cranefield and B. F. Hoffman, *J. Gen. Physiol.*, 41:633 (1958); B. F. Hoffman and P. F. Cranefield: "Electrophysiology of the Heart," McGraw-Hill, New York, 1960.

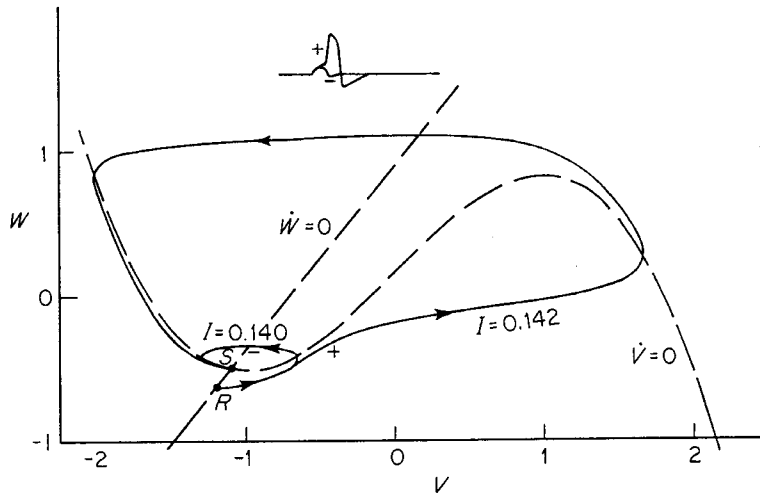


FIG. 3-3. BVP phase plane showing stimulation by step currents above ($I = 0.142$) and below ($I = 0.140$) rheobase. Vertical isocline ($\dot{V} = 0$) is raised by positive values of I . R = resting point, S = singular point.

carry the separatrix slightly past R , and an impulse occurs, with the trajectory (+) eventually returning to the new singular point S , which is +stable. Also shown in Fig. 3-3 is a trajectory (—) from a different phase plane, in which I_1 is slightly too small for excitation to occur. The intermediate value of I_1 for which the separatrix just passes through R is called *rheobase*, meaning the threshold amplitude of a step-current stimulus.

If the value of I_1 is increased still more, S passes onto the middle branch of the vertical isocline and becomes —stable. The stability of S is calculated as follows. Let V_S and W_S be the coordinates of S . Linearize Eqs. (3-6) about S , introducing the new variables v , w , and i :

$$\begin{aligned} v &= V - V_S & w &= W - W_S & i &= I - I_1 \\ \begin{bmatrix} \dot{v} \\ \dot{w} \end{bmatrix} &= \begin{bmatrix} 1 - V_S^2 & -1 \\ \phi & -b\phi \end{bmatrix} \begin{bmatrix} v \\ w \end{bmatrix} + \begin{bmatrix} i \\ 0 \end{bmatrix} \end{aligned} \quad (3-8)$$

The characteristic equation is (see Appendix B)

$$p^2 + [b\phi - (1 - V_S^2)]p + \phi[1 - b(1 - V_S^2)] = 0 \quad (3-9)$$

As V_S is varied, the stability type of the singular point S changes [1, 4, 5]. Analysis of the location of the roots of Eq. (3-9) on the complex plane shows that, depending on the value of V_S , the singular point S can be any of the following types:

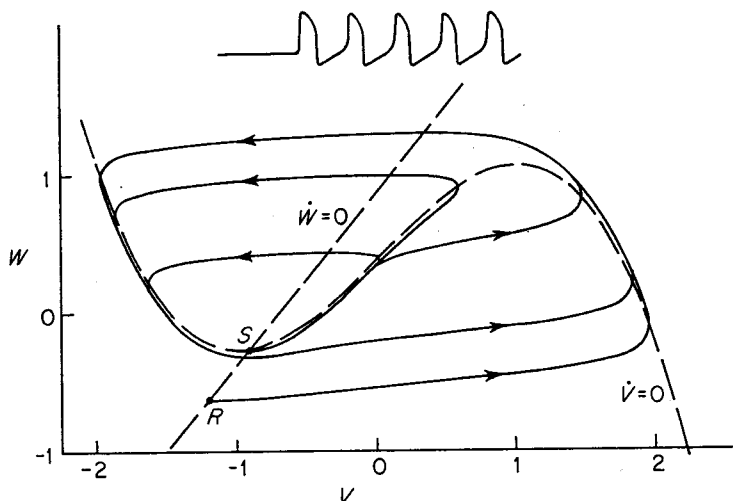
$0 < V_S^2 < 1 + b\phi = 0.593$	—stable node
$1 + b\phi - 2\sqrt{\phi} < V_S^2 < 1 - b\phi = 0.96$	—stable focus
$1 - b\phi < V_S^2 < 1 + b\phi + 2\sqrt{\phi} = 1.487$	+stable focus
$1 + b\phi + 2\sqrt{\phi} < V_S^2$	+stable node

The resting point R , where $V_S = V_R = -1.1994$, is a +stable focus. As I_1 is increased, S changes from a +stable to a -stable focus; this occurs on its middle branch, slightly past the minimum of the vertical isocline (V at minimum = -1). In this instance, the state point returning through the relatively refractory region is not stopped by S , but continues on past it to produce another impulse. This occurs repeatedly, and the trajectory approaches a +stable limit cycle (Fig. 3-4). An endless train of impulses results. As the amplitude of the current step is increased, the impulse frequency increases. Eventually, in this model, the impulses become symmetrical with the part of the waveform between the impulses; and further increases of I prolong the impulses and produce what a physiologist would call a "train of inverted impulses." Still higher values of I makes S +stable again.

One reason for introducing Young's model in Sec. 2 is to show its relation to the BVP model and thereby to the HH model (Sec. 4). This can best be done by comparing the phase planes in Figs. 2-1 and 2-2 with the corresponding ones for the BVP model in Figs. 3-2 and 3-3. The horizontal isocline of Young's model is straight instead of curved, as in the BVP model, but near the resting point the slopes of the isoclines, the position of the separatrix, and the general form of the trajectories are similar.

The property of the BVP model of producing only single impulses or infinite trains (which is shared also by the HH model described in Sec. 4) disagrees with the experimental results of Hagiwara and Oomura [44] from current-clamped squid axons, in which step-current stimulation produces either single impulses or finite trains of up to four impulses, but nothing resembling an infinite train. It is obvious that something is missing from

FIG. 3-4. BVP phase plane for step current $I = 0.4$, with a -stable singular point S and a +stable limit cycle. Inset above: endless train of action potentials. R = resting point.



the BVP model, namely, an adaptation variable of type 4 that has a long relaxation time compared to those of V and W .

An adaptation variable is provided by the Hill-Katz model, described in Sec. 2. The addition of such a variable to electronic models of the neuron [29] does produce finite trains, but the form of the action potentials obtained still does not satisfactorily duplicate the experimental curves of Hagiwara and Oomura [44]. This point is discussed further in Sec. 7, page 69.

To prepare for the explanation of the properties of the HH model in the next section, a somewhat different way of looking at the BVP model, the method of reduced systems, will now be described. First, the relaxation times (see Appendix B) of V and W are calculated as follows:

$$\begin{aligned}\tau_V &= \frac{1}{\partial \dot{V} / \partial V} = \frac{1}{1 - V^2} \\ \tau_W &= \frac{1}{\partial \dot{W} / \partial W} = \frac{-1}{b\phi}\end{aligned}\quad (3-10)$$

τ_V varies with V , but its magnitude exceeds that of τ_W only in two very small regions near $V = \pm 1$. V is thus a faster variable than W , on the average, V being of type 1 and W of type 3 (see Sec. 1).

In Eqs. (3-6) consider the limiting case in which ϕ is zero, making W zero and W constant at its resting value W_R . The model then becomes a one-variable system, the "V reduced model," describable by a one-dimensional phase space or V phase line. If this phase line is drawn horizontally through the resting point R in the VW phase plane (Fig. 3-2), its singular points are given by the intersection of that line with the vertical isocline ($\dot{V} = 0$). It has three singular points, two +stable with a -stable one between, forming a bistable system. The left-hand +stable point is at the resting state. The -stable point provides a threshold phenomenon of a different type from that occurring in the complete BVP model, where the trajectory dividing the sub- and suprathreshold conditions is the nonsingular threshold separatrix (see Sec. 5). The +stable point at the right corresponds to a +stable excited state, from which there is no recovery, in the reduced model.

Now consider the effect of changing the constant value of W . As W increases, the V phase line rises in the VW plane, and the positions of its singular points, determined by its intersections with the cubic curve, change. The -stable threshold point and the +stable excited point approach each other and, above a critical value of W , are absent, leaving only the +stable resting point.

Finally, instead of keeping W constant, let it vary according to its own differential equation (3-6). Since τ_W is, in general, much larger than τ_V , the behavior of the whole system can be approximated by that of the V reduced system during short time intervals. Initially, after a suprathreshold

brief shock, the state point in the reduced system approaches the $+s$ table excited point. Then, as W changes, the position of this point moves in the negative direction in V , and the state point follows it. When the excited singular point disappears, the state point then moves more rapidly back to the only remaining singular point, which is now at a V value negative to V_R . W starts decreasing again, and finally V and W return slowly toward their resting values.

How this alternative explanation of the BVP model leads to a better understanding of how the HH model works will become clear in the next section.

One effect not previously described for the BVP model is the decreased sharpness of threshold during the relative refractory period, a phenomenon that has been studied experimentally by Grundfest.[†] Although it is not evident in Fig. 3-2, the sharpness with which the trajectories veer away from the threshold separatrix decreases as one travels upward along the separatrix into the region of W values characteristic of relative refractoriness. This can be shown analytically by studying how τ_V at the $-s$ table singular point of the V reduced model varies with increasing W .

4. HODGKIN-HUXLEY MODEL OF THE SQUID GIANT AXON MEMBRANE

Description and Properties

In 1952 Hodgkin and Huxley published the first relatively complete mathematical model of a nerve membrane, that of the squid giant axon [31]. The HH model represents a basic advance in neuron theory; it contributes to our knowledge of the physical mechanisms of nerve excitation and conduction and gives the theory an adequate mathematical foundation for the first time. It is a remarkable achievement, combining difficult experimental technique with sound intuition and the intelligent use of applied mathematics. For this work Hodgkin and Huxley won a Nobel Prize in 1963.

Their model was obtained from an analysis of a series of voltage-clamp experiments, in which a short section of a squid axon was subjected to step changes in electric potential controlled by an electronic feedback circuit, connected through electrodes inside and outside the axon.[‡] This technique was first developed by K. S. Cole[§] and has since become one of the most important tools for the study of the nerve membrane.

By various techniques, including the use of solutions of varying sodium concentration in the solution bathing the axon, experimental curves of

[†] *Biol. Bull.*, 109:348 (1955).

[‡] A. L. Hodgkin, A. F. Huxley, and B. Katz, *J. Physiol.*, 116:424 (1952); A. L. Hodgkin and A. F. Huxley, *J. Physiol.*, 116:449, 473, 497 (1952).

[§] *Arch. Sci. Physiol.*, 3:253 (1949).

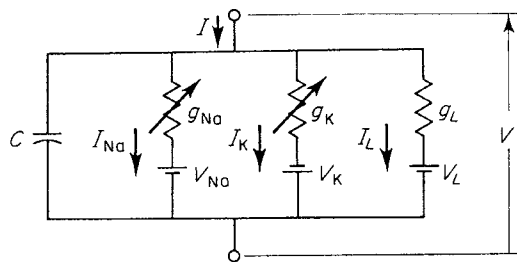


FIG. 4-1. Equivalent circuit of the Hodgkin-Huxley model, showing three ionic pathways, for sodium, potassium, and leakage ions, and the membrane capacitor. Redrawn from [31, fig. 1]. The g 's are conductances.

membrane current made during voltage clamp were separated into three components carried by different ions: sodium, potassium, and an unidentified "leakage" current. Empirical differential equations were derived to produce matching theoretical curves for a range of clamping potentials. On the basis of this separation, an equivalent circuit was derived (Fig. 4-1) for the membrane. The circuit contains, in addition to the three ionic current pathways, a membrane capacity, which had been measured earlier by H. J. Curtis and K. S. Cole.[†] The voltage-clamp technique eliminates the effect of the membrane capacity. The reason is that a capacity produces, in response to a step voltage, only a very brief current pulse which is finished before the ionic currents begin to change.

The main physical assumptions on which the model is based are as follows:

1. The current through the membrane is carried by sodium, potassium, and physically unidentified leakage ions.
2. The three ionic currents flow independently of one another.
3. The difference of concentration of each ion on the two sides of the membrane produces a chemical driving force on the ion which can be represented electrically by an emf equal to the ionic equilibrium potential, $(RT/F) \ln(C_i/C_o)$. C_i and C_o are the concentrations inside and outside, R is the gas constant, T is the absolute temperature, and F is the faraday.
4. The conductance of the membrane to potassium is determined by a variable of state n called the *potassium activation*, which is controlled by the variations of membrane potential. For sodium there are two variables, *sodium activation m* and *sodium inactivation h*. The physical nature of these three variables is still unknown. The leakage conductance is constant.
5. The membrane has a capacitance of $1 \mu F/cm^2$ in parallel with the three ionic pathways.

[†] *J. Gen. Physiol.*, 21:757 (1938).

6. The only effect of temperature is to change the rates of change of m , h , and n .

By using the variables defined in Appendix D, the HH equations for the standard temperature 6.3°C are written as follows:[†]

$$I = CV + I_i \quad (4-1)$$

$$I_i = \bar{g}_{\text{Na}}m^3h(V - V_{\text{Na}}) + \bar{g}_{\text{K}}n^4(V - V_{\text{K}}) + \bar{g}_L(V - V_L) \quad (4-2)$$

$$\dot{m} = \frac{m_\infty(V) - m}{\tau_m(V)} = \alpha_m(V)(1 - m) - \beta_m(V)m \quad (4-3)$$

$$\dot{h} = \frac{h_\infty(V) - h}{\tau_h(V)} = \alpha_h(V)(1 - h) - \beta_h(V)h \quad (4-4)$$

$$\dot{n} = \frac{n_\infty(V) - n}{\tau_n(V)} = \alpha_n(V)(1 - n) - \beta_n(V)n \quad (4-5)$$

Equations (4-1) to (4-5) are a special example of Eqs. (1-1), obtained by setting $\mu = 3$, $W_1 = m$, $W_2 = h$, $W_3 = n$.

A dot over a variable denotes its first derivative with respect to time t . Curves of the functions $m_\infty(V)$, $\tau_m(V)$, $h_\infty(V)$, etc., representing the steady-state values and relaxation times of m , h , n , are shown in Fig. 4-2. These curves are calculated from the rate-coefficient functions $\alpha_m(V)$, $\beta_m(V)$, $\alpha_h(V)$, etc., in Eqs. (4-3) to (4-5), which are defined as follows:

$$\begin{aligned} \alpha_m(V) &= \frac{0.1(25 - V)}{e^{0.1(25-V)} - 1} \\ \beta_m(V) &= 4e^{-V/18} \\ \alpha_h(V) &= 0.07e^{-V/20} \\ \beta_h(V) &= \frac{1}{e^{0.1(30-V)} + 1} \\ \alpha_n(V) &= \frac{0.01(10 - V)}{e^{0.1(10-V)} - 1} \\ \beta_n(V) &= 0.125e^{-V/80} \end{aligned} \quad (4-6)$$

The relaxation time and steady-state value for m in Eq. (4-3) are defined as follows:

$$\tau_m = \frac{1}{\alpha_m + \beta_m} \quad m_\infty = \alpha_m \tau_m \quad (4-7)$$

[†] Here the sign convention for V and I has been changed from that used in Hodgkin and Huxley's original paper, to agree with recent physiological practice, in which a depolarization of the membrane is taken to be positive. In this new convention, a cathodal current stimulating pulse I is positive, an anodal one negative.

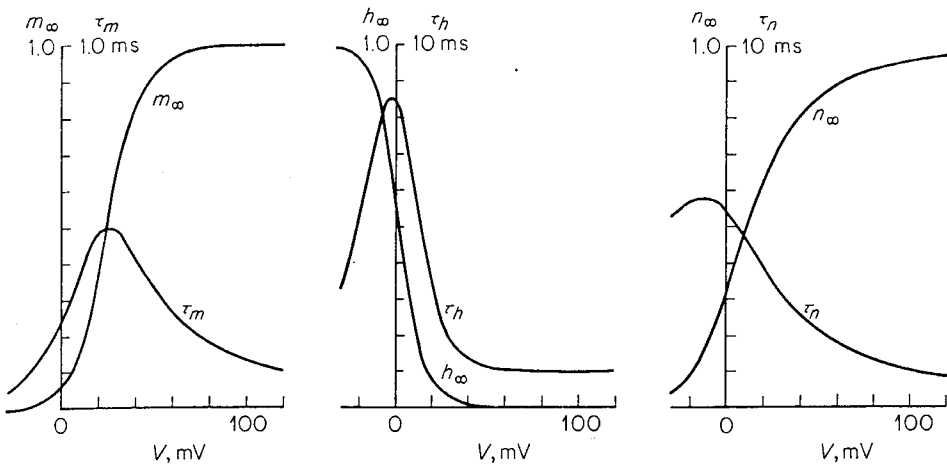


FIG. 4-2. Curves of the steady-state values and relaxation times of m , h , and n , as functions of V , for the HH model. [Redrawn from fig. 19 of K. S. Cole, *Biophys. J.*, 2 (no. 2, part 2), 101 (1962).]

and those for h and n in Eqs. (4-4) and (4-5) similarly. For temperatures different from 6.3°C , the right sides of Eqs. (4-3) to (4-5) are multiplied by the following factor:

$$\phi = 3^{(T-6.3)/10} \quad (4-8)$$

In a voltage-clamp experiment, the potential V is controlled as an input variable (step function), and the total current I and the separate terms of the ionic current I_i are measured. Since the equations were derived from voltage-clamp data, it is not surprising that they should predict such data well. What is more remarkable is that they should also reproduce experimental curves obtained under a different condition, that of a current clamp, in which the total current I is controlled as an input variable, and the membrane potential V is the output variable measured.

Figure 4-3a shows the results of stimulating the current-clamped model with instantaneous current shocks (proportional to delta functions) of different amplitudes. These resemble experimental curves closely.[†] Figure 4.3b shows the corresponding curves for m , h , and n . Many other sorts of experimental results have been successfully duplicated (see under "Verification and Criticisms" below), and this provides evidence for the essential correctness of this model.

[†] These theoretical action potentials duplicate those of the squid axon much better than do those of the BVP model (Fig. 3-2, inset). The latter have a conspicuous shoulder high on the descending phase, and the return of V to its resting value after the undershoot is too rapid. This is the result of having the relaxation time τ_w of the recovery variable w constant; τ_h and τ_n of the HH model, on the contrary, are functions of V , and are smaller near the peak of the action potential than near the resting potential (Fig. 4-2). This speeds the return from the peak and slows the recovery after the undershoot. For computing Fig. 3-2, ϕ [and therefore τ_w , Eqs. (3-10)] was adjusted to provide a compromise fit to an experimental action potential.

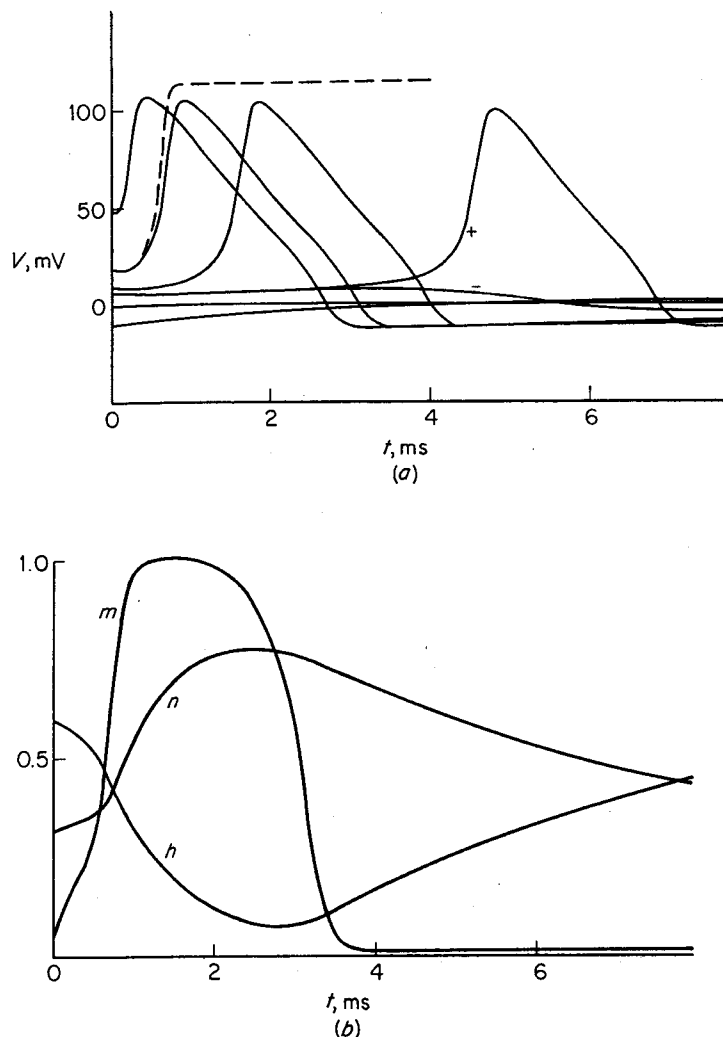


FIG. 4-3. (a) Solid curves: action potentials of the HH model for 6.3°C , following instantaneous current shocks of various intensities applied at $t = 0$. + and - correspond to stimuli slightly above and below threshold. Broken curve: plateau action potential of infinite duration for V_m reduced system (h and n constant at resting values), for $V(0) = 20$ mV. (b) Curves of m , h , and n corresponding to the action-potential curve for $V(0) = 20$ mV.

Other models based on different physical assumptions might, of course, behave similarly, and there is still debate among physiologists concerning the correctness of the HH model. The subsection, "Description and Properties," is concerned with analyzing the equations mathematically and explaining why they do behave like a real nerve membrane; the subsection, "Verification and Criticisms," mentions criticisms of the model.

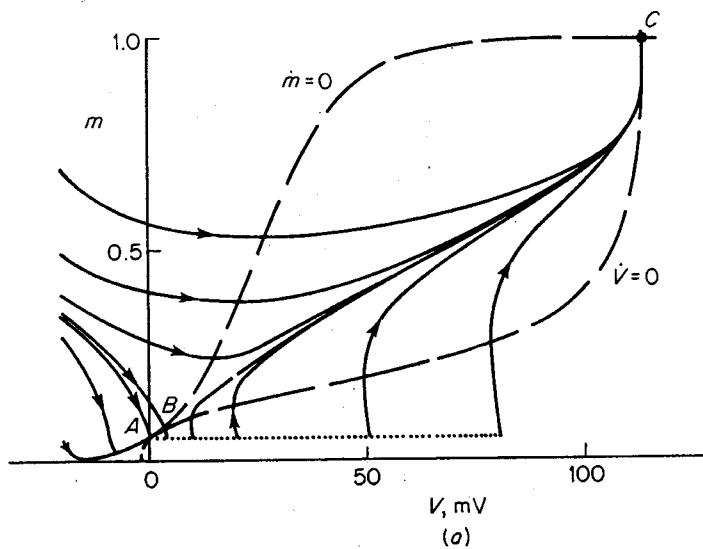
The analysis of the HH model is carried out by the method of reduced systems [25], described in Sec. 3. The four variables of state are arranged,

according to the order of magnitude of their relaxation times, into two classes: the fast variables V (type 1) and m (type 2), and the slow variables h and n (type 3). The relaxation time for V is simply the electrical RC "time constant" for the membrane, where R stands for the combined resistance of the sodium, potassium, and leakage pathways. The relaxation times for m , h , and n are τ_m , τ_h , τ_n . The latter three quantities are functions of V [Eqs. (4-6) and (4-7)], and the electrical time constant is a function of all four variables. RC and τ_m (0.1 to 1.0 ms) are roughly one-tenth as large as τ_h and τ_n (1.0 to 10 ms). If h and n , instead of being allowed to vary slowly according to their differential equations, are kept constant at their resting values (i.e., τ_h and τ_n made infinite), the remaining two differential equations for V and m form a Vm reduced system of equations.

The behavior of this system can be studied on the Vm phase plane (Fig. 4-4). The horizontal and vertical isoclines are defined by setting \dot{V} and \dot{m} equal to zero in Eqs. (4-1) and (4-3). The horizontal isocline is the curve of m_∞ as a function of V , while the vertical isocline is the Thévenin potential† V of the membrane as a function of m . The isoclines intersect at three singular points; a $+stable$ quiescent point A , a \pm stable threshold saddle point B , and a $+stable$ excited point C , making the system bistable. Stimulation by an instantaneous current shock displaces the state point from A along the horizontal dotted line toward the right. A threshold shock is one that displaces it just to the separatrix of the threshold saddle point (Fig. 4-4b). After a smaller (subthreshold) shock, the state point returns toward A . After a larger (suprathreshold) shock, it travels to the right and approaches C . In the Vm reduced system, excitation is followed by a plateau action potential of infinite duration in which V remains at the level determined by the excited singular point C (Fig. 4-3a, broken curve). The excited state is $+stable$ and there is no recovery, because the variables responsible for recovery from the excited state (h and n) are kept constant.

The next step in the analysis is to allow h and n to vary according to their differential equations (4-4) and (4-5). After excitation, V changes in a positive direction. Then, as seen from the curves of h_∞ and n_∞ in Fig. 4-2, h decreases and n increases. Giving h and n the values that they assume in the complete system of equations at various times during the impulse (Fig. 4-3b) raises the vertical isocline in the Vm phase plane (Fig. 4-5). Point C in the reduced system moves so as to make V , after it has increased to a maximum which is the peak of the spike, start decreasing. B and C approach each other, coalesce, and vanish, leaving only one singular point A in the reduced system, at a somewhat negative V value. Since A is $+stable$, it is

† The open-circuit potential, or emf, of the equivalent circuit appearing in the Thévenin-Pollard theorem [E. U. Condon and H. Odishaw, "Handbook of Physics," McGraw-Hill, New York, 1958].



(a)

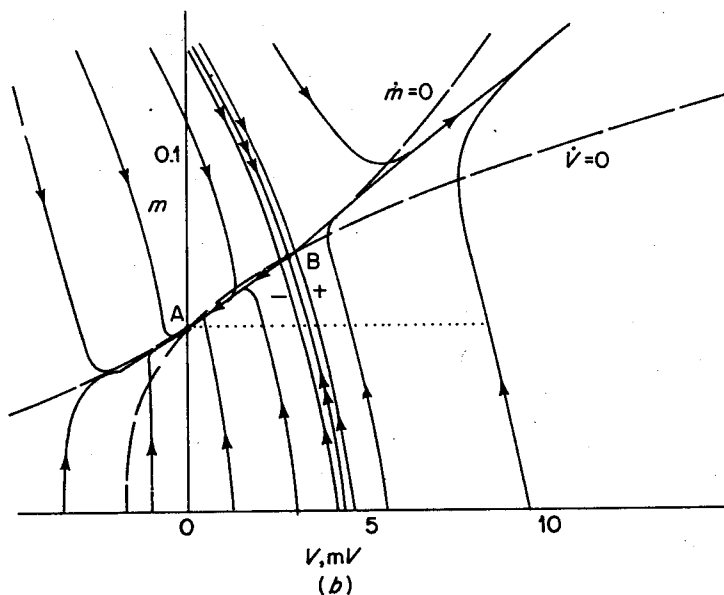


FIG. 4-4. (a) Phase plane for the HH V_m reduced system. Broken curves: horizontal ($\dot{m} = 0$) and vertical ($\dot{V} = 0$) isoclines. Solid curves with arrowheads: trajectories. Dotted line: locus of initial points following instantaneous shocks of various amplitudes. A , B , C : singular points. C is $+ \text{stable}$ and represents the excited state. (b) Region near A and B enlarged. A is the $+ \text{stable}$ quiescent point, B the $\pm \text{stable}$ threshold saddle point. A threshold shock displaces the state point along dotted line from A to the threshold separatrix (double arrowheads), which divides the all from the none trajectories (all-or-none law).

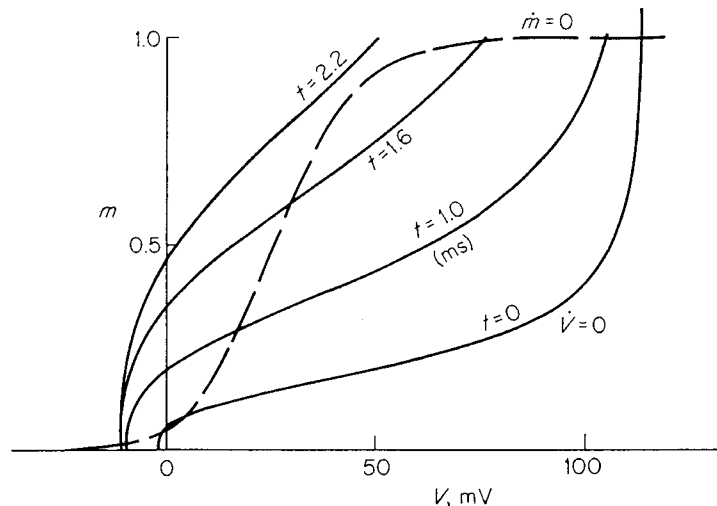


FIG. 4-5. Phase plane of the HH V_m reduced system. Broken curve: horizontal isocline. Solid curves: vertical isocline at various times during the action potential for which $V(0) = 20$ mV.

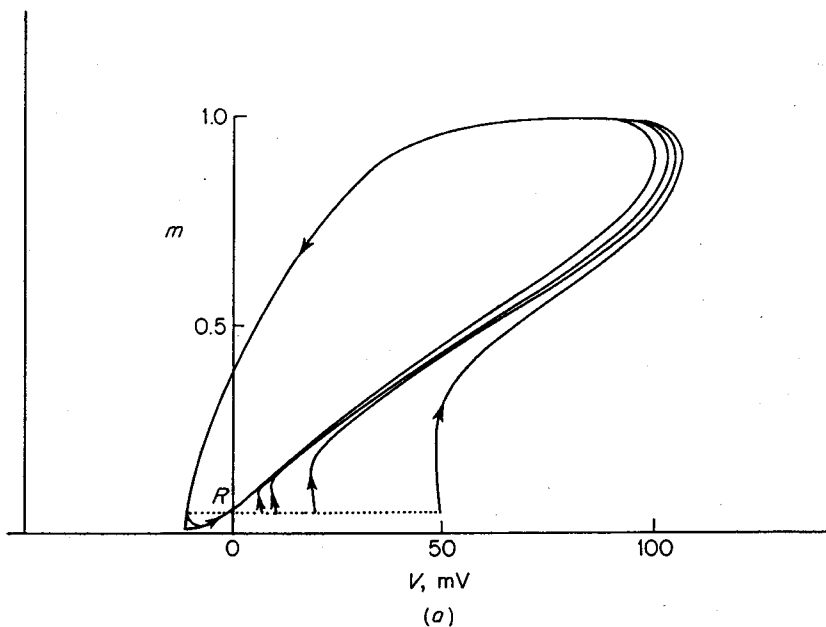
approached by the state point of the system, forming the undershoot at the end of the spike. The changes of V are shown in Fig. 4-3a; and the simultaneous changes of m , h , and n are shown in Fig. 4-3b. The trajectories in the V_m plane are shown in Fig. 4-6a. The enlarged detail in 4-6b shows that the form of the trajectories near threshold for the complete HH system is quite different from that for the V_m reduced system (Fig. 4-4b). If the stimulus is adjusted accurately enough with a digital computer, intermediate-sized action potentials result (see next subsection).

This section completes the description of the logical sequence of models of increasing complexity and accuracy: Blair,[†] Hill-Rashevsky-Young, BVP, and HH. They are all useful for simulating various aspects of neuronal function, the earlier ones being simpler to work with mathematically.

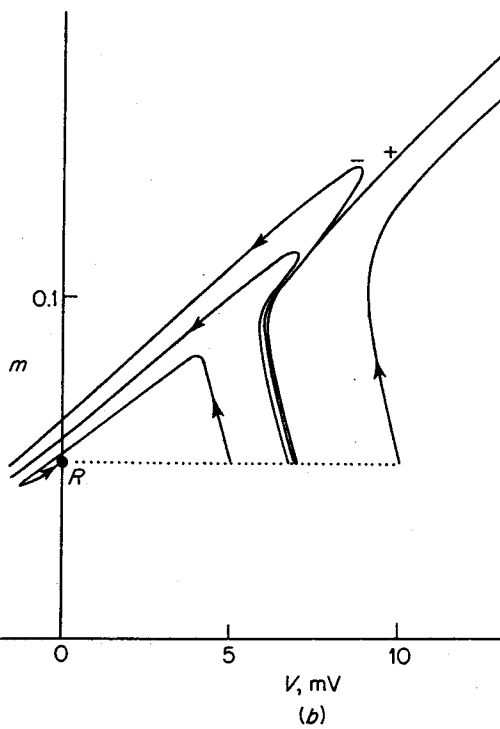
Verification and Criticisms

Like all theories, the HH model of the squid giant axon membrane requires testing. Predictions of the results of a variety of experiments have been made, starting from their equations, of which some do and some do not agree with experimental results. Agreement of predictions with experiment does not constitute a proof of the theory, since another theory might turn out later to provide equally valid predictions. This is particularly important to remember with regard to the HH equations, since the study of

[†] A one-variable special case of Young's model, without accommodation—see footnote in Sec. 2.



(a)



(b)

FIG. 4-6. (a) Trajectories projected from the HH $V_m h_n$ phase space into the V_m plane. (b) Detail near resting point R showing continuous type of threshold phenomenon.

two-variable models, of which the BVP models described in Sec. 3 are examples, suggests that it might be possible to find another set of equations, based on different physical assumptions from those of Hodgkin and Huxley, which would be a mathematical analog of the HH model and give equally good predictions. In the absence of any equally detailed competitor for the HH model, this accumulation of successful predictions provides convincing evidence in its favor. Nevertheless, the HH model is not universally accepted (see below); there are some predictions from the model which are definitely false, and these indicate that even if the model is basically valid, it needs to be modified.

In this subsection will be described some recent work on testing the model. (The physiological terms used below are mostly defined in Appendix A, and some of them have been discussed in Sec. 3 above.)

In their original paper [31], Hodgkin and Huxley, solving the differential equations by a numerical method with a desk calculator, found good agreement with experiment for the following phenomena: the membrane (space-clamped) action potential at two temperatures, the propagated action potential and velocity of conduction, the time course of impedance changes, net fluxes of potassium and sodium ions per impulse, absolute refractory period and recovery of excitability during the relative refractory period, the value of threshold to short current pulses, subthreshold responses, anodal break excitation, and subthreshold oscillations during a long rectangular current pulse.

Solving the equations with a desk calculator is so time-consuming that a digital computer was programmed to do this [18, 26]. Membrane action potentials computed at very near threshold show not only the variation of spike height to be expected from experiment, but also an apparently continuous gradation of responses of all intermediate heights between subthreshold active response and a full-sized action potential. This is an apparent violation of the all-or-none law which forbids such intermediate-sized responses and which is obeyed by the squid axon experimentally. The discrepancy is, however, only apparent, the result of the greater accuracy of the digital computer than that of a real axon. The latter is affected by spontaneous fluctuations that practically eliminate the possibility of intermediate responses in a normal axon. This is shown by the fact that when the stimulus is set just as threshold, a real axon gives action potentials for only a certain proportion of stimuli, whereas the equations, not containing any statistical variation, always give the same result.[†] No attempt has been made to include statistical variation in the equations in order to represent this phenomenon. This apparent disagreement between the model and

[†] The analog computer, with its electrical noise, also shows randomness near threshold, and is thus more lifelike than the digital computer.

experiment is therefore not serious, and the question of intermediate responses and the all-or-none law is discussed more fully below in Sec. 5.

The digital computations provide good agreement with experimental results for the strength-duration relation, and for additional propagated action-potential curves.

Some repetitions of the voltage-clamp experiments† have produced spatial nonuniformities of membrane potentials and oscillatory membrane currents of a form different from those on which Hodgkin and Huxley based their model. This failure of the space clamp has been shown to be the result of instability produced by more powerful membrane currents from axons in improved conditions, which can be overcome by the use of better technique: lower-resistance internal axial electrodes and a sufficiently short clamped length of axon.‡

During plateau action potentials obtained by injecting tetraethylammonium chloride (TEA) into a squid axon, the membrane exhibits bistable behavior, which has been taken as being contrary to the HH model [51]. However, if the equations are modified by increasing the relaxation time of variable n by a factor of 100 or so, plateau action potentials with bistable behavior result which closely imitate the experiments.§

Stimulation of the space-clamped squid giant axon membrane by a step current produces a finite train of up to four impulses [44]. For all constant-current strengths except those over a very narrow range [18, 26], however, the HH model produces an infinite train of impulses at a fixed frequency characteristic of the current strength [24]. A linearly increasing current used as a stimulus results in either a single impulse, or (for rates of increase of current below a threshold value) no impulse. The HH model, on the other hand, responds to such a stimulus by firing repetitively, the train of impulses lasting as long as the current is within that range of amplitudes for which infinite trains are produced by constant-current stimulation. Moreover, there is no threshold value of the rate of increase of the current, since any current that is linearly increasing, if it lasts long enough, will reach the range of repetitive excitation. As discussed under "Impulse Trains" in Sec. 7 these results indicate the need for an additional variable of type 4 to provide adaptation. Attempts to duplicate these experimental curves (unpublished) have so far been only partially successful.||

† I. Tasaki and A. F. Bak, *Amer. J. Physiol.*, **193**:301 (1958); I. Tasaki and C. S. Spyropoulos, *ibid.*, **309** (1958).

‡ Refs. 15, 17, 43; also R. E. Taylor, J. W. Moore, and K. S. Cole, *Biophys. J.*, **1**:161 (1960); J. W. Moore and K. S. Cole, chapter in "Physical Techniques in Biological Research," vol. 6, Academic, New York (1963).

§ Ref. 23; also E. P. George, *Nature*, **186**:889 (1960); E. P. George and E. A. Johnson, *Australian J. Exptl. Biol. Med. Sci.*, **39**:275 (1961).

|| For other comparisons of the HH model with experiment, see A. L. Hodgkin, "The Conduction of the Nerve Impulse," Liverpool University Press, Liverpool, 1964.

The effect of temperature on threshold in the HH model has been studied, assuming that temperature changes (1) the relaxation times of m , h , and n and (2) the conductance constants \bar{g}_{Na} , \bar{g}_K , and \bar{g}_L .[†] Curves of threshold to an instantaneous stimulus pulse versus temperature are U-shaped, whereas rheobase increases monotonically with temperature. These results agree qualitatively with experiment.

Although criticisms of the HH model have been made, no equally detailed model has been proposed as an alternative from which one might make predictions of experimental results for comparison. Until this is done, the HH model will remain as the best theoretical treatment of the squid giant axon membrane, though still subject to improvement, and a starting point for models for other excitable membranes.

Modifications‡

In this section are indicated a few ways in which the HH model can be modified or improved. For most experiments, a giant axon is dissected out of the squid, and then placed in a plastic chamber and circulated with solutions, but action potentials recorded from axons *in situ* in the living squid show larger resting potentials and more slowly decaying undershoots (positive after-potentials) than do either excised axons or the HH model.[§] Axons in the best condition have maximum sodium and potassium currents several times larger than those of the HH model [43]. Voltage-clamp records of potassium currents obtained after strong hyperpolarization show rises that are delayed more than those provided by the HH model.^{||}

A modification of the HH model for duplicating the results obtained with injected TEA has been mentioned under "Verification and Criticisms" above.

Computations by Huxley [32] on the effect of changes of calcium concentration on the squid axon were made by changing $m_\infty(V)$ to $m_\infty(V + \Delta V)$, $\tau_m(V)$ to $\tau_m(V + \Delta V)$, and $h_\infty(V)$, $\tau_h(V)$, $n_\infty(V)$, $\tau_n(V)$ similarly. Here $\Delta V = K \ln [(Ca)/(Ca)_n]$, (Ca) is the calcium concentration used, $(Ca)_n$ is the normal concentration, and $K = -9.32$ mV. These changes were based on experimental findings.[¶] The effect of these changes is to shift all the steady-state and relaxation time functions (Fig. 4-2) along the V axis to the right for an increase of (Ca) . These computations give resting and action potentials in good general agreement with experimental data.

[†] R. FitzHugh, *J. Gen. Physiol.*, **49**:989 (1966).

[‡] For a review article covering this section, see D. Noble, *Physiol. Rev.*, **46**:1 (1966).

[§] Work of Hodgkin and Keynes referred to in Fig. 3 of A. L. Hodgkin, *Proc. Roy. Soc. London*, **B148**:1 (1958); also J. W. Moore and K. S. Cole, *J. Gen. Physiol.*, **43**:961 (1960).

^{||} K. S. Cole and J. W. Moore, *Biophys. J.*, **1**:1 (1960).

[¶] B. Frankenhaeuser and A. L. Hodgkin, *J. Physiol.*, **137**:218 (1957).

E. B. Wright and T. Tomita† have used the HH equations to predict the effect of changing external sodium and potassium concentrations, by changing the values of V_{Na} and V_K . When this is done, it is necessary to compute new resting values of V , m , h , and n , to use as the initial conditions when computing the effect of applying a stimulus to a resting axon. Instead, Wright and Tomita used $V = 0$ and reset m , h , and n to arbitrary values for their initial conditions, thus introducing some error into their solutions.

There are other excitable membranes, both nerve and muscle, for which it would be useful to have mathematical models like that of Hodgkin and Huxley for the squid giant axon membrane. Since, with many of these, voltage-clamp techniques are less advanced or more difficult than for the squid axon, it is natural to take the HH model as a starting point and try to modify it to describe the new membranes, instead of starting all over again from the beginning to develop a new model. (This is a useful procedure, as long as its dangers are recognized—it might turn out later that a different cell operates on different principles than does the squid giant axon.)

The voltage-clamp technique has been applied to the single node of Ranvier of the myelinated nerve fibers of the frog and toad, and modifications of the HH model have been found which duplicates these results.‡ They differ from the HH equations (4-1) to (4-6) in the functions used for the steady-state values and relaxation times, in some of the constants, and in the fact that the terms on the right of the equation for I_i , representing the sodium and potassium currents, are nonlinear in V .

Before this improved model for the frog node appeared, the HH model was modified by only a change in the value of the membrane capacitance C and used in combination with a partial differential equation describing the myelinated axon, which is electrically equivalent to a passive linear leaky cable interrupted periodically by the excitable nodes [25]. The computed potential curves agree with experimental results.§

The HH equations have also been modified so as to describe the Purkinje muscle fibers of the heart.|| The principal change made is the addition of a potassium conductance with the characteristics of a rectifier directed inward across the membrane, in parallel with the potassium conductance g_K of the original HH model (Fig. 4-1). This change is in agreement with the observed fact that depolarization decreases the steady-state membrane conductance in these cells. τ_n is increased by a factor of 100 in order to slow the change of potassium conductance; this produces a plateau action potential similar

† *J. Cellular Comp. Physiol.*, **65**:211 (1965).

‡ Refs. 19, 21, 28, 41; also B. Frankenhaeuser and A. B. Vallbo, *Acta Physiol. Scand.*, **63**:1 (1965); B. Frankenhaeuser, *J. Physiol.*, **180**, 780 (1965).

§ A. F. Huxley and R. Stämpfli, *J. Physiol.*, **108**:315 (1949); J. Hodler, R. Stämpfli, and I. Tasaki, *Amer. J. Physiol.*, **170**:375 (1952).

|| D. Noble, *J. Physiol.*, **160**:317 (1962).

to that computed for the squid axon injected with TEA [24]. These changes, together with adjustment of various constants to agree with experimental data, provide a model that produces an infinite train of plateau action potentials and membrane impedance curves agreeing with those recorded from rhythmically beating heart-muscle fibers. Abolition and repetitive stimulation by applied current shocks are also successfully reproduced. This same model has been applied to a sheetlike membrane[†] to reproduce experimental current-voltage measurements made on the wall of the heart ventricle.[‡]

More recent experiments[§] indicate that the slow process governing the duration of the plateau is a slow sodium inactivation rather than a potassium activation. These results await mathematical description.

5. THRESHOLD PHENOMENA^{||}

A basic property of the nerve membrane is its possession of a threshold to stimulation. A stimulus above a certain value (the threshold) produces a nerve impulse. The electrical component of the impulse (which is a complex electrochemical process) is a pulse-shaped action potential lasting about a millisecond. Stimuli below threshold produce no impulse. The impulse is the indivisible unit of nervous activity, and its presence or absence in an axon, according to the magnitude of the stimulus, constitutes the threshold phenomenon. The *all-or-none law* of physiology states that an impulse occurs either full size or not at all, with no intermediate responses possible. The height of the action potential and its time of occurrence may vary, depending on the magnitude of the stimulus, but not so much as to make identification doubtful. On the other hand, nonthreshold *graded responses* which do not obey the all-or-none law, do occur under certain conditions, and mathematical models can also represent these.

Some of the properties of threshold phenomena can be shown with a *stimulus-response curve* (*SR* curve). The stimulus strength S is plotted horizontally, and some variable R serving as a measure of the response (usually the height or area of the action potential) is plotted vertically. Two types of *SR* curve are shown in Fig. 5-1. The discontinuous type (e.g., for a space-clamped nerve membrane obeying the all-or-none law) has a discontinuous jump in R at the threshold value S_T of S (left). A membrane exhibiting a graded response (e.g., in the relatively refractory state or in narcosis) has a *SR* curve which is continuous (right). In this instance the

[†] D. Noble, *Biophys. J.* **2**:381 (1962).

[‡] E. A. Johnson and J. Tille, *Australian J. Exptl. Biol. Med. Sci.*, **38**:509 (1960); *Nature*, **192**:663 (1961).

[§] K. A. Deck and W. Trautwein, *Pfluegers Arch. Ges. Physiol.*, **280**:63 (1964).

^{||} Ref. 22.

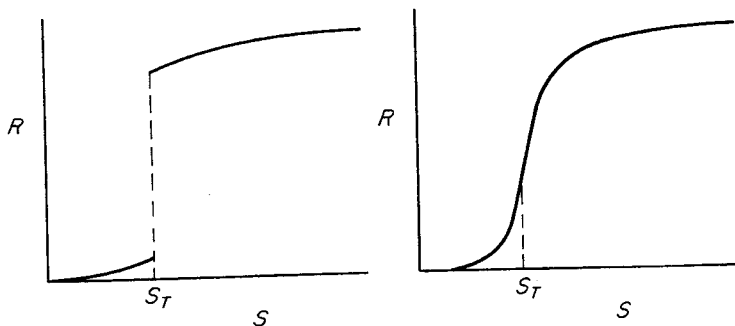


FIG. 5-1. Sketches of the two types of stimulus-response (SR) curve, in which response R is plotted against stimulus S . Left: discontinuous type, having a step discontinuity at a threshold value S_T of S . Right: continuous type, in which the maximum slope (at $S = S_T$) is a measure of the sharpness of the threshold phenomenon.

point of maximum slope may be taken as the position of the threshold value S_T . The maximum slope of the continuous type is called the sharpness of the threshold phenomenon; the sharpness of the discontinuous type may be taken as infinite. Although the two types of SR curve are mathematically distinct, a continuous SR curve obtained by computation may have a maximum slope so great that it is in practice indistinguishable from a discontinuous one.

The mathematical representation of threshold phenomena, of the all-or-none law and of graded responses is the subject of this section.[†] A threshold phenomenon is essentially a nonlinear one. A stable resting state and a threshold phenomenon cannot occur together in a system described by linear differential equations, which can have at most one isolated singular point. Three distinct mathematical types of threshold phenomena occur in nerve models. These will be described for two-variable models with a phase plane, but they can be generalized to phase spaces of any dimension.[‡]

Saddle-point Threshold Model

Figure 4-4b shows a threshold saddle point (point B). A saddle point in a phase plane is a \pm stable singular point having one real positive and one real negative eigenvalue. It has a pair of $+$ stable trajectories and a pair of

[†] A detailed theoretical analysis of threshold phenomena and stimulus-response curves by D. Noble and R. B. Stern, *J. Physiol.*, 187:126 (1966), unfortunately appeared too late to be discussed in this chapter.

[‡] See Appendix B and the references on stability theory in the bibliography. Much of the theoretical work on nonlinear differential equations has been directed toward the problem of predicting the existence of oscillations, which is important in engineering design, but the representation of threshold phenomena has received much less attention. Oscillations in nerve models are considered in Sec. 7.

—stable ones; in Fig. 4-4b these are the curves that touch the saddle point B and have arrowheads pointing toward or away from the saddle point. All the other trajectories in the neighborhood of the saddle point are hyperbolic (i.e., they do not approach the saddle point, but pass by it, looking somewhat like members of a family of hyperbolas near their common center). The curve composed of the two +stable trajectories and the saddle point itself, called the *threshold separatrix*, is of particular importance. In Fig. 4-4b it is denoted by double arrowheads. Consider the set of trajectories that start from points on the dotted line, the locus of initial points, following an instantaneous shock stimulus of adjustable amplitude. As the initial point is moved along this locus across the separatrix, the geometric form of the corresponding trajectories undergoes a sudden change. The separatrix forms the boundary between two classes of trajectory with qualitatively different properties. By letting two classes of trajectory correspond to the all and the none responses of the all-or-none law, one can use a saddle point to describe a threshold phenomenon mathematically. The corresponding SR curve is of the discontinuous type (Fig. 5-1, left).

The apparent discontinuity between the trajectories of the two classes seems to contradict a well-known theorem, but actually does not; a brief discussion of this point will help to clarify the nature of a saddle-point threshold model. From the Cauchy-Lipschitz theorem [4] on the existence and uniqueness of the solution of an analytic ordinary differential equation in t , one can show that the solution is a continuous function not only of t , but also of the initial conditions. Therefore, if one moved the initial point continuously along the locus of initial points, one would expect the corresponding trajectory to change continuously instead of discontinuously, as predicted by the all-or-none law. Nevertheless, this contradiction is only apparent, not real. For definiteness, consider an n -dimensional phase space with coordinates x_1, x_2, \dots, x_n , and focus attention on variable x_1 . The existence of the solution of the differential equation defines x_1 as a continuous function of t and also of the initial point P in the phase space, e.g., $x_1 = g(t, P)$; that is, at any fixed value of t , x_1 varies continuously with P . In a saddle-point threshold model, the discontinuous transition from an impulse to no impulse cannot, therefore, take place at any finite value of time. Instead, as the stimulus approaches its threshold value from above, the action potential occurs later and later, retreating, as it were, to infinite time, when the transition to the subthreshold response takes place.

The reason for this behavior can be made clearer as follows. A phase point moving along the separatrix approaches the saddle point as t approaches infinity. Phase points moving along neighboring hyperbolic trajectories, corresponding to stimuli very near threshold, come close to the saddle point, where they move so slowly that an arbitrarily large value of t can be reached before the phase point finally veers away from the saddle point.

For the suprathreshold case, this delays the appearance of the impulse for a correspondingly long time.

The physiological term for the time from the beginning of a stimulus pulse to the appearance of an action potential (measured, say, as the time at which it reaches half its full height), is *latency*. The above discussion can be summed up by saying that a saddle-point threshold model has an unbounded latency. This is in contradiction to experimental results, where there is usually a definite limit to the values of latency that are measured.

The notion of a saddle point can be generalized to phase spaces of other dimensions (n) than two. On a phase line ($n = 1$), a threshold saddle point is simply a $-$ -stable singular point, and the separatrix is the singular point itself. In a three-dimensional phase space, a threshold saddle point has for its separatrix a two-dimensional surface passing through it, composed of trajectories that approach the saddle point as t approaches infinity. A one-dimensional curve intersects this surface at the saddle point and is composed of two trajectories that approach the saddle point, one from each side of the separatrix, as t approaches infinity. The other nearby trajectories are divided by the separatrix into two classes, along which a state point first travels approximately toward the saddle point, and then veers away from it in one of two general directions (roughly parallel to the two trajectories in the one-dimensional curve), depending on which side of the separatrix it is. In an n -dimensional phase space, a threshold saddle point is a singular point that has one real positive eigenvalue, all its other eigenvalues having negative real parts. This guarantees that there is an $(n - 1)$ -dimensional manifold (or hypersurface) in the phase space passing through the singular point composed of $+$ -stable trajectories [4]—this manifold is the separatrix. Saddle-point threshold phenomena appear in the BVP (V) reduced system and in the HH (V_m) reduced system, in which recovery (type-3) variables are absent, but not in the complete models (see next subsection).

Continuous Threshold Model†

In this type, as in the saddle-point type, there are two classes of trajectories, separated by a separatrix. In a phase plane ($n = 2$), this separatrix is composed of one trajectory (instead of two trajectories and a singular point as in the saddle-point type). Figures 3-2 and 4-6b show continuous threshold phenomena. A state point moving along a trajectory neighboring the separatrix tends to veer sharply to one side or the other away from it. This property of sharp veering of neighboring trajectories does not usually extend over the whole length of the separatrix trajectory; the latter has instead a certain section over which the veering is very marked, becoming less so near the ends of this section, which is therefore not precisely delimited. The

† Called “quasi-threshold phenomenon” (QTP) in Ref. 22.

choice of trajectory as separatrix is not unique, as in the saddle-point type, but is made so as to have approximately the longest possible section where local veering occurs.[†] As before, if $x_1 = g(t, P)$, x_1 varies continuously with P , but, because of the absence of a saddle point, the transition from an impulse to no impulse occurs at a finite time. Such a model therefore has a bounded latency, in contrast to the saddle-point type. This transition takes place over a nonzero interval of stimulus strengths, giving a continuous *SR* curve (Fig. 5-1, right). The value of threshold can be taken anywhere in this interval, say at the point of maximum slope. Since a continuous threshold model has a continuous *SR* curve, it is useful in describing a graded response, if its maximum slope is not too great. It is also possible for the maximum slope to be so large that for ordinary computing accuracies it appears to be discontinuous, and a highly accurate threshold value can be computed. It can therefore serve to represent a neuron obeying the all-or-none law.

By appropriate change of parameters in the model, the *SR* curve can change from apparently discontinuous to obviously continuous, and thus represent a neuron which can have a range of threshold sharpness, according to its condition. This property of varying in sharpness, from a graded response to an all-or-none response, according to the value of certain parameters of the system, is not possessed by a saddle-point threshold model. The distinction between an all-or-none and a graded response is also physiologically not absolute. For instance, in the early part of the relative refractory period following an impulse the response to a second stimulus is graded, but becomes gradually less so, the later the stimulus is applied. The threshold phenomenon becomes sharper and sharper until it returns to the normal all-or-none response of the resting neuron.[‡]

Continuous threshold phenomena appear in the complete BVP and HH models. The fact that reduced systems of both models have saddle-point threshold phenomena indicates a connection between the two types. A continuous threshold phenomenon can arise from a saddle point which exists in a reduced subsystem and which slowly changes its position in the phase space of that subsystem as a result of the changes of variables not in the subsystem.

Discontinuous Threshold Model

In the models of excitation of Rushton and of Offner, Weinberg, and Young, discussed in Sec. 6 below, a switch in the equivalent circuit of the model closes when the membrane potential reaches a certain critical value.

[†] If any reader is bothered by the lack of rigor in this discussion, I sympathize with him, but this is the sort of applied mathematical reasoning which I find useful in thinking about threshold models. More rigorous definitions are needed here.

[‡] C. Y. Kao and H. Grundfest, *Biol. Bull.*, **109**:348 (1955).

Mathematically, this corresponds to a discontinuity in the functions appearing in the differential equations of the model. Such a discontinuity forms the basis of a third type of threshold phenomenon. In the two-variable models of Hill and of Rashevsky and of others, discussed in Sec. 2, the differential equations are linear until the state point reaches a certain line, the barrier of excitation, in the phase plane. If the state point reaches this barrier, its velocity changes, though in a way that is not made explicit in the equations of the model.[†] However, if a different analytic function is assumed to define the velocity of the state point on the other side of the barrier, then there will exist a discontinuity at the barrier, either of the function or of some of its derivatives. Thus the threshold phenomena in these models may also be included under the discontinuous type.

6. THE PROPAGATED NERVE IMPULSE

So far this chapter has dealt with a simplified case of excitation which occurs only in the experimental condition of space and current clamp: the membrane current and potential of an axon vary with time but not with distance, and the current is a rectangular pulse in t . In an axon in a living animal or experimentally in an excised axon (without space clamp), there are circulating currents that cross the membrane and flow lengthwise inside and outside the axon, and the membrane current and potential vary with distance as well as with time. The circulating currents provide the mechanism of conduction. An excited region of axon stimulates an adjacent unexcited region, and this process is repeated continuously along the axon to form a traveling impulse. Trains of such impulses, conducted along axons, transmit messages between different parts of the nervous system.

One can set up a model of an axon by combining the equations for an excitable membrane with the differential equations for an electrical core conductor cable. This can be done in two ways: for a continuous axon having its whole surface excitable, such as the squid axon or a vertebrate unmyelinated axon, or for a noded (myelinated) axon of a vertebrate, which is excitable only at certain spots—the nodes of Ranvier—spaced evenly along an otherwise electrically passive axon [40]. For simplicity, the cell body and the terminal branching of the axon are ignored, and the axon is assumed to be an infinitely long cylinder.

Continuous Axon

Axon equations

The whole surface of this axon consists of excitable membrane. Inside the membrane is the semifluid conducting axoplasm; outside, a conducting

[†] A similar assumption is made in the neuron model of P. P. Nelson, *Bull. Math. Biophys.*, 24:159 (1962).

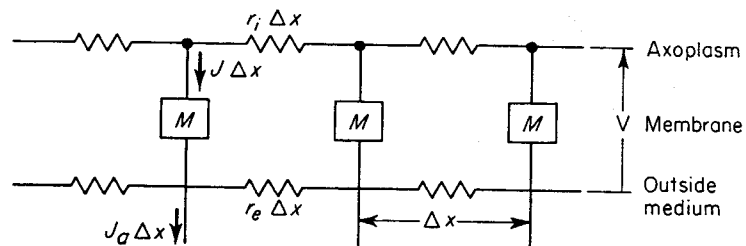


FIG. 6-1. Equivalent circuit of a continuous axon. M is the equivalent circuit of a section of membrane of length Δx .

salt solution. Figure 6-1 gives an equivalent ladder circuit in which the longitudinal dimension is divided into intervals of length Δx , and the internal and the external volume conductors are replaced by strings of resistors in series. The rungs of the ladder (labeled M) represent elements of membrane of length Δx . J and J_a are current densities per unit *length* of axon: J representing the total membrane current, and J_a the stimulating current applied externally through electrodes. In the limit, as Δx approaches zero, one obtains the following equation (for a more detailed derivation, see Ref. 40, p. 231, Eq. 7)

$$\frac{\partial^2 V}{\partial x^2} = (r_e + r_i)J - r_e J_a \quad (6-1)$$

For a cylindrical axon of diameter d , the current density per unit area of membrane is $I = J/\pi d$. Using this relation and Eq. (6-1), substitute for I in the general membrane equations (1-1) to get:

$$\begin{aligned} \frac{\partial V}{\partial t} &= \frac{I - I_i}{C} = \frac{1}{C} \left[\frac{1}{\pi d(r_e + r_i)} \left(\frac{\partial^2 V}{\partial x^2} + r_e J_a \right) - I_i \right] \\ \frac{\partial W_j}{\partial t} &= F_j(V, W_1, \dots, W_\mu) \end{aligned} \quad (6-2)$$

$$\begin{aligned} x \rightarrow \pm \infty \quad 0 \leq t < \infty: \quad &V \rightarrow V_R \quad W_j \rightarrow W_{jR} \\ t = 0 \quad -\infty < x < \infty: \quad &V = V_R \quad W_j = W_{jR} \end{aligned}$$

For the BVP equations (3-6), Eq. (6-2) becomes [assuming for simplicity that $C = 1$, $r_e = 1$, $\pi d(r_e + r_i) = 1$]

$$\frac{\partial V}{\partial t} = \frac{\partial^2 V}{\partial x^2} + J_a + V - \frac{V^3}{3} - W \quad (6-3)$$

$$\frac{\partial W}{\partial t} = \phi(V + a - bW)$$

The mathematics is simplified greatly by ignoring the transient behavior and considering only the steady-state case of the uniformly propagated impulse with velocity θ . Assume that

$$s = t + \frac{x}{\theta} \quad (6-4)$$

$$V(x,t) = V^*(s) \quad W_j(x,t) = W_j^*(s)$$

The partial derivatives in Eqs. (6-2) become

$$\begin{aligned} \frac{\partial V}{\partial t} &= \frac{dV^*}{ds} & \frac{\partial^2 V}{\partial x^2} &= \theta^{-2} \frac{d^2 V^*}{ds^2} \\ \frac{\partial W_j}{\partial t} &= \frac{dW_j^*}{ds} \end{aligned} \quad (6-5)$$

Substituting from Eqs. (6-5) into Eqs. (6-2), letting $J_a = 0$, and omitting the asterisks gives a set of ordinary differential equations, with boundary conditions as follows:

$$\begin{aligned} \frac{d^2 V}{ds^2} &= K \left(\frac{dV}{ds} + \frac{I_i}{C} \right) \\ \frac{dW_j}{ds} &= F_j \end{aligned} \quad (6-6)$$

$$V \rightarrow V_R \quad W_j \rightarrow W_{jR} \quad \text{for } s \rightarrow \pm \infty$$

where

$$K = C\pi d(r_e + r_i)\theta^2 \quad (6-7)$$

Equations for the uniformly propagated impulse in the BVP and HH axon can be obtained from Eqs. (6-6) by making the substitutions for I_i and F_j , described in Secs. 3 and 4.

In order that the boundary conditions in Eqs. (6-6) be met, K must be set to some critical value K_c . This in turn determines θ , by Eq. (6-7). How this is done, and the difficulties encountered in computing solutions, are discussed below, for the special case of Eqs. (6-19).

Propagation without recovery

The differential equations for an axon can be simplified further by eliminating recovery, i.e., by making the type-3 variables constant and dealing with a reduced system in the remaining type-1 and 2 variables. Once the membrane is excited, V approaches its excited level and produces an infinitely long-lasting plateau action potential. This simplification provides good enough approximation for some purposes, and is easier to handle mathematically than a complete model.

Rushton's model.† The equivalent circuit for the membrane element consists of three elements in series, a resistor, an emf, and a resistor-shunted capacitor. When the charge on the capacitor reaches a threshold value, the emf disappears, causing excitation. This type of circuit does not belong in the general class considered here and will not be described in detail, but two theoretical concepts used by Rushton are worth mentioning, *liminal length* and *safety factor*.

If a cathodal current is applied to the model through a stimulating electrode, excitation takes place over an interval of distance surrounding the electrode and of a length depending on the strength of the stimulus. In order for an impulse to arise and be propagated away from the electrode, this interval must be longer than a certain value, called the liminal length. Otherwise the impulse dies away without propagation. Moreover, if the emf, E , is reduced below a certain value, E_0 , propagation fails, no matter how great the stimulus is. Rushton defines the safety factor to be $E/E_0 - 1$. The safety factor must exceed zero for propagation to occur.‡ Rushton calculated a value of 3 for the safety factor from his model. The safety factor is thus a measure of the excess energy available over the minimum value necessary for propagation.

Offner, Weinberg, and Young's model. [37] This is a special case of the general model [Eq. (1-1)]. The triggered event representing excitation is a decrease of a resistance rather than a change of emf. This assumption is in accordance with the discovery of Cole and Curtis (see Sec. 7, page 65) that the principal electrical change in the membrane during the nerve impulse is a decrease of the membrane resistance by a factor of about 40. One theoretical conclusion from this model is that the conduction velocity varies as the square root of the diameter of the axon, a result that is derived more generally below.§

BVP model. If recovery is omitted, the equation for the uniformly propagated action potential can be solved exactly by a method due to A. F. Huxley (unpublished personal communication). In equations (6-3), let $\phi = 0$ and $W = W_R$, to get

$$\frac{d^2V}{ds^2} = K \left(\frac{dV}{ds} V + -\frac{V^3}{3} + W_R \right) \quad (6-8)$$

† W. A. H. Rushton, *Proc. Roy. Soc. London*, **B124**:210 (1938).

‡ Other authors, e.g., Tasaki [50], define the safety factor as equivalent to Rushton's quantity plus one, so that it must exceed one for conduction to occur. This latter definition corresponds to Schmitt and Schmitt's "safety ratio" (see below).

§ A similar piecewise-linear model without recovery has been studied by A. C. Scott, *IRE Trans.*, **CT-9**:192 (1962). In a later paper by Scott [*Bull. Math. Biophys.*, **26**:247 (1964)] the plus sign in Eq. (14) should be a minus. When this error is corrected, a contradiction results [the left side of Eq. (14) is a positive quantity, the right side negative], which invalidates the approximation method.

If one uses the relation $W_R = V_R - V_R^3/3$, Eq. (6-8) is equivalent to

$$\frac{d^2V}{ds^2} = K \left[\frac{dV}{ds} + \frac{(V - V_R)(V - V_1)(V - V_2)}{3} \right] \quad (6-9)$$

where

$$V_1 = -V_R \frac{(1 - \sqrt{D})}{2} = -0.7863$$

$$V_2 = -V_R \frac{1 + \sqrt{D}}{2} = 1.9857 \quad (6-10)$$

$$D = \frac{12}{V_R^2} - 3 = 5.3417$$

Let $P = dV/ds$. Then $d^2V/ds^2 = P dP/dV$, and Eq. (6-9) becomes

$$\frac{dP}{dV} = K \left[1 + \frac{(V - V_R)(V - V_1)(V - V_2)}{3P} \right] \quad (6-11)$$

As a trial solution, assume that

$$P = -A(V - V_R)(V - V_2) \quad (6-12)$$

where A is a positive constant. This equation describes a trajectory in the VP phase plane which is a parabolic arc connecting a saddle point at $V = V_R$ with another at $V = V_2$. Substituting Eq. (6-12) into Eq. (6-11) gives

$$A(2V - V_R - V_2) + K \left(1 - \frac{V - V_1}{3A} \right) = 0 \quad (6-13)$$

If this linear equation in V is to hold for all V , the sum of the constant terms and the sum of the terms in V must each equal zero. This gives a pair of simultaneous equations in K and A . Solve them, using the fact, from Eqs. (6-10), that $V_R + V_1 + V_2 = 0$, to get

$$A = \frac{V_R + V_2 - 2V_1}{6} = -\frac{V_1}{2} \quad (6-14)$$

In order that A be positive, as assumed, it is necessary that

$$V_1 < 0.5(V_R + V_2)$$

or, equivalently, $V_1 < 0$. In Eq. (6-7), assume for simplicity that

$$C\pi d(r_o + r_i) = 1$$

so that $K = \theta^2$. Then the conduction velocity is

$$\theta = \pm \sqrt{\frac{3}{2}} V_1 \quad (6-15)$$

The \pm sign indicates that the impulse can travel either to the left or to the right along the x axis. Substitute from Eqs. (6-10), and let θ be positive. If $V_R = -1.1994$ (for $a = 0.7$ and $b = 0.8$, as in Sec. 3),

$$\theta = -\sqrt{3/8}V_R(\sqrt{12V_R^{-2} - 3} - 1) = 0.963 \quad (6-16)$$

Finally, Eq. (6-12) can be solved to give the form of the action potential:

$$\begin{aligned} V &= \frac{V_R + V_2 e^{[A(V_2 - V_R)s]}}{1 + e^{[A(V_2 - V_R)s]}} \\ &= V_R + \frac{V_2 - V_R}{2} \left[1 + \tanh \frac{A(V_2 - V_R)s}{2} \right] \end{aligned} \quad (6-17)$$

This is an increasing sigmoid function of s , which describes an infinitely long-lasting plateau action potential without recovery.

This model can be used to predict the effect of a shunt conductance g_s across the membrane, by subtracting the term $g_s(V - V_R)$ inside the parenthesis on the left side of Eq. (6-8). The conduction velocity becomes

$$\theta = -\sqrt{3/8}V_R[\sqrt{12(1 - g_s)V_R^{-2} - 3} - 1] \quad (6-18)$$

Equation (6-18) predicts that θ decreases with increasing g_s , and becomes zero at $g_s = g_K$, where $g_K = 1 - V_R^2/3$. For greater values of g_s conduction is impossible. The action-potential height, which is $V_2 - V_R$ ($= 3.19$) for $g_s = 0$, becomes $-2V_R$ ($= 2.40 = 75$ percent of 3.19) at $g_s = g_K$. The height thus decreases only 25 percent before disappearing abruptly when conduction is blocked by increasing g_s .

These predictions are qualitatively similar to the results of unpublished computations of conduction velocity for the HH equations with recovery. Experimentally, in an axon that has been removed from the squid and is deteriorating in the course of an experiment, the conducted impulse gradually decreases in height and conduction velocity, and then abruptly disappears. The above theoretical treatment suggests the possible explanation that deterioration may be the result of a decrease in membrane resistance.

Propagation with recovery

The inclusion of type-3 variables complicates the equations for propagation.

BVP model. Let ϕ be positive. Proceeding as before, one obtains from Eqs. (6-3) the following ordinary differential equations and boundary

conditions for a uniform traveling impulse:

$$\begin{aligned} \frac{d^2V}{ds^2} &= K\left(\frac{dV}{ds} - V + \frac{V^3}{3} + W\right) \\ \frac{dW}{ds} &= \phi(V + a - bW) \\ V \rightarrow V_R \quad \frac{dV}{ds} \rightarrow 0 \quad W \rightarrow W_R \quad \text{for } s \rightarrow \pm\infty \end{aligned} \tag{6-19}$$

Analysis by the methods of Appendix B shows that in the $(V, dV/ds, W)$ phase space there is just one singular point R , at the resting point $(V_R, 0, W_R)$. Since it has one positive real eigenvalue and two with negative real parts, it is \pm stable; it is a threshold saddle point.[†] Through it pass a one-dimensional curve containing two $-$ stable trajectories, and a two-dimensional surface consisting only of $+$ stable trajectories. In order to make the solution approach R as $s \rightarrow -\infty$, an initial condition is chosen close to R . In general, the solution of Eqs. (6-19) is such that all three variables eventually start increasing without limit. In order that the solution approach R as $s \rightarrow +\infty$, it is necessary (1) to have the initial condition on the correct side of the $+$ stable surface and (2) to adjust the parameter K to a critical value K_c . It is impossible with a computer to adjust K to K_c exactly, but two bracketing values can be found very close together such that V tends toward $+\infty$ for one of them and $-\infty$ for the other. K_c lies between the bracketing values. With $K = K_c$ approximately, it is possible to compute the conduction velocity θ to sufficient accuracy, even with the relatively inaccurate analog computer. Since, however, the solutions obtained for the two bracketing values of K tend toward $\pm\infty$, and with the analog computer this separation from the desired (bounded) solution occurs in most instances before the peak of the action potential, one cannot obtain even the action-potential height in this way. For this the greater accuracy of a digital computer is needed (Fig. 6-2a). Even then the separation of any pair of bracketing solutions prevents one from obtaining a reasonably complete curve of the action potential directly. To do this with a digital computer, it is necessary to use the method of repeated continuation [18, 26]. At a value of s where the separation between the pair of bracketing trajectories grows beyond a preassigned limit, the solution is stopped, and a pair of starting points for a new pair of bracketing solutions is found by interpolating between the pair of stopping points on the original pair of trajectories. This process is repeated as many times as desired to extend the solution. It can be done automatically with a digital computer.

[†] The fact that R , the resting singular point, is not $+$ stable seems surprising, since the resting state of the real axon is physically stable. It is, however, only a mathematical artifact introduced by the assumption (6-4), and has nothing to do with the stability of a patch of membrane.

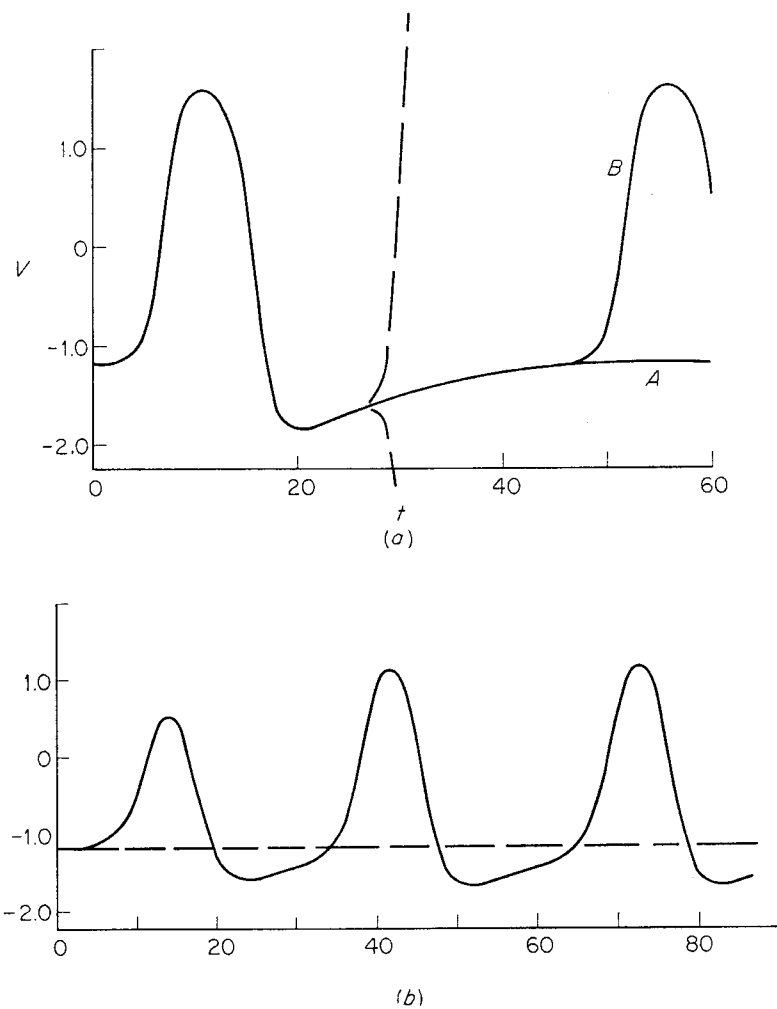


FIG. 6-2. Uniformly propagated action potentials for the BVP model. (a) and (b) correspond to upper and lower dots in Fig. 6.3. (a) Stable solution. Broken curves show neighboring solutions tending toward plus and minus infinity. Two curves, A and B , have nearly identical initial parts, but separate for large values of t . A corresponds to a single impulse, B to an infinite train of impulses. A and B were obtained by the use of different criteria for when V reached "infinity." (b) Unstable solution. Only an infinite train was obtained for this case.

When the conduction velocity for positive ϕ is computed, not one but two values of θ are found. Figure 6-3 shows θ plotted against ϕ . The curve is double valued and occupies only a bounded interval in ϕ . It has a vertex pointing to the right at a critical value ϕ_c of ϕ . For $\phi < \phi_c$, there are two possible conducted action potentials, with different conduction velocities. The upper branch of the curve corresponds to the normal impulse recorded from an axon experimentally, but the lower branch corresponds to a low-amplitude action potential of a type never recorded experimentally (Fig. 6-2b). This second theoretical propagated impulse was first found by Huxley [32] for the HH model, and he concluded that although it exists

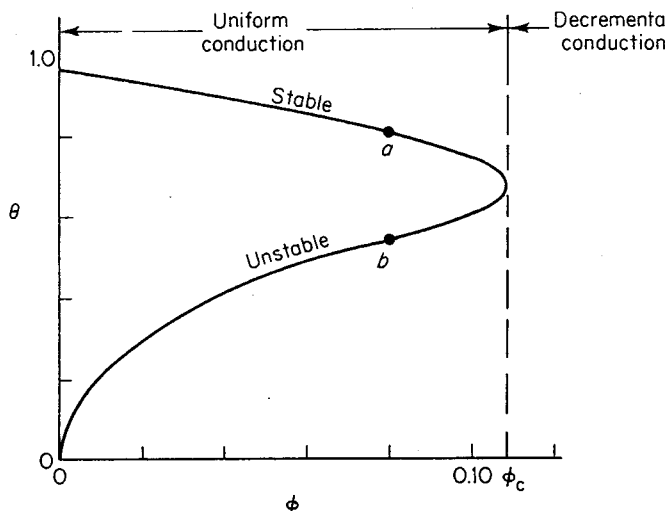


FIG. 6-3. Conduction velocity θ for uniform propagation vs. the temperaturelike parameter ϕ in the BVP equations. Upper and lower branches of curve correspond to stable and unstable impulses. Points *a* and *b* correspond to computations of Fig. 6-2*a* and *b*. Vertical broken line at $\phi = \phi_c$ is boundary for uniform conduction. [The point $\phi = 0$, $\theta = 0.963$ is given by Eq. (6-15).]

as a solution to the differential equations, it corresponds to a physically unstable condition which never occurs in a real axon. (A rigorous proof of the instability of this second solution has not been carried out, but could perhaps be done by a perturbation method.)

If ϕ is increased above ϕ_c , there is no uniformly propagated impulse, and conduction is said to be blocked. The parameter ϕ governs the rate at which the recovery process, represented by changes in the variable W , occurs, and plays somewhat the same role as does temperature in the HH model. Conduction block is a phenomenon that has been recorded under many different conditions experimentally. It can be caused by chemical changes in the bathing fluid or by pressure, as well as by high temperature.

Solutions of the partial differential equations (6-3) with J_a representing stimulating current pulses through point electrodes† show impulses originating at the electrodes and being propagated away, approaching a steady-state condition with constant velocity and waveform, in agreement with experiment.

HH model. The procedure is similar to that just described. The first computations of propagated action potentials were done by Hodgkin and Huxley [31] with a desk calculator, using a slightly different iterative method. Later ones were done with a digital computer [18, 26, 32]. Theoretical

† Digital computations with curves displayed as motion pictures [R. FitzHugh, *J. Appl. Physiol.*, **25**:628 (1968)].

values of net potassium and sodium ion flows during a propagated impulse computed from these solutions have recently been compared with experimental results [27]. J. Cooley, F. Dodge, and H. Cohen [20] have solved partial differential equations of the form of Eqs. (6-2) for the HH model and obtained strength-duration curves. For stimuli very near threshold, an unstable wave propagates a short distance from the electrode and either dies away or explodes into a full-sized propagated action potential. This unstable wave appears to be the same as the uniformly propagated wave of low amplitude found by Huxley [32].

Dimensional properties

Without solving the differential equations for the uniform propagated impulse for an axon model, one can still draw some general conclusions about the effects of changing its physical parameters, merely from the form of the equations. For several different models it has been shown that the conduction velocity varies as the square root of the axon diameter, and inversely as the square root of the longitudinal resistance.† This is true, in general, for the class of models considered here. If K_c is a critical value of K for which the solutions of Eqs. (6-6) are bounded, K_c depends on the properties of a unit area of the membrane model, but not on the non-membrane parameters d , r_e , and r_i , since they do not appear in Eqs. (6-6). The conduction velocity, from Eq. (6-7), is

$$\theta = \left[\frac{K_c}{C\pi d(r_e + r_i)} \right]^{\frac{1}{2}} \quad (6-20)$$

If the external shunting resistance r_e is increased by replacing the volume conductor surrounding the axon with a thin film of solution or reduced by shunting with external electrodes, θ varies as $(r_e + r_i)^{-\frac{1}{2}}$, as is found experimentally.‡

If the axon is surrounded by a large volume of conducting solution, r_e can be neglected in comparison with r_i . Take r_i to be the resistance of a cylinder of unit length, diameter d , and resistivity R_i . Then

$$r_i = \frac{4R_i}{\pi d^2} \quad (6-21)$$

$$\theta = \left(\frac{K_c d}{4CR_i} \right)^{\frac{1}{2}} \quad (6-22)$$

† Ref. [37]; A. Rosenblueth, N. Wiener, W. Pitts, and J. Garcia Ramos, *J. Cellular Comp. Physiol.*, 32:275 (1948); A. L. Hodgkin: *J. Physiol.*, 125:221 (1954).

‡ A. L. Hodgkin, *J. Physiol.*, 94:560 (1939); 106:305 (1947); B. Katz, *ibid.*, 106:411 (1947).

By Eq. (6-22) the conduction velocities of axons of similar constitution but different diameters vary with the square root of the diameter. This agrees only approximately with the measurements of Pumphrey and Young,[†] who found θ to be proportional to d^n with $n = 0.614 \pm 0.027$ instead of $n = 0.5$.

Del Castillo and Moore[‡] decreased R_i by inserting an axial wire electrode into squid axons, and obtained large increases in conduction velocity, but did not make a quantitative study of this effect.

The fact that conduction velocity increases with diameter shows, incidentally, why giant axons have evolved in the squid. These axons are the motor fibers that innervate the large muscles of the mantle. They are used in the escape reflex of the animal, in which it suddenly squeezes its mantle, squirts water through a nozzle, and whizzes away from a hungry enemy by aquatic jet propulsion. The speed of this reflex, and hence a high conduction velocity in the motor axons, is important for survival.

Other dimensional properties involving the parameters of the membrane itself are considered by Huxley [32]. In Eqs. (6-6), introduce dimensionless constants γ , η , and ϕ to provide changes of membrane capacitance and conductances and of the rate of change of the conductance variables W_j :[§]

$$\begin{aligned} \frac{d^2V}{ds^2} &= K \left(\frac{dV}{ds} + \frac{\eta I_i}{\gamma C} \right) \\ \frac{dW_j}{ds} &= \phi F_j \end{aligned} \quad (6-23)$$

Make the substitutions (6-24) into Eqs. (6-23) to get Eqs. (6-25):

$$\sigma = \phi s \quad \kappa = \frac{K}{\phi} \quad \beta = \frac{\eta}{\phi \gamma} \quad (6-24)$$

$$\begin{aligned} \frac{d^2V}{d\sigma^2} &= \kappa \left(\frac{dV}{d\sigma} + \frac{\beta I_i}{C} \right) \\ \frac{dW_j}{d\sigma} &= F_j \end{aligned} \quad (6-25)$$

Equations (6-25) are the same as Eqs. (6-6), except for the replacement of C by C/β and changes of notation. For every value of β , therefore, there is a critical value κ_c of κ for which the solution of Eqs. (6-25) is bounded. There is a corresponding one-parameter family of solutions of Eqs. (6-25) which determines a solution of Eqs. (6-23) for any set of values of γ , η , and

[†] *J. Exptl. Biol.*, 12:453 (1938). R. Hodes [*J. Neurophysiol.*, 16:145 (1953)] found that conduction velocity was proportional to diameter instead of to its square root.

[‡] *J. Physiol.*, 148:665 (1959).

[§] For the BVP model, ϕ already appears in the differential equation for W .

ϕ . $\kappa_c(\beta)$ can be obtained by computation. Figure 20 of [32] gives it for the HH model; it is an increasing function of β . The conduction velocity for Eqs. (6-23) is [see Eqs. (6-7) and (6-20)]

$$\theta = \left[\frac{\phi \kappa_c}{\gamma C \pi d(r_e + r_i)} \right]^{\frac{1}{2}} \quad (6-26)$$

The effects of varying the membrane parameters on conduction velocity can now be predicted. An increase of γ (i.e., capacitance) decreases β , κ_c , and θ . An increase of η (conductance) increases β , κ_c , and θ . An increase of ϕ has a twofold effect. It decreases β , thereby tending to decrease κ_c , but also tends to increase θ by its presence in the numerator of Eq. (6-26). The net effect, in terms of differentials, is given by

$$\begin{aligned} \frac{d \log \theta}{d \log \phi} &= \frac{1}{2} \frac{d \log K_c}{d \log \phi} = \frac{1}{2} \left(1 + \frac{d \log \kappa_c}{d \log \phi} \right) \\ &= \frac{1}{2} \left(1 - \frac{d \log \kappa_c}{d \log \beta} \right) \end{aligned} \quad (6-27)$$

From Fig. 20 of Ref. 32, $(d \log \kappa_c/d \log \beta) - 1$ changes sign from plus to minus as β increases. Thus increasing ϕ increases θ for small ϕ (large β), but decreases θ for large ϕ . In the HH model, ϕ increases with temperature [see Eq. (4-8)]. Figure 17 of Ref. 32 shows how increasing temperature first increases and then decreases the conduction velocity.[†]

A modification of Huxley's dimensional analysis has been used to study the effect of temperature on the ionic fluxes during a propagated impulse in the squid giant axon [27].

Impulse stability and decremental conduction

The use of an axon as a transmission line for neural information depends on its ability to conduct impulses of a constant size and at a constant velocity for long distances. Such impulse conduction is called *uniform conduction*. The active excitable membrane continuously delivers energy to the uniformly conducted impulse at a rate just sufficient to offset the resistive energy losses in the membrane, axoplasm, and external medium. But if, as the result of a very powerful applied stimulus, the action potential is initially larger than can be maintained in this way, it decreases in size as the impulse is propagated, approaching the condition of uniform conduction with a smaller action potential. Such a transient approach to uniform conduction from

[†] Experimental measurements of conduction velocity in the squid giant axon made by R. A. Chapman [*Nature*, 213:1143 (1967)] agree with Huxley's curve in the temperature range from 5 to 25°C, but fall below it for higher and lower temperatures.

above is called *decremental conduction*.[†] Similarly, an increase in size of the action potential up to the value for uniform conduction is called *incremental conduction*. Decremental conduction may also occur if the applied stimulus is slightly below the threshold for conduction. In this case a small impulse arises but dies away and disappears. Under certain conditions of high temperature or treatment by drugs, uniform conduction may be impossible, and only decremental conduction occurs, no matter how large a stimulus is used.

The dynamics of the process whereby the action-potential size and shape are automatically regulated [35] can be understood theoretically by considering stimulus-response curves for neighboring regions of an axon. The experimental *SR* curve of a space and current-clamped patch of squid axon membrane is of the discontinuous type (Fig. 5-1, left) [31]. (Theoretically, the *HH* model gives a continuous curve, but it has such a large maximum slope that the usual computed curves are indistinguishable from discontinuous ones.) *SR* curves recorded from an axon near a stimulating electrode are, however, obviously continuous (Fig. 5-1, right) [48, fig. 10]. The difference in sharpness is the result of loading the stimulated patch of membrane with the rest of the axon, which, being at rest, acts very much like a passive linear core-conductor cable. (This result appears in unpublished computations of a *HH* membrane element with an *RC* shunt.) *SR* curves of this type are used by Nasonov [14, 36] to explain some of the qualitative properties of axonal conduction. He assumes that the axon is divided into patches of length h , each of which responds to stimulation as a unit and in turn acts as the stimulus for the neighboring patch. By means of circulating currents, the excitation is passed along from patch to patch, and a propagated impulse travels along the axon. The magnitude of the impulse in each patch is measured by a single variable which can be either the height or the area of the action potential. These assumptions ignore (1) the spatial nonuniformity of the response in a single patch, (2) the interaction of patches that are not immediate neighbors, and (3) variations in shape of the action potential not reflected in the single magnitude variable chosen. Objection 1 is most serious for h large and objection 2 for h small. Assume that h is chosen to provide a satisfactory compromise between these two objections.

Figure 6-4 shows an *SR* curve. The variable describing the impulse size in each patch appears twice in this diagram, once as the response R

[†] Decremental conduction was found to occur in the squid giant axon by Schmitt and Schmitt [48]. Interest in decremental conduction has increased recently, after a lapse of some decades. See papers by Nasonov [36] and by Lorente de Nò and Condouris [*Proc. Natl. Acad. Sci.*, 45:592 (1959)]. In the experiments described in these papers, impulses were recorded from whole nerves containing many axons, instead of from single axons, and it is possible that some individual fibers were dropping out rather than true decremental conduction occurring in all fibers.

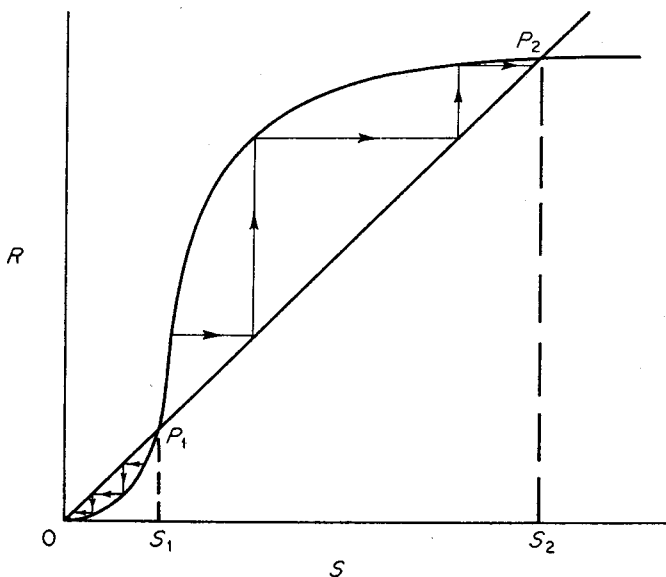


FIG. 6-4. Nasonov diagram consisting of an SR curve and a straight line, for demonstrating the stability of uniform propagated impulses. Lines with arrowheads show how S and R values approach either O or P_2 as impulse travels along axon.

to previous stimulation, and once as the stimulus S for the neighboring resting patch. The line of unit slope through the origin ($R = S$) intersects the SR curve at three points, O (the origin), P_1 , and P_2 , where $S = 0$, S_1 , and S_2 . Given any value of R in a given patch, project horizontally to the straight line to get the S value for the next patch. Then project vertically to the SR curve to find the R value for that patch, and so on. This process is shown by the straight lines with arrowheads in Fig. 6-4. It is the same as the ordinary iteration process used in finding a numerical approximation to the root of an algebraic equation [13]. As in that process, the roots, indicated by the points O , P_1 , and P_2 , are either stable or unstable, in the sense that repeated iterations bring one either toward or away from the point under consideration. The root is stable if the slope of the SR curve is less than one at the root, unstable if it is greater. Points O and P_2 are stable. P_2 corresponds to a uniform propagated impulse, O to the absence of an impulse. P_1 is unstable and corresponds to a uniformly conducted impulse which is never recorded experimentally, but which does appear as the solution to the equations for uniform conduction [for example, Eqs. (6-6)]. In the regions between O and P_1 , and beyond P_2 , conduction is decremental; in the regions between P_1 and P_2 , conduction is incremental.

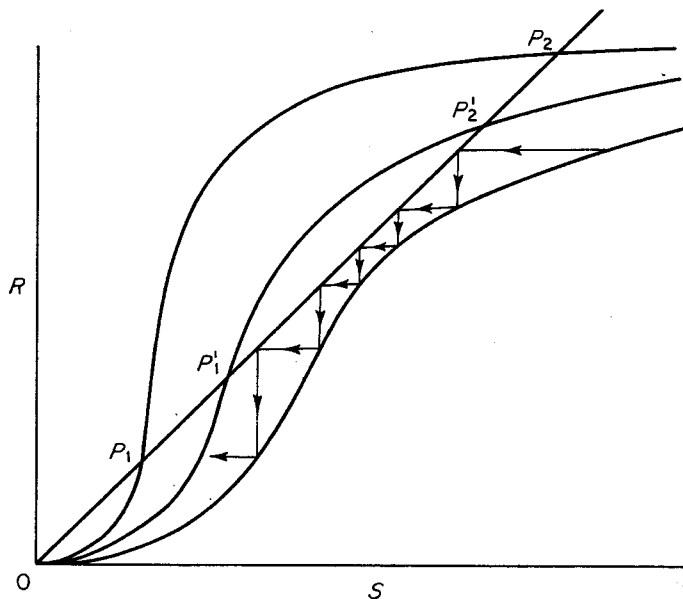
This admittedly rather crude treatment provides a simple way to study the transient behavior of the propagated impulse in an axon, starting from a model of a membrane element. A more adequate treatment, involving the behavior of the stationary solutions of nonlinear partial differential

equations of the type of Eqs. (6-2) is needed, and poses an interesting mathematical problem for research.

The Nasonov diagram can be used to predict qualitatively the properties of the curves of conduction velocity versus temperature or other agent, as described above (page 51), for example, the $\phi\theta$ curve for the BVP model in Fig. 6-3. If the effect of increasing temperature is to speed up the recovery variable W , this lowers the action-potential size and decreases the sharpness of the threshold phenomenon. The effect on the Nasonov diagram is sketched in Fig. 6-5, where the SR curve becomes lower and rises more gradually as temperature is increased. This brings the points P_1 and P_2 closer together (P'_1 and P'_2), until above a critical value of temperature they vanish. This eliminates both the stable and unstable impulses. By following the iteration procedure, one can show that an impulse of any initial size will eventually die away and disappear, so that only decremental conduction is possible in such an axon.

Figure 6-5 can also be used to explain the recovery and refractoriness of a propagated impulse. As the recovery (type-3) variables increase as the result of the change of membrane potential during the action potential, the SR curve is lowered. This eliminates the intersections P'_1 and P'_2 and brings about the return of V to its resting value and the end of the action potential. After the end of the action potential, the type-3 variables begin to return to their resting values, and the SR curve slowly rises again. As long as

FIG. 6-5. Nasonov diagram showing the effect of changing some parameter such as temperature or drug dosage. As parameter changes, SR curve is lowered; points P_1 and P_2 approach each other (P'_1, P'_2) and disappear, eliminating uniform conduction. Lines with arrowheads (as in Fig. 6-4) illustrate decremental conduction.



there is only one intersection O , the membrane patch is absolutely refractory. When P_2 first reappears, the patch is relatively refractory. This analysis can be compared to what has been said earlier (Secs. 3 and 4) with regard to the sequence of physiological states in the BVP and HH models.

The concept of safety factor can be illustrated with the help of the Nasonov diagram. Schmitt and Schmitt [48] define what they call the *safety ratio*, as "the ratio of the output of a unit area of membrane or a unit length of fiber to the lowest input excitation which would, under the same conditions, produce an output equal to itself." In Fig. 6-4 this corresponds to the ratio S_2/S_1 . When the safety ratio is less than one, propagation fails (it thus corresponds to Rushton's safety factor plus one). In Fig. 6-5, the effect of increasing temperature or other harmful agent is to decrease the safety ratio. When it falls below a value of one, block occurs.

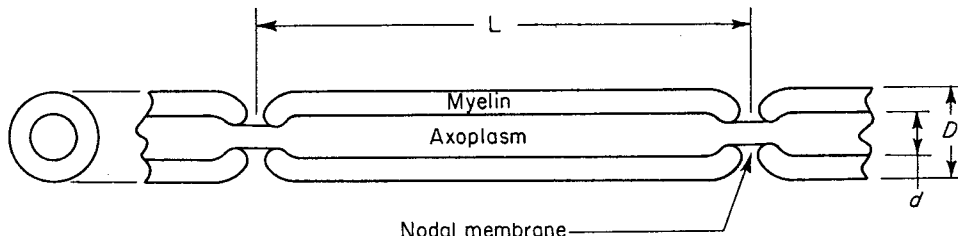
Noded Axon†

Axon equations

The axon is a cylinder of diameter d , encased in a thick layer of a lipoid substance called myelin, with an outer diameter D (Fig. 6-6). The myelin layer is interrupted periodically along the axon to expose the excitable axon surface, which is constricted there. These bare sections of membrane, called *nodes*, are spaced a distance L apart. The exposed area of membrane at the nodes is α . The sections of axon between the nodes are called *internodes*. The myelin layer is electrically passive and a fairly good insulator, and little current crosses the membrane except at the nodes, where excitation occurs. Since the excitation jumps from node to node during impulse conduction, this process is called *saltatory conduction*.

The membrane current density I_v through the v th node can be considered as constant over the whole node. The total current through that node is $J_v = \alpha I_v$. The geometry of the axon can be simplified by assuming that each node occupies a single point on the x axis. The myelin has the electrical

FIG. 6-6. Diagrammatic longitudinal section of a noded axon. Not to scale; radial dimensions are exaggerated for clarity.



† For a short general review, see Ref. 49.

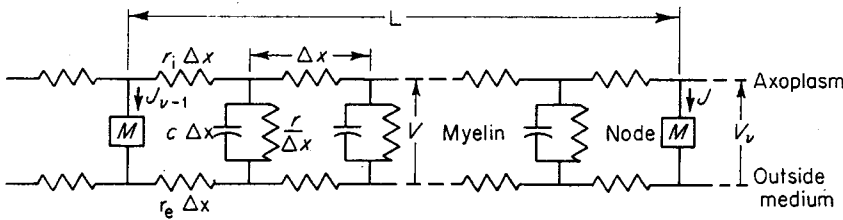


FIG. 6-7. Equivalent circuit of a noded axon. M is the equivalent circuit of a patch of membrane of area α , at a node.

properties of a distributed leaky capacitance. Figure 6-7 shows the equivalent circuit, with the internodes divided into sections of length Δx . In the limit, as Δx approaches zero, one obtains the equations for current flow in a noded axon, corresponding to Eq. (6-1) for a continuous axon:

$$x \neq \nu L \quad c \frac{\partial V}{\partial t} = \frac{1}{r_e + r_i} \frac{\partial^2 V}{\partial x^2} - \frac{V}{r}$$

$$\lim_{x \rightarrow \nu L} V(x, t) = V_\nu(t) \quad \nu = \dots, -2, -1, 0, 1, 2, \dots \quad (6-28)$$

$$J_\nu = \frac{1}{r_e + r_i} \left(\lim_{x \rightarrow \nu L+0} \frac{\partial V}{\partial x} - \lim_{x \rightarrow \nu L-0} \frac{\partial V}{\partial x} \right)$$

where $V(x, t)$ is the potential across the myelin, and $V_\nu(t)$ is the membrane potential at the ν th node. A set of equations of the form of Eqs. (1-1) in V_ν and $W_{\nu 0}$ for each node completes the description.

Propagation without recovery

The analytic approach has been less well developed for a noded axon than for a continuous one because of the greater geometrical complexity of the former. H. D. Landahl and R. J. Podolsky† use a model with nonconducting, noncapacitative myelin [$c = 0$, $r = \infty$ in Eqs. (6-28)]. They represent excitation at the nodes by Blair's one-variable model (see Sec. 2).

When excitation occurs at a given node, the electric circuit of the nodal membrane changes from an emf and a resistor in series to a short circuit. From this model they conclude that there is an optimal value of L at which the conduction velocity is maximum, and a maximum value of L at which the velocity is zero and above which conduction is impossible. There is also a critical value of axon radius, below which conduction is impossible.

The model of Huxley and Stämpfli [33], which includes the effect of the capacity of the myelin, is discussed below under "Dimensional Properties."

† *Bull. Math. Biophys.*, 11:19 (1949). See also Ref. 38.

Propagation with recovery

The partial differential equations (6-28) for a noded axon with the HH model representing the membrane at the nodes has been solved with a digital computer to simulate a noded axon [25]. If a rectangular stimulating pulse is applied to the axon at node zero, and if the pulse amplitude is above threshold, an impulse arises there, grows, and is propagated away to achieve constant size and velocity. In fig. 3 of Ref. 25, the action-potential height at node zero is only just detectably less than the (constant) height at all the neighboring nodes, suggesting incremental conduction. It was not possible to compute a case of excitation very near threshold, which might have shown this effect more strongly, because the greater delay in the appearance of the action potential would have exceeded the time and memory limitations of the computer (an IBM 704). Other details of experimental findings, including the differences in shape of the action potential recorded at a node and that recorded in the middle of an internode, are reproduced by these computations.

L. Goldman and J. S. Albus† have more recently done improved computations using the Frankenhaeuser-Huxley equations [28] for the nodal membrane.

Dimensional properties

A. F. Huxley and R. Stämpfli [33] use the dimensional method to examine the relation between node spacing and conduction velocity. To make the problem tractable mathematically, they make some simplifying assumptions. The ionic current I_i of the unexcited node is assumed to be zero, so that its equivalent circuit consists only of a capacitance $C\alpha$. When V_v , the potential of the node, reaches a critical triggering value V_c , the equivalent circuit is changed to an emf in series with a resistor. There is no recovery.

The details of their analysis are omitted here. They conclude that as node spacing L is increased, the conduction velocity θ first increases and then decreases, with θ a maximum at some optimal value of L . Unfortunately, their assumptions eliminate the possibility of block at large values of L . Because the myelin resistance r is infinite, the space constant [Eq. (6-35) below] is infinite, so that after a long enough delay, the potential at an inactive node approaches arbitrarily near to the constant potential at a neighboring active node, no matter how far apart the two nodes are. Moreover, since there is no recovery, the action potential of the active node does, in every case, last long enough to excite the inactive one. In a real axon, however, if the effective node separation were increased sufficiently, one

† *Biophys. J.*, 8:596 (1968).

would expect the rising potential at the inactive node to be both decreased and delayed so much that it would never reach the critical firing level, and the axon would be blocked. The effect of incipient block on conduction velocity may overshadow the effect of the myelin capacity, as studied with this model.

W. A. H. Rushton [39] applies the dimensional method in a different way. He considers that the design of a noded axon is determined in nature by three main physiological factors. A high conduction velocity decreases the reaction time of an animal's reflex, a low energy consumption per impulse decreases the demands on its metabolic system, and a high safety ratio protects it against deterioration of axonal function by fatigue, injury, or disease. All these factors have survival value, but it is, in general, impossible to optimize a system with respect to more than one criterion at a time. For instance, the greater the distance between nodes, the higher the conduction velocity and the lower the total energy expenditure, but the lower the safety ratio, because of partial shunting through the myelin of the circulating currents by which excitation is passed from node to node. One would expect, however, that natural selection would act to produce the best possible compromise among these three requirements, to favor survival.

Let R_i be the resistivity of the axoplasm, and ρ and ϵ the resistivity and dielectric constant of the myelin. Then, in Eqs. (6-28),

$$\begin{aligned} r_i &= \frac{4R_i}{\pi d^2} \\ r &= \frac{\rho}{2\pi} \ln \frac{D}{d} \\ c &= \frac{2\pi\epsilon\epsilon_0}{\ln(D/d)} \end{aligned} \tag{6-29}$$

where ϵ_0 is the permittivity of a vacuum (a physical constant equal to 1 in electrostatic units). Assume that with a large-volume conductor outside the axon, r_e can be ignored in comparison with r_i . Now transform x in Eqs. (6-28) to a dimensionless spatial coordinate $\xi = x/L$. The nodes lie at the integer positions on the ξ axis. The membrane at the nodes is described by Eqs. (1-1). Let T be the time delay between the appearances of the uniformly conducted impulse at two successive nodes. The conditions for a uniformly conducted impulse are as follows [see Eqs. (6-4) for the continuous axon]:

$$\begin{aligned} \xi \neq v &\quad V(\xi, t) = V(\xi - 1, t + T) \\ V_v(t) &= V_{v-1}(t + T) \\ W_{j,v}(t) &= W_{j,v-1}(t + T) \end{aligned} \tag{6-30}$$

With these assumptions, uniform conduction in a noded axon is described as follows:

$$\xi \neq v \quad \frac{\partial V}{\partial t} = P_1 \frac{\partial^2 V}{\partial \xi^2} - \frac{V}{\rho \epsilon \epsilon_0} \quad (6-31)$$

$$\lim_{\xi \rightarrow v} V(\xi, t) = V_v(t) \quad (6-32)$$

$$\frac{dV_v}{dt} = \frac{1}{C} \left[P_2 \left(\lim_{\xi \rightarrow v+0} \frac{\partial V}{\partial \xi} - \lim_{\xi \rightarrow v-0} \frac{\partial V}{\partial \xi} \right) - I_i(V_v, W_{1,v}, \dots, W_{\mu,v}) \right] \quad (6-33)$$

where

$$P_1 = \frac{d^2 \ln(D/d)}{8R_i \epsilon \epsilon_0 L^2} \quad (6-34)$$

$$P_2 = \frac{\pi d^2}{4\alpha R_i L} \quad (6-35)$$

From Eq. (6-34),

$$L = P_3 d \sqrt{\ln \frac{D}{d}} \quad P_3 = \frac{1}{\sqrt{8R_i \epsilon \epsilon_0 P_1}} \quad (6-36)$$

The properties of this set of equations have not been studied in detail, but by analogy with those of Eqs. (6-6) for the continuous axon, one may guess that if all constants except T are specified in advance, there are critical values T_c of T for which the solution remains bounded as x approaches infinity. T_c in turn determines the conduction velocity θ ($= L/T_c$).

The parameters of these equations are of two types: the spatial parameters (L, d, D, α), and the material parameters (C, R_i, ρ, ϵ). The latter, together with the functions I_i and F_j , depend only on the properties of the material out of which the axon is made.

Consider the material parameters to be fixed. They are limited by the possible chemical structures of nerve, of which little is known. Of the dimensional parameters, assume only that D is fixed by space limitations. How the available space in the body is distributed among the individual axons depends on a compromise between large, rapidly conducting axons which provide rapid reflex responses, and small, slower axons which provide a greater information flow per unit volume of nerve. This problem has not been studied quantitatively, but is discussed by Rushton.

The two constants P_1 and P_2 contain all the spatial parameters [Eqs. (6-35) and (6-36)]. A given pair of values of P_1 and P_2 determine both T_c and the form of the action potential as a function of t . Simultaneous changes of two or more dimensional parameters which do not change the values of P_1 and P_2 leave T_c and the action potential unchanged.

If two points on two different axons have the same value of ξ , Rushton refers to them as "corresponding points." If the equations (6-31) and (6-33) for the two axons have the same functions $V(\xi, t)$ and $V_v(t)$ as solutions, he says that they are in "corresponding states" at every moment.

Here two axons with the same values of P_1 and P_2 will be said to be *dimensionally equivalent*, which means, in Rushton's terminology, that if each is appropriately stimulated, they can be put into and will remain in corresponding states.

The class of all axons with the same values of P_1 and P_2 form an *equivalence class*. Note that if d , D , L , and α are all multiplied by the same factor, the values of P_1 and P_2 are unchanged. All members of an equivalence class have the same waveforms and time relations for the uniformly conducted impulse.

The noded axons of a vertebrate are divided experimentally into different groups, distinguished by different spike durations, afterpotentials, and time course of refractoriness following the spike. Rushton's principal hypothesis is that all the axons in a given group belong to a single-dimensional equivalence class. First let us compare the consequences of this assumption with the experimental facts, and then examine possible theoretical justifications for it.

Since the value of the ratio d/D can vary within an equivalence class of axons, the assumption that all axons in a given group belong to a single equivalence class does not determine d/D . The measurements of F. K. Sanders [47, fig. 3] on rabbit axons show d/D to be an increasing function of D , increasing from 0.15 to 0.8 as D increases from 1 to 20 μm . Using this observed function, Rushton employs relation (6-35) to plot D as a function of L . By adjusting the value of the constant P_1 , he obtains a good fit to the measurements of J. B. Hursh [46, fig. 3] on cat axons. (All the measurements that one wants are unfortunately not always available in the literature for the same species of animal!) This supports his assumption that P_1 is a constant. Although the theoretical curve so derived is slightly concave toward the D axis, the measured points have so much scatter that they can be fitted almost as well by a straight line through the origin in the LD plane. Such a straight line also results theoretically from the simpler assumption that d/D is a constant as D varies. Thus the variation of d/D turns out to be of relatively minor importance in determining the shape of the L versus D curve, and one can say that L is nearly proportional to D .†

The second assumption, that P_2 is a constant, is not directly testable, for lack of detailed measurements of nodal area α in mammals.‡

† B. G. Cragg and P. K. Thomas [*J. Physiol.*, 171:164 (1964)] obtain a straight line in the LD plane which does not go exactly through the origin, for rabbit nerve.

‡ J. D. Robertson [*Progr. Biophys. Biophys. Chem.*, 10:344 (1960)] shows sections of nodes of several different-sized axons (of frog) and remarks that some large axons may actually have smaller nodal areas than some smaller ones. Even if α were a constant for all D , and if L were proportional to D , d/D would decrease as D increased, contrary to measurements on mammals. Measurements of D , L , and α on a single species are needed to decide whether P_2 is actually constant.

However, if both P_1 and P_2 are assumed constant, then T_e is also constant,† since it is theoretically a function of P_1 and P_2 alone. Since $\theta = L/T_e$, θ should vary in the same way with D as L does. Rushton's theoretical curve derived in this way agrees well with the measurements of Hursh [46, fig. 2]. Again, the relation is very nearly one of direct proportionality between θ and D .

Thus Rushton's assumption that all the axons in a given species and fiber group belong to a given equivalence class fits the data rather well, although it does not predict the relation between d and D .

A theoretical argument for the constancy of P_1 can be made by considering the safety ratio of transmission of excitation from node to node.

The efficiency of transmission of excitation from one node to the next by circulating currents depends on the electrical properties of the internode. It is shown below that transmission is most effective when the length constant of the internode, defined as follows [40], is a maximum, relative to L :

$$\lambda = \sqrt{\frac{r}{r_i}} = \frac{d}{2} \sqrt{\frac{\rho \ln (D/d)}{2R_i}} \quad (6-37)$$

The general idea of this derivation is that the greater λ is, the farther a potential signal generated at one node spreads along the internode before decaying to any specified value. Consider a solution of Eq. (6-31) between two neighboring nodes, say numbers 0 and 1. The initial condition for the axon at rest is $V(\xi, 0) = 0$. The potentials at the two nodes are $V_0(t)$ and $V_1(t)$. Let $\bar{V}(\xi, p)$ and $\bar{V}_j(p)$ be the Laplace transforms of $V(\xi, t)$ and $V_j(t)$. Then the transformed solution of Eq. (6-31) with the initial and boundary conditions just given is obtained by standard methods:

$$\bar{V}(\xi, p) = \bar{V}_0(p)F(1 - \xi, p) + \bar{V}_1(p)F(\xi, p) \quad (6-38)$$

where

$$F(\xi, p) = \frac{\sinh q\xi}{\sinh q} \quad (6-39)$$

$$q = \sqrt{\frac{p + 1/\rho\epsilon\epsilon_0}{P_1}}$$

The longitudinal current at the end of the internode near node 1, and its transform, are

$$I_1(t) = -\frac{1}{r_i} \frac{\partial V(\xi, t)}{\partial \xi} \Big|_{\xi=1}$$

$$\bar{I}_1(p) = -\frac{1}{r_i} \frac{\partial \bar{V}(\xi, p)}{\partial \xi} \Big|_{\xi=1} \quad (6-40)$$

$$= -\frac{1}{r_i} [-\bar{V}_0(p)G(0, p) + \bar{V}_1(p)G(1, p)]$$

† Tasaki [50] found both conduction velocity and node length to be proportional to axon diameter D in the frog, thus showing T_e to be, in fact, independent of D .

where

$$G(\xi, p) = \frac{\partial F(\xi, p)}{\partial \xi} = \frac{q \cosh q \xi}{\sinh q} \quad (6-41)$$

Let the impedance transfer function of the membrane at node 1 be $Z(p)$, and the admittance of the rest of the axon beyond node 1 be $A(p)$. (Since the nodes numbered 1 and greater are near their resting state, not having been excited yet, they can be considered as linear elements.) Let $J_1(t)$ be the membrane current and $\bar{J}_1(p)$ its transform. Then

$$I_1(p) = \bar{J}_1(p) + A(p)\bar{V}_1(p) \quad (6-42)$$

$$\bar{V}_1(p) = Z(p)\bar{J}_1(p) \quad (6-43)$$

Eliminate $I_1(p)$ and $\bar{V}_1(p)$ from Eqs. (6-40), (6-42), and (6-43), and use Eq. (6-41) to get

$$\bar{J}_1(p) = \frac{\bar{V}_0(p)}{r_i(\sinh q)[1 + A(p)Z(p)]/q + \cosh q} \quad (6-44)$$

As a measure of the magnitudes of the node response and stimulus, take the following expressions for their total areas, derived using a standard limit formula of Laplace transform theory:

$$\begin{aligned} \int_0^\infty V_0(t) dt &= \lim_{t \rightarrow \infty} \int_0^t V_0(s) ds \\ &= \lim_{p \rightarrow 0} p \mathcal{L} \left[\int_0^t V_0(s) ds \right] = \bar{V}_0(0) \quad (6-45) \\ \int_0^\infty J_1(t) dt &= \bar{J}_1(0) \end{aligned}$$

Let $\bar{J}_T(0)$ be the threshold value of $\bar{J}_1(0)$ which will just cause excitation at node 1. Define the safety ratio as follows:

$$\sigma = \frac{\bar{J}_1(0)}{\bar{J}_T(0)} = \frac{\bar{V}_0(0)}{\bar{J}_T(0)\{(\lambda/L)r_i \sinh(L/\lambda)[1 + A(0)Z(0)] + \cosh(L/\lambda)\}} \quad (6-46)$$

since from Eqs. (6-35), (6-37), and (6-39),

$$\frac{\lambda}{L} = \sqrt{P_1 \rho \epsilon \epsilon_0} \quad (6-47)$$

$$\lim_{p \rightarrow 0} q = \frac{L}{\lambda} \quad (6-48)$$

If the excited node O , which has a relatively low internal impedance, is considered simply as a potential source, then $\bar{V}_0(0)$ is a constant. $A(0)$ and $Z(0)$ are a steady-state conductance and resistance and are positive.

σ is an increasing function of λ/L , and maximizing σ is therefore equivalent to maximizing λ/L , as was to be proved.

By Eq. (6-47), λ/L is a function of P_1 only, and is thus a constant for all members of an equivalence class of axons.

As mentioned above, an axon cannot be optimized with respect to all three quantities, θ , Q , and σ , at once; a compromise is necessary. To evolve a theory of the optimal design of noded axons, one might assume a cost function of these three quantities (the simplest would be some kind of a weighted sum) and minimize that. This will not be attempted here. It can be pointed out, however, that Rushton's assumption that all the axons in a group belong to one equivalence class implies that all axons in a group have the same value of safety ratio. Perhaps this is the minimum possible safety ratio compatible with dependable functioning in a given species, and natural selection has eliminated all individuals with axons having safety ratios smaller than this. At the same time the antagonistic effects of other selection processes with regard to θ and Q would have eliminated higher values of σ . This hypothesis would be most reasonable if the survival value of the safety ratio changed rapidly at a certain critical value of σ . In fact, noded axons, with a measured value of safety ratio of 5, conduct impulses even when a single node becomes totally inexcitable between two excitable ones [50], but normally two inexcitable nodes are not passable by the impulse [49]. If the safety ratio is adjusted to satisfy this requirement, it would help to explain the constancy of P_1 in a given group of axons.[†]

It is not clear how the axon might be optimized with respect to conduction velocity θ and to energy consumption. Let Q be the energy consumption per impulse per unit area of excitable membrane. Then from Eqs. (6-35) and (6-36),

$$\theta = \frac{L}{T_c(P_1, P_2)} = \frac{P_3 d \sqrt{\ln(D/d)}}{T_c(P_1, P_2)} \quad (6-49)$$

$$Q \sim \frac{\alpha}{L} = \frac{P_4}{\ln(D/d)} \quad P_4 = \frac{\pi}{4R_i P_3^2 P_2} \quad (6-50)$$

From Eq. (6-49), the maximum value of θ occurs for $d/D = \exp(-1/2) = 0.61$.[‡] From Eqs. (6-50), however, Q is minimized by making d/D as small

[†] The conclusions stated here are different from Rushton's. He argues that maximizing the space constant within an equivalence class leads to the constant value for d/D of 0.61, which maximizes the safety ratio. But since, as shown above, λ/L is constant within a given equivalence class, L always increases by the same factor as λ , actually leaving the safety ratio unchanged. It is intuitively obvious, for example, that changing the safety ratio from a value greater than one to a value less than one would eliminate the action potential and be incompatible with membership in the same equivalence class. Moreover, the data which he quotes [47] show, in fact, that d/D , instead of being constant, has a clear functional dependence on D .

[‡] This is the value derived by Rushton, though for a different reason. See previous footnote.

as possible. The actual value of d/D might be determined by a compromise between these two criteria. If low energy expenditure were more important for small fibers (since there are more of them) and a high conduction velocity for larger ones (since the most rapid reflexes depend on them), this would explain the observed monotonic increase of d/D with D , up to a value of 0.61, but not the occurrence of still larger values of d/D for the largest fibers.

The problem of the dimensional properties and optimal design of noded axons is still only partially solved, and requires more measurements of the various parameters concerned on the same species of animal than are available now.†

Impulse stability and decremental conduction

A Nasonov diagram like Fig. 6-4 can also be used to study impulse stability for the noded axon. S can be taken as the spike height at one node, and R the spike height that is evoked by S at the next node. This assumes that the stimulating effect of the spike at one node does not extend appreciably beyond the neighboring one which is not strictly true, since, as mentioned above, an axon can still conduct even though alternate nodes are not functioning.

The safety ratio for a noded axon can be defined as S_2/S_1 , where S_1 and S_2 are the abscissa values of points P_1 and P_2 in Fig. 6-4. The other qualitative conclusions regarding impulse stability and decremental conduction follow as for the continuous axon.

7. OSCILLATORY PHENOMENA

Impedances and Space-clamp Stability

The phenomena of excitation and propagation are nonlinear phenomena. As described in Appendix B, the presence or absence of oscillations in a model can, however, be determined by linearizing the nonlinear differential equations and calculating the stability of their singular points.‡ Alternately

† A. S. Paintal [*J. Physiol.*, 184:791 (1966)] finds that in noded nerves of the cat the spike duration decreases with increasing conduction velocity, in disagreement with Rushton's assumption that P_1 and P_2 are constant.

‡ As noted in the last footnote of Appendix B, this criterion is a test only for soft oscillations, i.e., those accompanied by an unstable stationary state from which they can arise without a stimulus of minimum size. Hard oscillations (in a system which also has a stable nonoscillatory stationary state) would be overlooked by the method described. In fact, Cooley, Dodge, and Cohen [20] have found a narrow interval at the lower end of the oscillatory range of the input current I in which hard oscillations occur. These were overlooked in earlier analog computations.

one can study the stability of a linearized electric system by examining its complex impedance.

Experimental measurements of the impedance of the membrane of the squid giant axon were first made by K. S. Cole and coworkers.[†] They found that the membrane in the resting state could be described approximately by a distributed equivalent circuit consisting of a capacitance of $1 \mu\text{F}/\text{cm}^2$ in parallel with a branch composed of a resistance of $1,000 \Omega\text{-cm}^2$ in series with an inductance of $0.2 \text{ H}\cdot\text{cm}^2$. During the nerve impulse the resistance fell to a value of $25 \Omega\text{-cm}^2$. The inductance is not electro-magnetic in nature, but arises from the kinetics of the process of conductance.[‡]

Using the voltage-clamp technique, one can measure current-potential (IV) curves of the membrane showing a region of negative slope resistance. These curves are of the dynatron type, describing a system which in the negative-resistance region is stable under potential control but not under current control. They are curves of membrane current (exclusive of capacitive current) measured either at fixed times following the onset of the voltage pulse (isochronal curves) or at the peak value of the inward (mostly sodium) current, plotted against membrane potential. Neither type of curve is, strictly speaking, the characteristic of the membrane in any particular state, but the concept of such a negative resistance is a useful one that can be made theoretically precise. One way to do this is to use steady-state IV curves of reduced systems. The other, which is more useful in predicting the existence of oscillations, is to use theoretical expressions for membrane impedance (or its reciprocal, admittance). The latter approach will be described for Young's model, the BVP model, and the HH model.

To find the admittance of Young's model, let

$$\begin{aligned} v &= v_0 e^{j\omega t} \\ w &= w_0 e^{j\omega t} \\ i &= i_0 e^{j\omega t} \end{aligned} \tag{7-1}$$

where $v = V - V_R$, $w = W - W_R$, $i = I$.

Substitute these expressions into Eqs. (2-1), eliminate w_0 , and solve for the admittance Y :

$$Y(j\omega) = \frac{i_0}{v_0} = j\omega C + G + \frac{1}{j\omega L + R} \tag{7-2}$$

[†] K. S. Cole and H. J. Curtis, *Nature*, **142**:209 (1938); *J. Gen. Physiol.*, **22**:649 (1939); Curtis and Cole, *ibid.*, **21**:757 (1938); Cole and R. F. Baker, *ibid.*, **24**:771 (1941).

[‡] See Ref. 16, where K. S. Cole used an equivalent circuit like that in Fig. 7-1 (but with $G = 0$) to provide a physical representation of the generalized two-variable model of

where $C = 1$, $G = -k_{11}$, $R = k_{22}/k_{12}k_{21}$, and $L = 1/k_{12}k_{21}$. An equivalent ac circuit having this admittance [16] is shown in Fig. 7-1. Since Eqs. (2-1) are linear, the same circuit values apply if the model is linearized about any operating point in its phase space.

The same equivalent circuit is obtainable from the BVP model as linearized about an operating point (V_S, W_S, I_1) . Making the substitutions (7-1) into Eqs. (3-8), then Eq. (7-2) again results, with $C = 1$, $G = V_S^2 - 1$, $L = 1/\phi$. All the circuit elements except G are constant throughout the phase space, but G is now a function of V_S . For the resting state, $V_S = V_R$ and $G = 0.439$. In the range $-1 < V_S < 1$, G is negative. $G = -1$ for $V_S = 0$, corresponding to a point about halfway up the action potential.

Consider the circuit of Fig. 7-1 shunted by a conductance g_s . Experimentally, g_s is the output conductance of the clamping circuit. To study the stability of this combined circuit, replace $j\omega$ in Eq. (7-2) by the complex variable p . $Y(p)$ is the transfer function of the BVP model. Equating the currents through the two parts of the circuit and canceling potential gives

$$Y(p) = -g \quad (7-3)$$

Equation (7-3) is the characteristic equation of the linearized operating point. The operating point is +stable only if all the roots of Eq. (7-3) are in the left-half complex plane.[†] Equation (7-3) can be put into the form of a quadratic in p :

$$LCp^2 + [RC + L(G + g_s)]p + R(G + g_s) + 1 = 0 \quad (7-4)$$

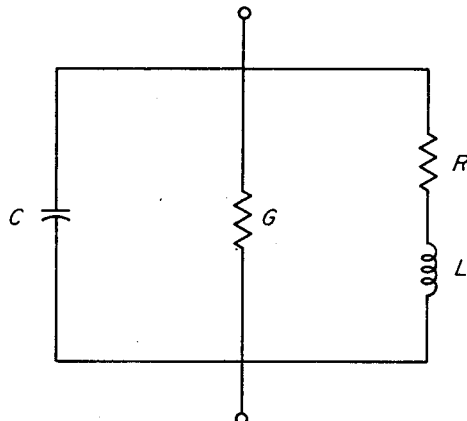


FIG. 7-1. Ac equivalent circuit of Young's model or the BVP model, obtained by linearizing the equations about an operating point in phase space [Eq. (7-2)]. G is a conductance, R a resistance.

[†] The cases in which a root lies on the axis of imaginaries is ignored; this is a special borderline case of little practical importance here.

When $g_s = 0$, Eq. (7-4) is the same as Eq. (3-9) except for differences in notation. By examining the formula for the solution of the general quadratic equation, one can show that the necessary condition for both roots to have negative real parts, and therefore for +stability, is that both the constant term and the coefficient of p be positive [1, 5], or:

$$g_s > -G + \max\left(\frac{-RC}{L}, \frac{-1}{R}\right) \quad (7-5)$$

Since G is a function of membrane potential, the necessary requirement for +stability under all conditions is found by making g_s always greater than g_c , the maximum of the right side of inequality (7-5):

$$\begin{aligned} g_s &> g_c = \max(-G) + \max\left(\frac{-RC}{L}, \frac{-1}{R}\right) \\ g_c &= 1 - \min\left(b\phi, \frac{1}{b}\right) \end{aligned} \quad (7-6)$$

Here "min" and "max" indicate the minimum or maximum value of the quantities in parenthesis, as V is varied. g_c is called the critical clamping conductance. g_c is of great practical importance for voltage-clamp experiments, since it sets a limit to the internal resistance of the clamping circuit to be used. This resistance consists of the output resistance not only of the electronic circuit, which can be made very small, but also of the electrodes, the electrolytes, and the connective tissue covering the membrane. The latter sources of resistance can cause undesirable instability in a clamping circuit. This problem has been the subject of several papers.[†]

As mentioned earlier, another theoretical method for estimating g_c is provided by the reduced system. If, in the first equation (3-5), one lets $W = W_R$ and solves for I , one gets the IV curve of the V reduced system. Its slope is G ; $\max(-G)$ is the magnitude of its greatest negative slope, which is, however, not exactly the same as g_c [Eqs. (7-6)]. For the BVP parameter values used, however, the difference is small: $\min(b\phi, 1/b) = b\phi = 0.064$, which is small compared to 1 in Eqs. (7-6). The negative slope of the IV curve of the reduced model therefore provides, in the BVP model at least, a good estimate of g_c .

For the squid giant axon, dynatron curves were obtained in several ways by Hodgkin, Huxley, and Katz: isochronal curves obtained after a brief

[†] I. Tasaki and A. F. Bak: *Amer. J. Physiol.*, **193**:301 (1958); I. Tasaki and C. S. Spyropoulos: *ibid.*, **193**:309 (1958); K. S. Cole and J. W. Moore, *J. Gen. Physiol.*, **44**:123 (1960); R. E. Taylor, J. W. Moore, and K. S. Cole, *Biophys. J.*, **1**:161 (1960); J. W. Moore and K. S. Cole, chap. 5 in "Physical Techniques in Biological Research," vol. 6, p. 263, Academic Press, Inc., New York 1963; refs. 17 and 15. In Ref. 17, Cole also studies the effect of clamped length of axon on its stability.

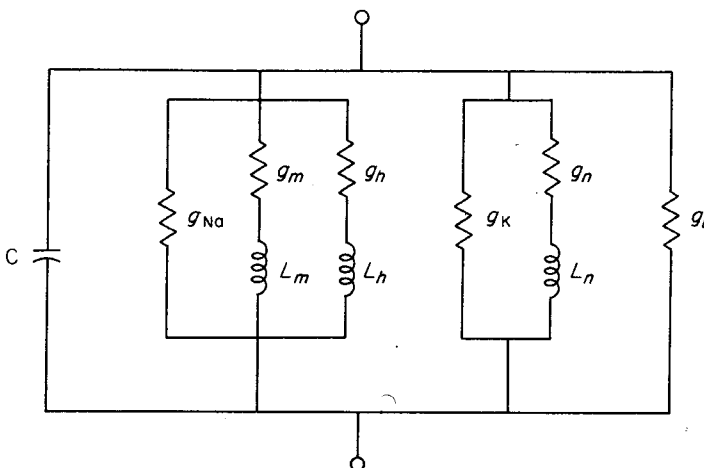


FIG. 7-2. Ac equivalent circuit of the HH model [Eq. (7-7)]. Redrawn from fig. 5 of [15]. The g 's are conductances.

current shock or during a potential pulse, and peak inward current curves.[†] The maximum negative slopes measured from such curves give estimates of g_c , since these curves are approximations of the IV curve for the V_m reduced system. These estimates can be compared with theoretical values computed from the HH model. The admittance of the HH model is[‡]

$$Y(p) = g_\infty + pC + \frac{1}{r_m + pL_m} + \frac{1}{r_h + pL_h} + \frac{1}{r_n + pL_n} \quad (7-7)$$

$$g_\infty = \bar{g}_{Na}m^3h + \bar{g}_Kn^4 + \bar{g}_L$$

Figure 7-2 shows the corresponding ac equivalent circuit.

No simple formula can be given for the critical clamping conductance g_c of the HH model, but computations of g_c , using the Nyquist method, have been made. The theoretical value of g_c is very close to the experimental value obtained from the voltage-clamped squid axon [15]. Such experimental measurements can therefore be used to find the maximum allowable source resistance for adequately space-clamping an axon.

Impulse Trains

Trains of impulses of varying frequency in neurons are the signals that transmit information in the nervous system. Impulse trains can be produced in single neurons and in neuron models by constant-current stimulation (see Secs. 3 and 4). In the BVP and HH models, these trains show a constant

[†] A. L. Hodgkin, A. F. Huxley, and B. Katz, *J. Physiol.*, **116**:424 (1952); Hodgkin and Huxley, *ibid.*, **449**:473 (1952).

[‡] Derived in Ref. 15, including expressions for the r 's and L 's.

impulse height and last indefinitely long, being based on the presence of a +stable limit cycle in phase space. In the space-clamped squid giant axon, however, Hagiwara and Oomura [44] obtained only short trains consisting of at most four impulses, with impulse height and frequency decreasing throughout the train. This disagreement between theory and experiment indicates that something is missing from the BVP and HH models. As mentioned in Sec. 2, the decrease of impulse frequency with time during a constant stimulus is called *adaptation*. To make the BVP and HH models show adaptation, it is necessary to introduce an additional variable of state having a greater relaxation time than any of the other variables, which will serve to decrease the effectiveness of the stimulus, the longer it lasts. Such a variable belongs to type 4 of our classification of variable states.

The simplest way to introduce an adaptation variable into the HH model is by using the Hill-Katz model (Sec. 2). In Eq. (2-8) let $Z_R = 0$; then in Eq. (4-1) replace I by Z . If I in Eq. (2-8) is a step function of time, then Z , the effective stimulating current, is a decaying exponential with time constant λ . Computations with this assumption show a finite burst of impulses with frequency that decreases with time during the burst. They do not, however, duplicate the experimental curves of Hagiwara and Oomura. In the latter, the potential values of the undershoots of successive action potentials in the burst are higher and higher, whereas in the computations just mentioned the successive undershoots fall. (This is reasonable because the effect of a decreased stimulation current is, in general, to lower the value of V .) A number of other ways of introducing an adaptation variable into the HH equations have been tried, none of them completely successful (FitzHugh, unpublished). This work is incomplete and requires further study.

8. CONCLUSION

The analysis of systems of nonlinear differential equations is a difficult but rapidly developing field. For lack of adequate analytic methods it has been necessary to make many simplifying assumptions and approximations in the previous sections of this chapter, without always providing adequate justification and estimates of the resulting errors. Mathematicians have received much stimulation from the practical problems arising from nonlinear systems studied by engineers, with particular emphasis on the prediction of oscillations. Perhaps some mathematical reader will find the nonlinear nerve models described here of equal interest and will be stimulated to contribute some badly needed analysis, particularly of the stability properties of the partial differential equations (6-2) describing propagation in continuous and noded axons. More accurate approximations than provided by the Nasonov model, for instance, would also be of great help

in this work. The ordinary differential equations (6-5) for the uniform propagated impulse, are, at the critical value of conduction velocity, an example of a structurally unstable system, and the topology of its phase space has not been described.

From the physiologist's viewpoint, different problems are important. He wants models that are as accurate as possible in describing the results of his experiments. The present models are unsatisfying in that they lack an adequate basis in molecular biophysics. What is needed is a description of the membrane itself in terms of the molecules which make it up and the kinetics of the changes in ionic conductance which form the basis of excitability. Exploratory work on this major problem is now progressing, using both space-clamped nerve membranes and artificial thin-film membranes of known composition. Only experimental work can provide the solutions to these problems. This chapter has little to contribute directly here,[†] but when kinetic equations of molecular models can be derived, the principles presented here ought to help in analyzing their properties before actual computing is started.

It is easy for some one without experimental experience to forget one important way in which real nerve cells differ from their mathematical models, namely, in their variability. A squid giant axon, for example, is not really a cylinder, but tapers, has lumps and flattened places, and sends off tiny branches (which go to the mantle muscle) all along its length. This causes spatial irregularities in its properties. The experimenter tries to find all these branches and cut them off far enough from the axon to prevent the resulting injury from spreading to it during the experiment (he may not succeed). An axon is delicate; as soon as dissection starts, it begins to degenerate. The squid itself, having recently been through the unpleasant experience of being trapped and imprisoned in a small aquarium, may not be in the best of health. Add to this the inevitable gremlins and snafus inherent in the experimental apparatus itself, to say nothing of the fallibility of the experimenters. Even if the experiment starts well, the axon may give up the unequal struggle against a roomful of electronic equipment and research geniuses, and die before a set of measurements has been completed. A really successful experiment is unusual, and getting several which agree with one another is rare. The fact that so many data have in fact been collected is a tribute to the skill and pertinacity of investigators.

The difficulty of obtaining reasonably consistent, complete, and accurate experimental results complicates the task of the theorist, because he must try to evaluate the data, and try to judge the extent to which their inconsistencies have been affected by differences in technique and experimental conditions.

[†] See however, R. FitzHugh, *J. Cellular Comp. Physiol.*, **66** (suppl. 2; part 2):111 (1965).

For this reason, it is important that he be in close touch with and work with experimenters, if he is not an experimenter himself.

APPENDIX A

Definitions of Physiological Terms

Absolute refractory period the period following an impulse during which the neuron is inexcitable.

Accommodation the decrease of excitability during a subthreshold constant stimulus.

Action potential the curve of membrane potential versus time during the nerve impulse.

Active response a response due to the nonlinear properties of the membrane; the opposite of passive response.

Adaptation the progressive decrease of frequency and, in some cases, cessation of an impulse train resulting from a prolonged constant stimulus.

Afterpotential a relatively slow variation of membrane potential following the spike.

All-or-none law the principle that the response to a stimulus is either a full-sized impulse or no impulse, no intermediate response being possible.

Anodal break excitation excitation occurring after the end of an anodal stimulus pulse.

Anodal current stimulus an applied current passing positively inward through the membrane.

Axon a fine cylindrical outgrowth from a neuron which transmits messages between different parts of the nervous system by means of impulses.

Axoplasm the semifluid conducting medium inside an axon.

Cathodal current stimulus an applied current passing positively outward through the membrane, the usual direction for stimulating currents to be effective.

Circulating currents electric currents through the axon and surrounding solution by which an impulse at one region of an axon membrane stimulates an adjacent region, resulting in conduction of the impulse.

Conduction the movement of an impulse along an axon.

Current clamp an experimental technique in which the membrane current is controlled and the time course of the membrane potential recorded.

Decremental conduction impulse conduction with ever-decreasing action-potential size, eventually leading either to an impulse of constant size or to extinction of the impulse.

Depressed state a state following a subthreshold stimulus in which the threshold is greater than the resting value.

Enhanced state a state following a subthreshold stimulus in which the threshold is lower than the resting value.

Excitation the initial stage of impulse production, just following a suprathreshold stimulus.

Impulse a sequence of electrical and chemical events in a neuron, serving as a unit signal in the nervous system.

Latency the time between the beginning of a suprathreshold stimulus and the appearance of the resulting impulse.

Local response a response that occurs and remains only near the stimulating electrode.

Membrane action potential an action potential recorded from a space-clamped axon or a small, uniformly responding patch of membrane.

Myelinated axon an axon in which only short, equally spaced sections of its surface (nodes) are excitable, the intervening regions being insulated by the lipoid substance, myelin.

Nerve cell neuron.

Nerve fiber axon.

Nerve membrane the thin surface layer of a neuron in which the chemical and electrical changes responsible for excitation and impulse production occur.

Neuron nerve cell, the fundamental functional unit of the nervous system.

Nondecremental conduction impulse conduction with constant velocity and action-potential size.

Passive response a response that has an amplitude proportional to the amplitude of the stimulus; a linear response.

Propagation conduction.

Refractory state the state following an impulse during which the neuron is first inexcitable (absolute refractory period) and then has a threshold above the resting value (relatively refractory period).

Relative refractory period the period following an impulse during which the threshold is greater than the resting value.

Response an electrochemical change, either an impulse or a subthreshold active response, resulting from applying a stimulus to a neuron.

Resting state the stationary condition of a neuron which has received no stimuli recently.

Space clamp an experimental technique in which the membrane potential and current are kept uniform over a short length of axon. Can be used for either current- or voltage-clamp experiments.

Spike the large initial, sharply peaked part of the action potential, which is followed by the afterpotential.

Stationary impulse an impulse that occurs locally in an axon and is not propagated.

Stimulus any physical agent acting on a neuron that can serve to produce an impulse.

Stimulus-response curve (SR curve) a curve of action-potential size versus stimulus intensity.

Strength-duration curve a curve showing the threshold amplitude of a rectangular stimulating pulse plotted against its duration.

Subthreshold stimulus a stimulus too small to produce an impulse.

Suprathreshold stimulus a stimulus large enough to produce an impulse.

Threshold the value of stimulus just large enough to produce an impulse.

Undershoot a minimum in the membrane potential following the spike of an action potential.

Uniform conduction nondecremental conduction.

Voltage clamp an experimental technique in which the membrane potential is controlled by electronic feedback and the time course of the membrane current recorded.

APPENDIX B

Brief Outline of Stability Theory

Some of the topics in the theory of the stability of solutions of ordinary differential equations which are used in this chapter are given here. For a fuller and more rigorous treatment, see the references on this subject in the bibliography.[†] Since this appendix is rather abstract, in the interests of reasonable brevity, readers who are not familiar with this subject are advised to read first one of the many introductory treatments of stability theory which appeal better to the eye and the intuition, such as are contained in Refs. 1, 3, and 5.

Vector and matrix notation is used. A column vector with elements x_j ($j = 1, \dots, n$) is denoted in boldface as \mathbf{x} . An $n \times n$ square matrix with elements A_{ij} is denoted as \mathbf{A} . A dot over a scalar or vector denotes its first derivative with respect to time t (e.g., $\dot{\mathbf{x}}$). $\mathbf{0}$ and \mathbf{I} are the zero vector and the unit matrix of order n . Complex conjugates are indicated by an asterisk.

The state of a system with n variables of state, x_j , can be represented in two equivalent ways, either geometrically as a *state point* in an n -dimensional euclidean *state space* with coordinates x_j , or analytically as a *state vector* \mathbf{x} with components x_j . A state space is called a *phase space* when the motion of a state point in it is determined by a differential equation of the general form (B-1) or (B-2).

$$\dot{\mathbf{x}} = \mathbf{f}(\mathbf{x}) \quad (\text{B-1})$$

$$\dot{\mathbf{x}} = \mathbf{f}(\mathbf{x}, t) \quad (\text{B-2})$$

[†] Some of the terms used here are not standard (eigenlines, eigenplanes, +stable, -stable, \pm stable).

Since Eq. (B-1) does not contain t explicitly, it is called *autonomous*. Such an equation can be used to describe a physical system having properties that do not vary with time. Equation (B-2) is *nonautonomous*; such equations appear in certain applications. A curve in a phase space along which the state point moves is called a *trajectory*. If, for some value s of \mathbf{x} in Eq. (B-1),

$$\mathbf{f}(\mathbf{s}) = \mathbf{0} \quad (\text{B-3})$$

then s is called a *singular point*, which is a degenerate trajectory. Assume that $\mathbf{f}(\mathbf{x})$ can be expanded in the multivariable Taylor series about the point s . Because of Eq. (B-3), the constant term is zero, and for present purposes the terms of second and higher degree can be ignored. This leaves the following linear approximation to Eq. (B-1),

$$\dot{\mathbf{x}} = \mathbf{A} \cdot (\mathbf{x} - \mathbf{s}) \quad (\text{B-4})$$

where

$$A_{jk} = \frac{\partial f_j}{\partial x_k} \quad (\text{B-5})$$

Equation (B-4) is called the linearized differential equation at the singular point s . Move the origin of coordinates to s by the transformation $\mathbf{u} = \mathbf{x} - \mathbf{s}$. Equation (B-4) becomes

$$\dot{\mathbf{u}} = \mathbf{A} \cdot \mathbf{u} \quad (\text{B-6})$$

Consider a trial solution of Eq. (B-6) of the form

$$\mathbf{u} = \mathbf{z} e^{pt} \quad (\text{B-7})$$

Substitution of Eq. (B-7) into Eq. (B-6) gives, after canceling the exponential term,

$$(\mathbf{A} - p\mathbf{I}) \cdot \mathbf{z} = \mathbf{0} \quad (\text{B-8})$$

In order for Eq. (B-8) to have a solution not identically zero, it is necessary that the following determinant be zero:

$$|\mathbf{A} - p\mathbf{I}| = 0 \quad (\text{B-9})$$

Equation (B-9) is the *characteristic equation* of (B-6). It is a polynomial equation in p of degree n and has n roots, real or complex, called the *characteristic roots* or *eigenvalues*. We will consider only the case in which all the eigenvalues are distinct. Since all the coefficients in Eq. (B-9) are real, complex eigenvalues occur only in complex conjugate pairs. To each eigenvalue there corresponds a solution \mathbf{z} of Eq. (B-8). Since Eq. (B-8) is linear, any multiple of \mathbf{z} by a scalar is also a solution of Eq. (B-8). If an eigenvalue p is real, the corresponding eigenvector can be chosen real; if p is complex, this is, in general, not possible. Distinguish the n eigenvalues by subscripts: p_j ($j = 1, \dots, n$).

The eigenvectors can be shown to be linearly independent [2]. This means that any vector \mathbf{u} can be expressed as a linear combination of the eigenvectors, of the form

$$u_j = \sum_{k=1}^n y_k (\mathbf{z}_k)_j, \quad (B-10)$$

where $(\mathbf{z}_k)_j$ is the j th component of the k th eigenvector. Let \mathbf{Z} be the matrix having \mathbf{z}_k as its k th column. Equation (B-10) is equivalent to the matrix equation

$$\mathbf{u} = \sum_{k=1}^n y_k \mathbf{z}_k = \mathbf{Z} \cdot \mathbf{y} \quad (B-11)$$

Equation (B-11) provides a transformation of coordinates from \mathbf{u} to \mathbf{y} by which Eq. (B-6) can be simplified. If \mathbf{P} is the diagonal matrix of the eigenvalues ($P_{jj} = p_j$, $P_{jk} = 0$ if $j \neq k$), the n equations (B-8), one for each eigenvalue, can be written together in matrix form:

$$\mathbf{A} \cdot \mathbf{Z} = \mathbf{Z} \cdot \mathbf{P} \quad (B-12)$$

The differential equation for \mathbf{y} is, using Eqs. (B-6), (B-12), and (B-11),

$$\dot{\mathbf{y}} = \mathbf{P} \cdot \mathbf{y} \quad (B-13)$$

Since \mathbf{P} is diagonal, there are no cross terms in the differential equation for y_j :

$$\dot{y}_j = p_j y_j \quad (B-14)$$

Equation (B-14) has a simple solution,

$$y_j = y_j^0 e^{p_j t} \quad (B-15)$$

where y_j^0 is the initial value of y_j .

If p_j is real, \mathbf{z}_j is a real vector. If all the components of \mathbf{y} are zero except one, say y_j , then by Eq. (B-11), $\mathbf{u} = y_j \mathbf{z}_j$. y_j is thus a measure of distance along the line which passes through the singular point s in the direction of \mathbf{z}_j . Call this line the *j*th eigenline. Equation (B-14) makes the *j*th eigenline into a one-dimensional phase space or *phase line*. It consists of two infinitely long trajectories separated by s at $y_j = 0$.

From Eq. (B-15) a state point \mathbf{u} which is on the *j*th eigenline, but not at s , approaches s as $t \rightarrow +\infty$ if $p_j < 0$. In this case, s is called *+stable* on the eigenline. If $p_j > 0$, \mathbf{u} approaches s as $t \rightarrow -\infty$, and s is *-stable*. The case $p_j = 0$ is special and is neglected here.

If all eigenvalues are real, the eigenlines provide a set of oblique axes (the principal axes of the matrix \mathbf{A}) with its origin at s . Certain trajectories, as just mentioned, lie entirely in the eigenlines. The others can be constructed as follows. Any vector \mathbf{u} is resolved into components in the directions of the eigenlines by Eq. (B-11). The component in the k th direction ends on a point $y_k \mathbf{z}_k$, called the *k*th projection point of \mathbf{u} . The resultant vector of the n moving projection points is \mathbf{u} ; this determines the motion

of \mathbf{u} in the phase space. If all $p_j < 0$, \mathbf{s} is +stable on each eigenline, and \mathbf{u} approaches \mathbf{s} ; \mathbf{s} is then called +stable in the phase space. If all $p_j > 0$, \mathbf{s} is -stable on each eigenline, and also in the phase space. If, however, some eigenvalues are positive and some negative, \mathbf{s} is +stable on some eigenlines and -stable on others, and \mathbf{u} does not approach \mathbf{s} at all (unless its nonzero projection points happen to lie only on +stable or -stable eigenlines). In this case \mathbf{s} is called \pm stable. \pm stable points play an important role in the mathematical representation of threshold phenomena.

If p_j and p_{j+1} are complex conjugates ($p_{j+1} = p_j^*$), p_j can be expressed as follows in terms of its real and imaginary parts:

$$\begin{aligned} p_j &= \pi_j - i\pi_{j+1} \\ p_{j+1} &= \pi_j + i\pi_{j+1} \end{aligned} \quad (\text{B-16})$$

\mathbf{z}_j , \mathbf{z}_{j+1} , y_j , and y_{j+1} are in general complex, but in Eqs. (B-8) and (B-15) we can choose $\mathbf{z}_{j+1} = \mathbf{z}_j^*$ and $y_{j+1} = y_j^*$. Let

$$\begin{aligned} \mathbf{z}_j &= \zeta_j + i\zeta_{j+1} \\ \mathbf{z}_{j+1} &= \zeta_j - i\zeta_{j+1} \end{aligned} \quad (\text{B-17})$$

$$y_j = \frac{\eta_j + i\eta_{j+1}}{2} \quad (\text{B-18})$$

$$y_{j+1} = \frac{\eta_j - i\eta_{j+1}}{2}$$

Differentiate the first equation of (B-18), and separate into real and imaginary parts, using Eqs. (B-14) and (B-16):

$$\begin{aligned} \dot{\eta}_j &= \pi_j \eta_j - \pi_{j+1} \eta_{j+1} \\ \dot{\eta}_{j+1} &= \pi_{j+1} \eta_j + \pi_j \eta_{j+1} \end{aligned} \quad (\text{B-19})$$

Instead of two independent differential equations (B-14) for y_j and y_{j+1} , we have the pair of simultaneous equations (B-19) with cross terms. The general solution of Eqs. (B-19) is

$$\begin{aligned} \eta_j &= [\eta_j^0 \cos(\pi_{j+1}t) - \eta_{j+1}^0 \sin(\pi_{j+1}t)]e^{\pi_j t} \\ \eta_{j+1} &= [\eta_{j+1}^0 \cos(\pi_{j+1}t) + \eta_j^0 \sin(\pi_{j+1}t)]e^{\pi_j t} \end{aligned} \quad (\text{B-20})$$

If all the components of \mathbf{y} are zero except y_j and y_{j+1} , then by (Eq. B-11)

$$\mathbf{u} = y_j \mathbf{z}_j + y_{j+1} \mathbf{z}_{j+1} \quad (\text{B-21})$$

Using Eqs. (B-17) and (B-18),

$$\mathbf{u} = \eta_j \zeta_j + \eta_{j+1} \zeta_{j+1} \quad (\text{B-22})$$

\mathbf{u} lies in the plane through the singular point \mathbf{s} generated by the two vectors ζ_j and ζ_{j+1} . Call this plane the *eigenplane* corresponding to the eigenvalues p_j and p_{j+1} . η_j and η_{j+1} provide a pair of coordinates for this eigenplane, and Eqs. (B-19) make it into a two-dimensional phase space or *phase plane*, by defining the motion of the state point in it. If π_j , the real part of the eigenvalue pair, is negative, \mathbf{s} is $+$ stable in the eigenplane. If $\pi_j > 0$, \mathbf{s} is $-$ stable. The trajectories spiral around \mathbf{s} with an angular frequency π_{j+1} .

In general, if some eigenvalues are real and others occur in complex conjugate pairs, any trajectory can be constructed by the use of projected points moving in the eigenlines and eigenplanes through \mathbf{s} . There are many types of singular point, depending on the location of the eigenvalues in the complex plane. In a phase plane ($n = 2$), if both eigenvalues are real and of the same sign, the singular point is a *node*; if the eigenvalues are complex conjugates, it is a *focus*; if they are real and of opposite sign, it is a *saddle point*. A node or a focus can be either $+$ stable or $-$ stable; a saddle point is \pm stable. Drawings of different types of singular point and their surrounding trajectories for a phase plane are illustrated in several of the references. Those in phase spaces with $n > 3$ cannot be visualized, but their stability properties can be deduced from the preceding method of projected points.

We can now state a criterion for the stability of the singular point of a linear differential equation such as Eq. (B-4) [1, 2].† A singular point is $+$ stable if and only if all its eigenlines and eigenplanes, considered as phase subspaces of the original phase space, are $+$ stable. This in turn is true if and only if the real parts of all eigenvalues are negative. Similarly, the point is $-$ stable if and only if all eigenvalues have positive real parts. Otherwise it is \pm stable. An important further result is that the stability of the singular point of a nonlinear equation (B-1), in cases of practical interest,‡ is the same as that of the linearized equation (B-4). It is possible therefore to study the stability of the singular points of a nonlinear differential equation and obtain valuable information about its qualitative behavior, even though no general solution is available.

Another theorem [2, 4] states that if k of the n eigenvalues have negative [positive] real parts, there is a k -parameter family of solutions (i.e., one occupying a k -dimensional manifold or hypersurface in the n -dimensional phase space) which are $+$ stable [$-$ stable] at the singular point. An important case in the theory of threshold phenomena is a \pm stable singular point with one positive eigenvalue and $n - 1$ with negative real parts. There is then an $(n - 1)$ -dimensional hypersurface of solutions passing through the

† It is assumed here that no eigenvalues have zero real parts.

‡ Functions expandable in Taylor series, no repeated eigenvalues, no eigenvalues with zero real parts.

singular point, which forms a local barrier in the phase space separating two classes of trajectories, corresponding to subthreshold and suprathreshold stimulation. Such a singular point is called a *threshold saddle point*, and the $n - 1$ surface is the threshold separatrix. If $n = 2$, this is an ordinary saddle point in a phase plane, an example of which appears in Fig. 4-4b as point *B*. Threshold saddle points also appear at the resting state in the equations (6-5), (6-7), (6-18), (6-22), (6-24), for the uniformly propagated impulse.

Consider a system having a differential equation with the property that its solutions remains bounded, i.e., within a certain finite region R of its phase space. This is a necessary condition for any physical system. A state point traveling along a trajectory remains within R and approaches some connected subset of R , called the *limiting set* of the trajectory, as $t \rightarrow \infty$. Here only two types of limiting set are important. A limiting set can consist of a singular point which is $+$ stable, or of a trajectory in the form of a closed loop, called a *limit cycle*. More generally, a limit cycle is $+$ stable or $-$ stable or \pm stable, according to whether it is approached by state points only as $t \rightarrow -\infty$, or as $t \rightarrow +\infty$, or both. The stability of a limit cycle is harder to determine theoretically than that of a singular point. However, if the region R contains only one $-$ stable singular point in addition to a single limit cycle, then the limit cycle is $+$ stable and corresponds to an oscillation of the type responsible, for example, for endless impulse trains in nerve models. Whether a train or other oscillation will occur or not can thus be determined relatively easily by examining the stability of the singular point Sec. 7.^f

A useful concept is that of the *relaxation time* of a variable. One can linearize a differential equation (B-1) not only at a singular point, but at any point \mathbf{r} in a phase space,

$$\dot{\mathbf{x}} = \dot{\mathbf{x}}_r + \mathbf{A} \cdot (\mathbf{x} - \mathbf{r}) \quad (B-23)$$

where $\dot{\mathbf{x}}_r$ is the value of $\dot{\mathbf{x}}$ at $\mathbf{x} = \mathbf{r}$. The solutions of (Eq. B-23) approximate those of Eq. (B-1) near \mathbf{r} . Let $\mathbf{x}(t; \mathbf{x}_0)$ denote the solution of Eq. (B-23) such that $\mathbf{x}(0; \mathbf{x}_0) = \mathbf{x}_0$, and let $\mathbf{u} = \mathbf{x}(t; \mathbf{s}) - \mathbf{x}(t; \mathbf{r})$, where \mathbf{s} is any point near \mathbf{r} . Then $\dot{\mathbf{u}} = \dot{\mathbf{x}}_r + \mathbf{A} \cdot (\mathbf{x}(t; \mathbf{s}) - \mathbf{r}) - \dot{\mathbf{x}}_r - \mathbf{A} \cdot (\mathbf{x}(t; \mathbf{r}) - \mathbf{r}) = \mathbf{A} \cdot \mathbf{u}$, and \mathbf{u} obeys Eq. (B-6). Choose one variable u_j , and assume that all the other variables u_k ($k \neq j$) are held constant. Then u_j obeys the simple equation

$$\dot{u}_j = A_{jj} u_j \quad (B-24)$$

The relaxation time τ_j is defined to be $1/|A_{jj}|$. Equation (B-24) is in most cases not a very accurate approximation to Eq. (B-23) for u_j , but if one

^f The type of phase space considered here, with a $-$ stable singular point and a $+$ stable limit cycle as its only limiting sets, shows what engineers call a "soft oscillation." It is also theoretically possible to have both a $+$ stable singular point and a $+$ stable limit cycle, corresponding to a "hard oscillation." See the first footnote in Sec. 7.

relaxation time τ_j is much greater than the others, it may be useful for purposes of approximation to examine the reduced differential equation obtained from Eq. (B-1) by setting $\dot{u}_j = 0$ and solving for the remaining variables as functions of time. This method of reduced systems is used to analyze the HH equations and is the basis of the classification of variables of nerve models into types 1 to 4.

As an example of the methods described in this appendix, the equations for Young's model given in Sec. 2 are derived below.

Define the following vectors and matrix:

$$\mathbf{x} = \begin{bmatrix} V - V_R \\ W - W_R \end{bmatrix} \quad \mathbf{A} = \begin{bmatrix} k_{11} & k_{12} \\ k_{21} & k_{22} \end{bmatrix} \quad \mathbf{u} = \begin{bmatrix} a \\ 0 \end{bmatrix} \quad (\text{B-25})$$

Equations (2-1) and their initial condition become (to avoid confusion with the unit matrix I , denote the current by J)

$$\dot{\mathbf{x}} = \mathbf{A} \cdot \mathbf{x} + J\mathbf{u} \quad \mathbf{x}(0) = 0 \quad (\text{B-26})$$

The differential equation in (B-26) is the same as Eq. (B-4) if $s = -J\mathbf{A}^{-1} \cdot \mathbf{u}$. Equation (B-26) has the solution

$$\mathbf{x}(t) = J\mathbf{A}^{-1} \cdot (e^{\mathbf{A}t} - \mathbf{I}) \cdot \mathbf{u} \quad (\text{B-27})$$

Equation (B-12) can be used to eliminate \mathbf{A} from Eq. (B-27). Since $\mathbf{A} = \mathbf{Z} \cdot \mathbf{P} \cdot \mathbf{Z}^{-1}$ and $\mathbf{A}^n = \mathbf{Z} \cdot \mathbf{P}^n \cdot \mathbf{Z}^{-1}$, the power-series definition of $e^{\mathbf{A}t}$ gives $e^{\mathbf{A}t} = \mathbf{Z} \cdot e^{\mathbf{P}t} \cdot \mathbf{Z}^{-1}$. Then

$$\dot{\mathbf{x}}(t) = J\mathbf{Z} \cdot \mathbf{P}^{-1} \cdot (e^{\mathbf{P}t} - \mathbf{I}) \cdot \mathbf{Z}^{-1} \cdot \mathbf{u} \quad (\text{B-28})$$

Equation (B-9) becomes

$$p^2 - (k_{11} + k_{22})p + (k_{11}k_{22} - k_{12}k_{21}) = 0 \quad (\text{B-29})$$

with roots p_1, p_2 .

Define the matrices

$$\mathbf{I}_1 = \begin{bmatrix} 1 & 0 \\ 0 & 0 \end{bmatrix} \quad \mathbf{I}_2 = \begin{bmatrix} 0 & 0 \\ 0 & 1 \end{bmatrix} \quad (\text{B-30})$$

Then

$$e^{\mathbf{P}t} - \mathbf{I} = \begin{bmatrix} e^{p_1 t} - 1 & 0 \\ 0 & e^{p_2 t} - 1 \end{bmatrix} = (e^{p_1 t} - 1)\mathbf{I}_1 + (e^{p_2 t} - 1)\mathbf{I}_2 \quad (\text{B-31})$$

$$\mathbf{x}(t) = J[(e^{p_1 t} - 1)\mathbf{c}_1 + (e^{p_2 t} - 1)\mathbf{c}_2] \quad (\text{B-32})$$

where

$$\mathbf{c}_i = \mathbf{Z} \cdot \mathbf{P}^{-1} \cdot \mathbf{I}_i \cdot \mathbf{Z}^{-1} \cdot \mathbf{u} \quad (\text{B-33})$$

A current pulse of duration T is of threshold amplitude I if $\mathbf{x}(T)$ lies on the excitation barrier, i.e., if $V = W$ at $t = T$. Define the vector $\mathbf{j}' = [1, -1]$.

Then, from Eqs. (B-25),

$$\mathbf{j}' \cdot \mathbf{x}(T) = W_R - V_R \quad (\text{B-34})$$

Substitute for $\mathbf{x}(T)$ from Eq. (B-32) into Eq. (B-34) and solve for J to get

$$J = \frac{W_R - V_R}{C_1(e^{p_1 T} - 1) + C_2(e^{p_2 T} - 1)} = \frac{1}{K_1(e^{p_1 T} - 1) - K_2(e^{p_2 T} - 1)} \quad (\text{B-35})$$

where $C_i = \mathbf{j}' \cdot \mathbf{c}_i$ and $K_i = (-1)^{i-1} C_i / (W_R - V_R)$.

If J is at its rheobasic value, the trajectory is tangent to the excitation barrier at $t = T$; that is, the velocity vector $\dot{\mathbf{x}}(T)$ has unit slope

$$\mathbf{j}' \cdot \dot{\mathbf{x}}(T) = 0 \quad (\text{B-36})$$

Differentiate Eq. (B-32) and substitute in Eq. (B-36), setting $T = T_0$, to get

$$T_0 = \frac{1}{p_1 - p_2} \ln \frac{p_2 K_2}{p_1 K_1} \quad (\text{B-37})$$

By setting the derivative of J with respect to T , obtained from Eq. (B-35), equal to zero, one sees that an extremum (actually a minimum in cases of interest) in J exists at $T = T_0$. Values of J obtained from Eq. (B-35) for $T > T_0$ correspond to a trajectory crossing the excitation barrier (Figs. 2-1 and 2-2) for a second time, and thus do not lie on the strength-duration curve. Since a rheobasic pulse of any duration greater than T_0 is also just threshold, the formula for the complete strength-duration curve is as follows:

$$0 < T \leq T_0 \quad J(T) = \frac{1}{K_1(e^{p_1 t} - 1) - K_2(e^{p_2 t} - 1)} \quad (\text{B-38})$$

$$T_0 < T \quad J(T) = J(T_0)$$

APPENDIX C

Computation Methods

No general solutions are available for most of the nonlinear differential equations used in models of the axon. Both digital and analog computers have been used to solve such equations, and hybrid computers should also be useful for many problems. Since the use of computers is now widespread, there is no need for a general description of them here, but a brief description of their application to axon modeling may be useful.

Much work with nerve models requires an exploration of the properties by making various changes in the equations and observing their effects. The result of a change in a model can be seen at once from the solution curves and will suggest the next change to try. In such a trial-and-error search an analog computer, operated by the investigator, is most convenient. It

can be used, for instance, to solve ordinary differential equations of the form (2-1) to obtain curves of action potentials of a current- and space-clamped axon [23, 24]. The curves are displayed with high-speed repetitive operation on a cathode-ray oscilloscope screen, or more slowly drawn on an *XY* plotter. Because of the ease of modifying the program and the immediate availability of results, an analog computer is much more useful than a batch-processed digital computer, which may require a minimum turnaround time of several hours between submission of the input data and production of the results as printed columns of figures.

The use of remote computing stations connected to a time-shared central processor reduces turnaround time markedly, from hours to minutes or seconds. If a digital plotter is provided for plotting curves, the convenience of using a digital computer will be greatly increased. Special programming languages for simulating an analog computer such as MIDAS† may also help. Even so, a digital computer cannot approach the speed and accessibility of an analog computer with high-speed repetitive operation and with oscilloscopic display, for solving ordinary differential equations.

The principal disadvantage of an analog computer is its limited accuracy. The overall error in solving the HH equations with a medium-accuracy analog computer (0.1 to 0.5 percent accuracy of separate components) is between 1 and 5 percent, depending on the problem. This makes it hard to get dependable threshold measurements, especially if one is looking for a relatively small change in threshold resulting from some change in the equations. It is also impossible to compute with an analog computer the intermediate-sized action potentials which theoretically occur with a continuous threshold phenomenon (see Sec. 5 under "Continuous Threshold Model" and ref. [26]); for these a digital computer is needed. Another example is the equations (6-6) for the uniformly propagated impulse. With an analog computer, equations can be solved up to the point of divergence to plus and minus infinity (Fig. 6-2a), which is sufficient for computing the velocity, but to obtain a more complete curve showing the peak and later parts of the action potential requires the greater accuracy of a digital computer. Because of its logical capabilities, a digital computer can automatically carry out the search for velocity and the continuation of the action-potential curve by the process of repeated continuation (see Sec. 6 under "Propagation without Recovery").

For the solution of partial differential equations of the form (6-2) for variables of state which change with distance along the axon as well as with time, a digital computer has been used [20, 25]. Stability studies which require the computation of eigenvalues of a matrix or impedance curves can best be performed with a digital computer [15].

† G. H. Burgin, *Simulation*, 6:160 (1966).

Hybrid computers, which combine the speed and convenience of a high-speed repetitive-operation analog computer with the logical capabilities and memory of real-time digital computation, promise to be very useful for nerve-model work, but I have not had any personal experience using them.

APPENDIX D

List of Symbols†

a	= 0.7 = constant in BVP model	J_a	= electrode current applied to axon surface, per unit length
b	= 0.8 = constant in BVP model	K	= adjustable constant in equations for uniformly propagated impulse
C	= capacitance per unit area of membrane	K_c	= critical value of K
c	= capacitance of myelin per unit length	L	= node spacing
D	= outer diameter of myelin sheath	m	= sodium activation in HH model
d	= diameter of continuous axon or of axoplasm of noded axon	m_∞	= steady-state value of m , a function of V
F_j	= function defining dW_j/dt	n	= potassium activation in HH model
G	= variable conductance in ac equivalent circuit of BVP model	n_∞	= steady-state value of n , a function of V
\tilde{g}_{Na}	= $120 \text{ m}\Omega/\text{cm}^2$ = sodium conductance constant in HH model	P_1, P_2	= constants in dimensional analysis of noded axon
\tilde{g}_K	= $36 \text{ m}\Omega/\text{cm}^2$ = potassium conductance constant in HH model	p	= eigenvalue variable
\tilde{g}_L	= $0.3 \text{ m}\Omega/\text{cm}^2$ = leakage conductance constant in HH model	Q	= total charge in current pulse
g_c	= critical value of g_s	Q_0	= threshold value of Q for instantaneous pulse
g_s	= shunt conductance applied to membrane	R	= resting singular point; denotes value of variable at state R when used as a subscript; also response variable of stimulus-response curves
h	= sodium inactivation in HH model	R_1	= resistivity of axoplasm
h_∞	= steady-state value of h , a function of V	r	= resistance per unit length of myelin
I	= total current through membrane, per unit area	r_e	= resistance per unit length of external medium
I_i	= (ionic) current through membrane conductors, per unit area	r_i	= resistance per unit length of axoplasm
I_0	= rheobase	S	= singular point for nonzero I ; denotes value of variable at
I_1	= amplitude of step or pulse of current		
J	= total current through membrane, per unit length		

† Symbols used only in Appendix B, and those used only where defined, are omitted.

s	= state S when used as a subscript; also stimulus variable of stimulus-response curves	W_R	= resting value of W , equal to -0.6243 in the BVP model
T	= traveling spatial coordinate for uniformly propagated impulse	W_j	= j th variable of state, other than V and I
T_c	= node-to-node conduction time	x	= distance along axon
T_0	= critical value of T	α	= area of nodal membrane
T_1	= utilization time	$\alpha_h, \alpha_m, \alpha_n, \beta_h, \beta_m, \beta_n$	= functions for HH model defined in Eq. (4.6)
t	= duration of rectangular current pulse	Δx	= increment of x in equivalent circuits of axons
V	= time	ϵ	= dielectric constant of myelin
V_{Na}	= potential across membrane, or, in noded axon, across myelin	ϵ_0	= permittivity of vacuum
V_K	$= 115$ mV = sodium equilibrium potential in HH model	θ	= conducted velocity of propagated impulse
V_L	$= -12$ mV = potassium equilibrium potential in HH model	λ	= space constant of axon
V_R	$= 10.5989$ mV = leakage equilibrium potential in HH model	μ	= number of variables W_j
V_v	= resting potential $= -1.1994$ for the BVP model, 0 for the HH model	ν	= node number
W	= membrane potential at ν th node	ξ	= dimensionless spatial coordinate for noded axon
	= accommodation and recovery variable in Young and BVP models	τ	= (with subscript) = relaxation time of variable named in subscript
		ϕ	= temperature-scaling factor in BVP or HH model, also scaling factor for s

BIBLIOGRAPHY

Stability Theory

1. Andronow, A. A., and C. E. Chaikin: "Theory of Oscillations," Princeton University Press, Princeton, N.J., 1949.
2. Bellman, R.: "Stability Theory of Differential Equations," McGraw-Hill Book Company, New York, 1953.
3. Korn, G. A., and T. M. Korn: "Mathematical Handbook for Scientists and Engineers," pp. 264-270, McGraw-Hill Book Company, New York, 1961.
4. Lefschetz, S.: "Differential Equations: Geometric Theory," Interscience Publishers, Inc., New York, 1957.
5. Minorsky, N.: "Nonlinear Oscillations," D. Van Nostrand Company, Inc., Princeton, N.J., 1962.
6. Nemytskii, V. V., and V. V. Stepanov: "Qualitative Theory of Differential Equations," Princeton University Press, Princeton, N.J., 1960.

Computing Techniques

7. Johnson, C. L.: "Analog Computer Techniques," McGraw-Hill Book Company, New York, 1956.
8. Korn, G. A., and T. M. Korn: "Electronic Analog Computers," 2d ed., McGraw-Hill Book Company, New York, 1956.

9. McCracken, D. D.: "A Guide to Fortran Programming," John Wiley & Sons, Inc., New York, 1961.
10. Wrubel, M. H.: "A Primer of Programming for Digital Computers," McGraw-Hill Book Company, New York, 1959.

Numerical Techniques

11. National Physical Laboratory: "Modern Computing Methods," 2d ed., Philosophical Library, Inc., New York, 1961.
12. Ralston, A., and H. S. Wilf (ed.): "Mathematical Methods for Digital Computers," John Wiley & Sons, Inc., New York, 1960.
13. Scarborough, J. B.: "Numerical Mathematical Analysis," 4th ed., The Johns Hopkins Press, Baltimore, 1958.

Nerve Models

14. Averbakh, M. S., and D. N. Nasonov: *Fiziol. Zh. SSSR*, **36**:46 (1950).
15. Chandler, W. K., R. FitzHugh, and K. S. Cole: *Biophys. J.*, **2**(part 1):105 (1962).
16. Cole, K. S.: *J. Gen. Physiol.*, **25**:29 (1941).
17. Cole, K. S.: *Biophys. J.*, **1**:401 (1961).
18. Cole, K. S., H. A. Antosiewicz, and P. Rabinowitz: *J. Soc. Ind. Appl. Math.*, **3**:3 (1955).
19. Dodge, F. A.: "Biophysics of Physiological and Pharmacological Actions," p. 119, American Association for the Advancement of Science, Washington, D.C., 1961; also doctoral thesis, Rockefeller Institute, New York, 1963.
20. Cooley, J., F. Dodge, and H. Cohen: *J. Cellular Comp. Physiol.*, **66**(suppl. 2, part II):99 (1965).
21. Dodge, F. A., and B. Frankenhaeuser: *J. Physiol.*, **143**:76 (1958); **148**:188 (1959).
22. FitzHugh, R.: *Bull. Math. Biophys.*, **17**:257 (1955).
23. FitzHugh, R.: *J. Gen. Physiol.*, **43**:867 (1960).
24. FitzHugh, R.: *Biophys. J.*, **1**:445 (1961).
25. FitzHugh, R.: *Biophys. J.*, **2**:11 (1962).
26. FitzHugh, R., and H. A. Antosiewicz: *J. Soc. Ind. Appl. Math.*, **7**:447 (1959).
27. FitzHugh, R., and K. S. Cole: *Biophys. J.*, **4**:257 (1964).
28. Frankenhaeuser, B., and A. F. Huxley: *J. Physiol.*, **171**:302 (1964).
29. Harmon, L. D.: *Kybernetik*, **1**:89 (1961).
30. Hill, A. V.: *Proc. Roy. Soc. London*, **B119**:305 (1936).
31. Hodgkin, A. L., and A. F. Huxley: *J. Physiol.*, **117**:500 (1952).
32. Huxley, A. F.: *Ann. N.Y. Acad. Sci.*, **81**:221 (1959).
33. Huxley, A. F., and R. Stämpfli: *J. Physiol.*, **108**:315 (1949).
34. Katz, B.: "Electric Excitation of Nerve," Oxford University Press, London, 1939.
35. Nagumo, J., S. Arimoto, and S. Yoshizawa: *Proc. IRE*, **50**:2061 (1962).
36. Nasonov, D. N., and D. L. Rosental: *Usp. Sovrem. Biol.*, **34**:161 (1952).
37. Offner, F., A. Weinberg, and G. Young: *Bull. Math. Biophys.*, **2**:89 (1940).
38. Rashevsky, N.: "Mathematical Biophysics," 3d ed., 2 vols., Dover Publications, Inc., New York, 1960.
39. Rushton, W. A. H.: *J. Physiol.*, **115**:101 (1951).
40. Taylor, R. E.: Cable Theory, a chapter in "Physical Techniques in Biological Research," vol. 6, Academic Press, Inc., New York, 1963.

41. Vallbo, Å. B.: *Acta Physiol. Scand.*, **61**:1 (1964).

42. Young, G.: *Psychometrika*, **2**:103 (1937).

Experiments

43. Cole, K. S., and J. W. Moore: *J. Gen. Physiol.*, **44**:123 (1960).

44. Hagiwara, S., and Y. Oomura: *Japan. J. Physiol.*, **8**:234 (1958).

45. Hodgkin, A. L., and B. Katz: *J. Physiol.*, **108**:37 (1949).

46. Hursh, J. B.: *Amer. J. Physiol.*, **127**:131 (1939).

47. Sanders, F. K.: *Proc. Roy. Soc. London*, **B135**:323 (1947-1948).

48. Schmitt, F. O., and O. H. Schmitt: *J. Physiol.*, **98**:26 (1940).

49. Stämpfli, R.: *Physiol. Rev.*, **34**:101 (1954).

50. Tasaki, I.: "Nervous Transmission," Charles C. Thomas, Publisher, Springfield, Ill., 1953.

51. Tasaki, I., and S. Hagiwara: *J. Gen. Physiol.*, **40**:859 (1957).

Basic Neurophysiology

52. Brazier, M. A. B.: "The Electrical Activity of the Nervous System," rev. ed., Sir Isaac Pitman & Sons, Ltd., London, 1953.

53. Bullock, T. H., and G. A. Horridge: "Structure and Function in the Nervous System of Invertebrates," vol. I, chap. 3, W. H. Freeman and Company, San Francisco, 1965.

54. Field, J., (ed.): "Handbook of Physiology," sec. I: Neurophysiology, vol. I, chaps. 1-3. American Physiological Society, Washington, D.C., 1959.

55. Hodgkin, A. L.: "The Conduction of the Nerve Impulse," Charles C. Thomas, Publisher, Springfield, Ill., 1964.

56. Ochs, S.: "Elements of Neurophysiology," John Wiley & Sons, Inc., New York, 1965.